

-Deuterium Isotope Effects as Evidence for  $\alpha$ -Agostic Assistance in Ziegler-Natta Catalysts.

-Design, Synthesis, and Reactivity of a New Class of Highly Syndiospecific Ziegler-Natta Polymerization Catalysts.

Thesis by

Timothy A. Herzog

In Partial Fulfillment of the Degree of Doctor of Philosophy

Division of Chemistry and Chemical Engineering

California Institute of Technology  
Pasadena, California

1997

(Submitted June 17, 1996)

Dedicated to:

Valentin and Elizabeth Herzog

Allan and Francis Fackenthal

Mallene and Johannes Herzog

**Acknowledgment:**

It is impossible to thank all of the people who have helped me throughout the past six years. I have been blessed with many great friends and coworkers and I will try to mention most of them.

John Bercaw has created an unsurpassed environment in which to do science and I feel fortunate indeed to have been in his group and to learn from him. He is not only a great scientist, but a great person as well and I will spend my life trying to live up to his example. Throughout the years, the Bercaw group has gone through many changes, but I have always enjoyed working here and will miss it a great deal. Thanks to all of you who made this a fun place to work and to not work. A long time ago, it seems, Leroy Whinnery first talked to me about the Bercaw Group and introduced me to Toe's Tavern, perhaps in that order. Bryan Coughlin, Donnie Cotter, Erik Kelson, and Roger Quan all taught me how to do chemistry the Bercaw way. Bryan, especially, took me under his wing when I started out and I owe him a lot. Donnie Cotter convinced me to go on my first Bercaw group hike and somehow saddled me with the job of organizing the next three. When he wasn't crashing his bike, Bob Blake served as the driving force behind the band, Resbit Früm Hel, since he always brought the beer. Sharad Hajela taught me about isotope effects and took me out to see Dizzy Gillespie. My classmate Andy Kiely has always amazed me with his knowledge and insight into chemistry as well as everything else. Mike Abrams has kept the Blue Box squeaky clean and has always kept me honest. Shannon Stahl ran our birthday parties like a drill Sargent. Susan Brookhart was a great person to share a line with, despite the fact that she is so short, and dragged me out of the lab for ice cream when things got particularly depressing. Steve Miller taught me a lot about working with polymers and about polymer statistics. Antek Wong Foy is always up for a late night beer run and always keeps things interesting around the lab. Cory Nelson is never too busy to school me at basketball or golf. Jeff Yoder is never too busy to let me school him at basketball or golf. I have greatly enjoyed talking trash, and talking about chemistry, with Paul Chirik. Deanna Zubris has been a terrific line mate and has been a lot of fun to work with. I am happy that she will continue the project that I started.

Larry Henling solved both of the crystal structures in this thesis and was a great companion in the outfield. Bill Schaefer is an unbelievable source of information about the Sierras and taught me most of the little that I know about crystallography.

A number of post-docs and visiting faculty have come through and given a lot to the group and to me. Warren Piers started the  $\alpha$ -agostic project and unfortunately gave us the first slide from hell. Gui Bazan kept us all strong and fat with "motivation pulls" and by starting the "eating society." Gui also initiated the project of trying to make Group III syndiospecific catalysts. Dave Lyon was always up for a beer, even well before Hogs practice. John Mitchell was always a great source of synthetic advice as well as Stevie Ray Vaughn at Lucky Baldwins. Jim Gilchrist has helped me incredibly with his encyclopedic knowledge of organic synthesis. "Ask Jim!" is now my first answer to most synthetic questions but is usually followed by "Where's Jim?" Matt Holtkamp brought a breath of fresh, country air to the group and is never too busy to foul me mercilessly playing basketball. Dario Veghini has enlightened me with numerous interesting discussions about chemistry and life in general, as well as putting me up when I was homeless. Jun Okuda helped out a lot with (TMS)Cp chemistry and provided unpublished results regarding the deprotonation of BTCp. Les Field showed up just at the right time, as is his way, and he and Sharad Hajela showed me how to get great deuterium NMRs. Terry Burkhardt at Exxon Chemical in lovely Baytown, Texas, ran a polymerization for me and Chuck Ruff gave me a great  $^{13}\text{C}$  NMR of the polymer.

Alison McCurdy has been my best friend at Caltech and has helped to keep my life in perspective. Andy Kiely has been a great friend throughout the past six years and I will miss the sight of his protruding lower lip. Mike Abrams has been a great friend and hiking companion, when he isn't getting lost, and has often helped me answer the elusive question, "What do I like to do in my free time?" Michael Murray, Chris Kenyon, and Bob Blake always provided a nice atmosphere for quiet reflection. Chris, as well as Ken Brameld, took me skiing in places that I had no business going and made it fun. Toshi Takeuchi, Rudy Rico, Arnel Fajardo, Mike Abrams, Dario Veghini, and, ugh, Tom Shields were all great room mates. Ray Porter, my

soccer coach, finally convinced me that I couldn't score a goal to save my life and put me in defense where I finally found my place.

I wouldn't have accomplished anything in the past six years without the work of Pat Anderson, Dian Buchness, Fenton Harvey, Steve Gould, Ruth Brambilia, Rick Gerhart, and Guy Duremburg. They are the people that keep this place running.

Finally I want to thank my parents and grandparents, to whom I have dedicated this thesis. They have provided me with an incredible example of strength, commitment, and faith in the face of adversity. I will spend my life trying to live up to that example.

## ABSTRACT

By applying the concept of "isotopic perturbation of stereochemistry" to a number of Group III metallocene catalysts, further evidence for an  $\alpha$ -agostic interaction in the chain propagation step of Ziegler-Natta polymerization has been obtained. These results are in accord with the "modified Green-Rooney" mechanism. An  $\alpha$ -agostic interaction in the transition state of olefin insertion may contribute to the remarkable stereoselectivities of many Ziegler-Natta catalyst systems since it may restrict the possible orientations of the polymer chain such that it has a more significant impact on the orientation of the inserting olefin.

A new class of Group IV metallocene catalysts is presented for the syndiospecific polymerization of propylene. These catalysts incorporate what are thought to be the key characteristics of syndiospecific metallocene catalysts: Cs symmetry and rigidly linked cyclopentadienyls of greatly differing size. However, preliminary attempts to develop new syndiospecific catalysts have suggested another important characteristic: a pocket in the larger moiety to avoid undesirable steric interactions between the ligand framework and coordinated olefin. In order to accommodate this constraint, a ligand system with a 1,3-dialkylcyclopentadienyl doubly linked to a singly substituted cyclopentadienyl was chosen. Group IV metallocenes with these new ligands, in the presence of a cocatalyst (MAO), react rapidly with neat propylene to form highly syndiotactic polypropylene. This is the first example of a stereospecific doubly bridged olefin polymerization catalyst and is the first example of a highly syndiospecific polymerization catalyst not based on a fluorenyl like ligand. This catalyst system is also very versatile since straightforward changes in the alkyl group of the singly substituted cyclopentadienyl and in the reaction conditions lead to dramatic changes in the polymer microstructure. These catalysts should provide an excellent platform for mechanistic study and may be important industrially.

**TABLE OF CONTENTS**

Dedication.....	ii
Acknowledgment.....	iii
Abstract.....	vi
Table of Contents.....	vii
List of Figures.....	viii
List of Schemes.....	xii
List of Tables.....	xiii
Introduction.....	1
Chapter 1.....	3
Deuterium Isotope Effects as Evidence for $\alpha$ -Agostic Assistance in Ziegler-Natta Catalysis.	
Chapter 2.....	33
The Development of New $C_s$ Symmetric Catalysts for the Syndiospecific Polymerization of $\alpha$ -Olefins.	
Appendix A: $^1\text{H}$ and $^{13}\text{C}$ NMR data.....	104
Appendix B: Crystal Structure Data for $\text{HpZrCl}_2$ .....	120
Appendix C: Crystal Structure Data for $^i\text{PrThpZrCl}_2$ .....	128

## LIST OF FIGURES

## Chapter 1:

Figure 1: Cossee-Arlman mechanism.	6
Figure 2: Modified Green-Rooney mechanism.	6
Figure 3: Possible products of deuterocyclization of <i>trans,trans</i> -1,6- <i>d</i> <sub>2</sub> -1,5-hexadiene.	10
Figure 4: Hydrodimerization of <i>trans</i> -1- <i>d</i> <sub>1</sub> -1-hexene.	10
Figure 5: Transition states for <i>trans</i> -1- <i>d</i> <sub>1</sub> -1-hexene hydrodimerization.	11
Figure 6: Isotopic perturbation of molecular weight of polypropylene.	11
Figure 7: Presumed $\alpha$ -agostic assisted olefin insertion into BpY-R.	16
Figure 8: Two possible transition states for olefin insertion into a metal-alkyl.	19
Figure 9: G. C. analysis of hydrogenation of methylenecyclopentane and hydrocyclization of 1,5-hexadiene.	22
Figure 10: Hyperconjugative transition state for methylenecyclopentane hydrogenation.	22
Figure 11: Hyperconjugative transition state for methylenecyclohexane hydrogenation.	23

## Chapter 2:

Figure 1: Aspecific polymerization with $C_{2v}$ symmetric metallocenes.	36
Figure 2: Isospecific polymerization with $C_2$ symmetric metallocenes.	36
Figure 3: Polymerization with $C_1$ symmetric catalysts.	37
Figure 4: Microstructure of polymer from some $C_1$ symmetric catalysts.	37



Figure 5: Syndiospecific polymerization with $C_s$ symmetric metallocenes.	38
Figure 6: Generic features of syndiospecific systems.	38
Figure 7: Transition state for olefin insertion in isospecific systems.	40
Figure 8: Possible transition states for olefin insertion in syndiospecific systems.	41
Figure 9: Ewen's migratory insertion mechanism.	42
Figure 10: Mechanism of site isomerization.	43
Figure 11: Importance of chirality at the polymer $\beta$ -C.	44
Figure 12: Epimerization mechanism.	45
Figure 13: Target complexes.	46
Figure 14: CyFlCp ( <b>1</b> ) synthesis.	47
Figure 15: Synthesis of (CyFlCp)M-R ( <b>1B</b> , <b>1D</b> ).	47
Figure 16: Reaction of Sc-R with unprotected Cp-H bonds.	48
Figure 17: Proposed BTCp ligands.	49
Figure 18: Distribution of isomers in (BTCp) $R_2SiCl$ .	50
Figure 19: SiMe <sub>3</sub> migrations in deprotonation reactions.	50
Figure 20: Synthesis of HpH <sub>2</sub> ( <b>2</b> ) and K <sub>2</sub> Hp.	51
Figure 21: Synthesis of [HpYCl] <sub>2</sub> ( <b>2B</b> ).	51
Figure 22: Synthesis of HpZrCl <sub>2</sub> ( <b>2A</b> ).	52
Figure 23: <sup>13</sup> C NMR of atactic polypropylene from HpZrCl <sub>2</sub> / MAO.	53
Figure 24: An ORTEP drawing of HpZrCl <sub>2</sub> ( <b>2A</b> ) with 50% probability ellipsoids showing the numbering system.	54

Figure 25: An ORTEP drawing of $\text{HpZrCl}_2$ ( <b>2A</b> ) with 50% ellipsoids showing the asymmetry of the chlorine atoms.	55
Figure 26: Comparison between "pocket" of fluorene and $(\text{TMS})_2\text{Cp}$ .	57
Figure 27: 1,2-disubstituted vs. 1,3 disubstituted Cp ligands.	58
Figure 28: Brintzinger's doubly bridged metallocenes.	59
Figure 29: New ligand design.	60
Figure 30: Proposed transition states for olefin insertion with $\text{C}_s$ symmetric catalysts.	60
Figure 31: Synthetic scheme for doubly bridged ligands.	61
Figure 32: Preparation of 1,3-diisopropylcyclopentadiene.	62
Figure 33: Synthesis of singly bridged ligands.	63
Figure 34: Synthesis of doubly bridged ligands, R'Thp ( <b>3-7</b> ).	63
Figure 35: Ligand <b>3-7</b> names.	64
Figure 36: Deprotonation of R'Thp ( <b>3</b> , <b>5</b> , <b>6</b> , and <b>7</b> ).	64
Figure 37: Deprotonation of $^i\text{PrThp}$ ( <b>4</b> ).	65
Figure 38: Metallation of R'Thp ( <b>3-7</b> ) to form <b>3A-7A</b> .	65
Figure 39: Synthesis of $\text{R'ThpZrCl}_2$ ( <b>3B - 7B</b> ).	66
Figure 40: An ORTEP drawing of $^i\text{PrThpZrCl}_2$ ( <b>4B</b> ) with 50% probability ellipsoids showing the numbering system.	67
Figure 41: An ORTEP drawing of $^i\text{PrThpZrCl}_2$ ( <b>4B</b> ) with 50% probability ellipsoids.	68
Figure 42: Activation of $\text{R'ThpZrCl}_2$ ( <b>3B-7B</b> ) with MAO.	70
Figure 43 and Figure 44: Comparison of <b>4B</b> with Brintzinger's doubly bridged catalysts.	73

Figure 45: Effect of R' on the syndiospecificity of R'ThpZrCl <sub>2</sub> /MAO.	74
Figure 46: Proposed energy profile for C <sub>s</sub> symmetric catalysts (R' = H, <i>i</i> Pr, TMS, <i>t</i> Bu).	75
Figure 47: Proposed transition states for olefin insertion with C <sub>1</sub> symmetric catalysts <b>6B</b> and <b>7B</b> .	76
Figure 48: Proposed energy profile for C <sub>1</sub> symmetric catalysts <b>6B</b> and <b>7B</b> .	78
Figure 49: Proposed microstructure of polymer <b>7a</b> .	79

### Appendix B:

Figure 1: An ORTEP drawing of HpZrCl <sub>2</sub> ( <b>2A</b> ) with 50% probability ellipsoids showing the numbering system.	120
---	-----

### Appendix C:

Figure 1: An ORTEP drawing of <i>i</i> PrThpZrCl <sub>2</sub> ( <b>4B</b> ) with 50% probability ellipsoids showing the numbering system.	128
---	-----

**LIST OF SCHEMES****Chapter 1:**

Scheme 1: Origin of isotopic perturbation of stereochemistry in <i>trans, trans</i> -1,6- <i>d</i> <sub>2</sub> -1,5-hexadiene hydrocyclization.	8
Scheme 2: Hydrocyclization of 1,5-hexadiene with various Group III catalysts.	13
Scheme 3: Origin of isotopic perturbation of stereochemistry in <i>trans, trans</i> -1,7- <i>d</i> <sub>2</sub> -1,6-heptadiene hydrocyclization.	15
Scheme 4: Isotopic perturbation of stereochemistry in the hydrogenation of 2,6- <i>d</i> <sub>2</sub> -methylcyclopentane.	20
Scheme 5: $\beta$ -alkyl elimination?	21

**LIST OF TABLES:****Chapter 1:**

Table 1: Product ratios for various substrates with Group III catalysts.	18
Table 2: Product ratios for methylenecycloalkane hydrogenation with various catalysts.	24

**Chapter 2:**

Table 1: Some $C_s$ symmetric polymerization catalysts.	39
Table 2: Selected bond distances and angles for $HpZrCl_2$ ( <b>2A</b> ).	56
Table 3: Selected bond distances and angles for $^iPrThpZrCl_2$ ( <b>4B</b> ).	69
Table 4: Polymerization data for catalysts <b>3B-7B</b> .	71
Table 5: Comparison of polypropylene <b>3c</b> (from $ThpZrCl_2$ , ( <b>3B</b> )/ MAO) with polypropylene from $(^iPrFlCp)ZrCl_2$ / MAO.	72
Table 6: $^{13}C$ NMR data for polymers <b>3a-7d</b> .	72

**Appendix A:**

Table 1: $^1H$ and $^{13}C$ NMR data.	104
---------------------------------------	-----

**Appendix B:**

Table 1: Crystal and intensity collection data for $HpZrCl_2$ .	122
Table 2: Final heavy atom parameters for $HpZrCl_2$ .	123
Table 3: Complete distances and angles for $HpZrCl_2$ .	125

**Appendix C:**

Table 1: Crystal and intensity collection data for $i\text{PrThpZrCl}_2$ .	130
Table 2: Final heavy atom parameters for $i\text{PrThpZrCl}_2$ .	131
Table 3: Complete distances and angles for $i\text{PrThpZrCl}_2$ .	133

## INTRODUCTION

This thesis will describe the motivation, results, and ramifications of my research during my graduate studies at Caltech. The unifying theme of this thesis is the study of the mechanism of Ziegler-Natta polymerization of olefins. Ziegler-Natta polymerization is practiced on an enormous scale industrially and is the subject of volumes of academic research, but a number of mechanistic questions remain. The two chapters of this thesis address the mechanistic questions associated with Ziegler-Natta catalysts in different ways, but the goal of furthering the understanding of these systems is a constant throughout.

The first chapter of this thesis has a narrow focus and is dedicated almost exclusively to the issue of  $\alpha$ -agostic interactions in the carbon-carbon bond forming step of Ziegler-Natta reactions.  $\alpha$ -agostic interactions have been proposed to lower the transition state energy of carbon-carbon bond formation as well as playing a role in the incredibly high stereoselectivity of Ziegler-Natta catalysts. Since the current evidence regarding  $\alpha$ -agostic interactions is contradictory, chapter 1 presents an effort to look at different catalyst systems to further study the generality of  $\alpha$ -agostic interactions in Ziegler-Natta catalyst systems. Chapter 1 also presents an interesting side note which is a brief study of an unrelated isotope effect observed in a control experiment.

Chapter 2 is focused specifically on the syndiospecific polymerization of  $\alpha$ -olefins. The initial goal, which has evolved throughout this work, was to develop group III model complexes to study the mechanism of syndiospecific polymerization of  $\alpha$ -olefins. However, since the preparation of simple model complexes based on existing ligands was quite challenging and ultimately unsuccessful, I set out to develop new syndiospecific catalysts that would be more amenable to model studies. Therefore, in the process of trying to understand the mechanism of these reactions, the focus shifted more toward trying to understand the key characteristics of syndiospecific catalysts. The understanding which was gained through the failures of several different approaches facilitated the development of a new class of catalysts for syndiospecific polymerizations. Since this discovery came near the end of my time at Caltech, I have only been able to begin the process of using these new catalysts to study the mechanism of syndiospecific polymerization. However,

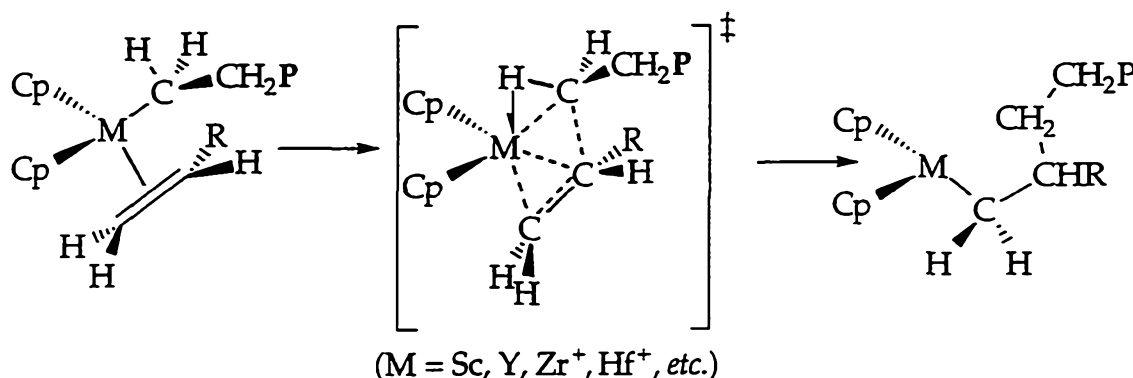
the preliminary results suggest a number of important experiments which should provide answers to many of the mechanistic questions regarding syndiospecific polymerization and Ziegler-Natta catalysts in general. This work is currently being pursued by a group of clever and enthusiastic people who will undoubtedly answer many of the questions that I could not.



**CHAPTER 1**  
**DEUTERIUM ISOTOPE EFFECTS AS EVIDENCE FOR  $\alpha$ -AGOSTIC**  
**ASSISTANCE IN ZIEGLER-NATTA CATALYSIS.**

**Abstract:**

By applying the concept of "isotopic perturbation of stereochemistry" to different Group III catalysts, further evidence for an  $\alpha$ -agostic interaction in the chain propagation step of Ziegler-Natta polymerization has been obtained. These results are in accord with the "modified Green-Rooney" mechanism as shown below.



An  $\alpha$ -agostic interaction in the transition state of olefin insertion may contribute to the remarkable stereoselectivities of many Ziegler-Natta catalyst systems since it may restrict the possible orientations of the polymer chain such that it has a more significant impact on the orientation of the inserting olefin.

During the course of this work, a different isotope effect was observed in the hydrogenation of labelled methylenecycloalkanes with a scandium catalyst. It is proposed that this other effect is a result of a hyperconjugative transition state for methylenecycloalkane insertion into an M-H bond. These results provide support for the idea that the transition state of these catalysts is polarized with positive charge buildup at the  $\beta$ -carbon of the inserting olefin.

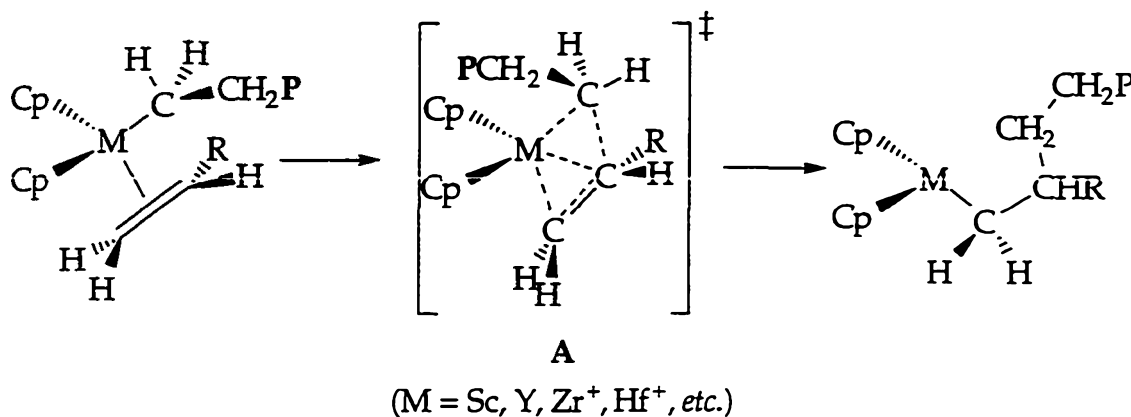
I. Introduction.....	5
Part 1. $\alpha$ -Agostic Assistance in Ziegler-Natta Catalysis.	
II. Results and Discussion.....	12
III. Conclusions from Part 1.....	18
Part 2. A hyperconjugative isotope effect in the hydrogenation of methylenecycloalkanes.	
IV. Results and Discussion.....	19
V. Conclusions from Part 2.....	25
Experimental Section.....	26
References and Notes.....	30

## I. Introduction

Ziegler-Natta polymerization of ethylene, propylene and copolymerization of ethylene with  $\alpha$ -olefins are practiced on enormous scales, yet only recently have organometallic chemists turned their attention to catalyst structure and the mechanisms of these remarkable processes.<sup>1-5</sup> Initial attempts to study the mechanism of these systems were hampered by the heterogeneous, ill defined nature of the catalyst systems. However, the development of homogenous, readily characterized metallocene catalysts has provided an unprecedented opportunity to examine the relationships between catalyst structure, activity and polymer microstructure.

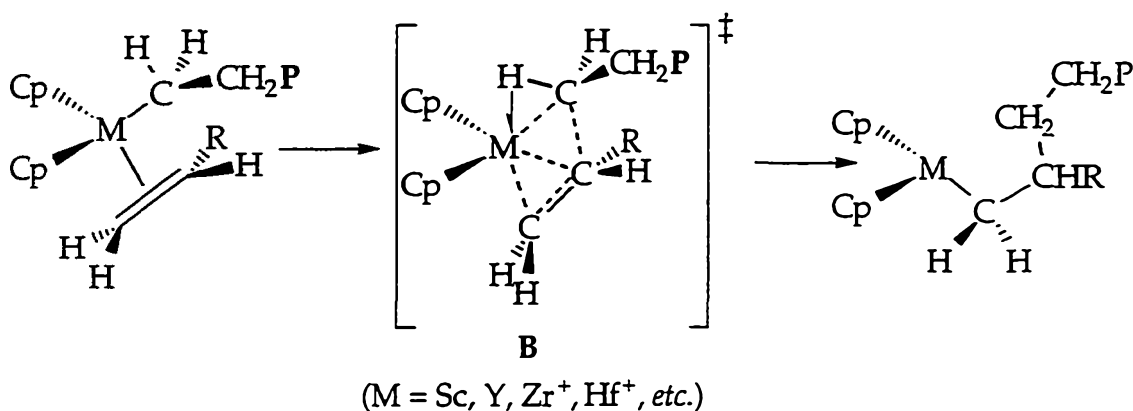
Most of these catalysts<sup>6</sup> share a common structural framework and electronic configuration:  $[\text{Cp}'_2\text{M-R}]^+$  ( $\text{Cp}'$  = cyclopentadienyl or variously substituted cyclopentadienyl;  $\text{M} = \text{Ti, Zr, Hf, Th}$ ;  $\text{R} = \text{H, alkyl}$ ) and  $\text{Cp}'_2\text{M-R}$  ( $\text{M} = \text{Sc, Y, lanthanide element}$ ). An empirical observation has been made: olefin insertion into the metal-carbon bond of these metallocene alkyls appears to require *two* vacant orbitals. Thus, even though they possess a vacant orbital for coordination of the in-coming olefin, the 16-electron alkyls, *e.g.*,  $(\eta^5\text{-C}_5\text{H}_5)_2\text{Zr}(\text{CH}_3)_2$ , are unreactive toward ethylene. The 14-electron analogs, *e.g.*,  $[(\eta^5\text{-C}_5\text{H}_5)_2\text{Zr-CH}_3]^+$ , react readily, even at low temperatures. The net positive charge undoubtedly contributes to the higher reactivity of the latter; however, neutral 14-electron  $(\eta^5\text{-C}_5\text{Me}_5)_2\text{M-CH}_3$  ( $\text{M} = \text{Sc, Y, lanthanide}$ ) also readily undergo ethylene insertion, even at  $-80^\circ\text{C}$ . Thus, the major factor responsible for increased reactivity appears to be the availability of a second vacant metal orbital.<sup>7</sup>

The Cossee-Arlman mechanism,<sup>8,9</sup> with transition state A as shown in figure 1, does not account for the apparent requirement of two vacant orbitals as only one orbital is required for olefin insertion.



**Figure 1: Cossee-Arlman mechanism.**

The modified Green-Rooney mechanism,<sup>10-12</sup> on the other hand, offers a possible explanation for the requirement of a vacant orbital in addition to that of coordinating the in-coming olefin since it invokes an  $\alpha$ -agostic interaction as shown in transition state **B** in figure 2.



**Figure 2: Modified Green-Rooney mechanism.**

Almost all of the experiments designed to probe for  $\alpha$ -agostic interactions in Ziegler-Natta catalysts are based on the original concept of "isotopic perturbation of stereochemistry"<sup>13</sup> introduced by Grubbs and co-workers. According to the modified Rooney-Green mechanism, placement of a single deuterium at the  $\alpha$  carbon of the alkyl could have a stereochemical outcome in forming the C-C bond if the insertion occurs with either a preferential cis or a preferential trans (as shown in **B**) arrangement of the alkyl ( $\text{CH}_2\text{P}$ ) and  $\alpha$ -olefin substituent (R) and the vibrational force

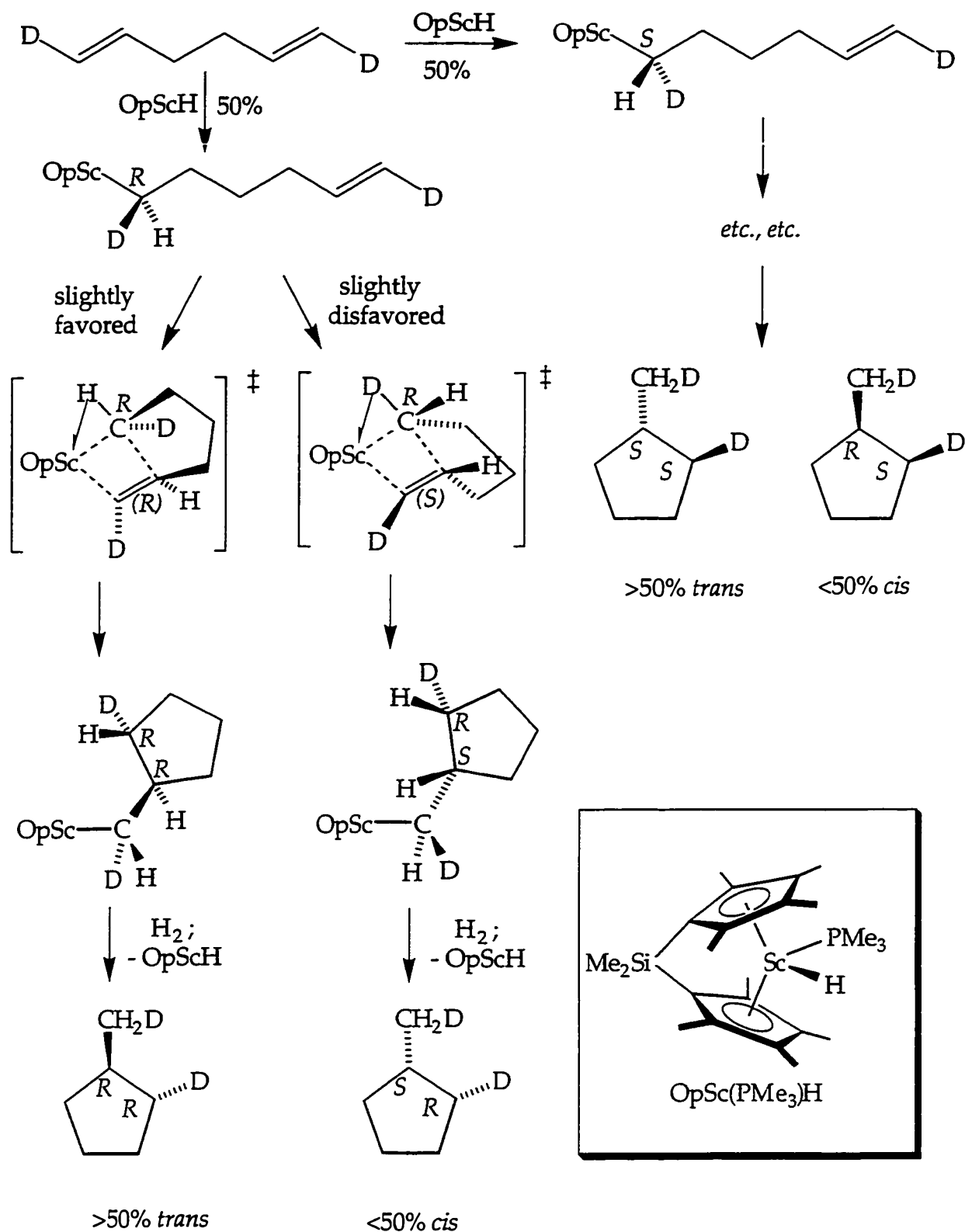
constants for the agostic and terminal  $\alpha$  C-H bonds are sufficiently different in transition state **B**.

Coordination of a C-H bond to an electrophilic metal center may considerably reduce  $\nu(\text{C-H})$  and  $\delta(\text{C-H})$  in stable structures.<sup>10,11,14,15</sup> In the case of a methyl-bridged trimer with  $[\text{Os}(\mu_2\text{-CHDR})\text{Os}]$  ( $\text{R} = \text{H}, \text{D}$ ) equilibrium isotope effects favoring coordination of C-H over C-D amount to approximately  $0.13 \text{ kcal}\cdot\text{mol}^{-1}$ , or to an equilibrium isotope effect of  $K_{\text{eq}} = 1.25$  at  $25^\circ\text{C}$ .<sup>16</sup> With strongly electrophilic metal centers, such as active Ziegler-Natta olefin polymerization catalysts, stronger agostic effects may be expected with commensurately greater  $K_{\text{eq}}$ 's.

The amount of this ground state agostic interaction that is realized in transition state **B** may be expected to vary, depending upon conformational restrictions and the energy of **B** relative to that for the reactants (*i.e.*, the activation energy for olefin insertion). Thus, the magnitude of the secondary deuterium kinetic isotope arising from a "modified Rooney-Green" C-C bond forming step *a priori* may be expected to be variable, much like the secondary DKIE's arising from hyperconjugative effects observed for the solvolysis of  $\beta$  deuterated alkyl halides, tosylates, *etc.*<sup>17</sup> A similar explanation has been presented by Grubbs and Coates.<sup>18</sup>

A number of different groups have looked for  $\alpha$ -agostic interactions in the C-C bond forming step of Ziegler-Natta catalysts with mixed results. Bercaw,<sup>19,20</sup> Brintzinger,<sup>21,22</sup> and Stille<sup>23</sup> have all found evidence in support of an  $\alpha$ -agostic transition state consistent with the modified Green-Rooney mechanism. Alternatively, Grubbs<sup>13</sup> and Brintzinger<sup>22</sup> have both found evidence contradictory to an  $\alpha$ -agostic transition state which thus support the more "conventional" Cossee-Arlman mechanism.

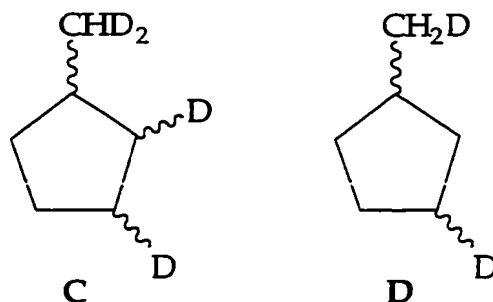
Piers and Bercaw have reported<sup>19</sup> that the  $\text{OpSc}(\text{PMe}_3)\text{H}$ -catalyzed ( $\text{Op} = \{(\eta^5\text{-C}_5\text{Me}_4)_2\text{SiMe}_2\}$ ) hydrocyclization of *trans, trans-1,6-d\_2-1,5-hexadiene* gives rise to a  $1:1.19 \pm 0.04$  ratio of *cis*- and *trans-d\_2*-methylcyclopentanes, implying a maximum  $k_{\text{H}}/k_{\text{D}}$  of 1.19(4) at  $25^\circ\text{C}$ . This number has since been refined to a  $k_{\text{H}}/k_{\text{D}}$  of 1.225 (12) at  $25^\circ\text{C}$  through the use of improved  $^2\text{H}$  NMR techniques.<sup>20</sup> These results provide support for an  $\alpha$ -agostic transition state as shown in scheme 1.



Scheme 1: Origin of isotopic perturbation of stereochemistry in *trans*, *trans*-1,6-*d*<sub>2</sub>-1,5-hexadiene hydrocyclization.

As shown in scheme 1, addition of achiral  $\alpha,\omega$ -diene to achiral OpScH yields precisely a 50:50 mixture of *R*- and *S*-1,6- $d_2$ -5-hexenyl-1-scandium complexes. Due to ring strain there should be a strong preference for *cis* fusion of the pseudo 4,5 ring system in the transition state for olefin insertion.<sup>24,25</sup> Face selection for insertion of the pendent olefin then depends on whether H or D occupies the  $\alpha$ -agostic position. If an  $\alpha$ -agostic interaction assists olefin insertion into the Sc-C bond, the expected preference for H to occupy the bridging position, based on the lower vibrational frequencies for agostic vs. terminal C-H bonds, leads to an excess of the *R,R* (*trans*) (and *S,S* (*trans*)) over the *R,S* (*cis*) (and *S,R* (*cis*)) products. In a similar experiment, a  $(k_H/k_D)_{max} = 1.21 \pm 0.05$  was measured for the corresponding hydrocyclization of 1,7- $d_2$ -1,6-heptadiene to a mixture of *cis*- and *trans*- $d_2$ -methylcyclohexanes.

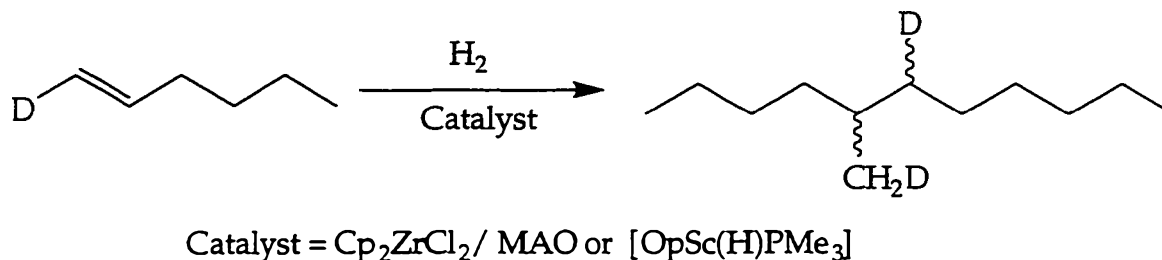
Additional experiments by Bercaw provide further support for the presumption that the partitioning of stereochemistry is due to a kinetic deuterium isotope effect operating at the  $\alpha$  methylene of the [OpScCHDCH<sub>2</sub>CH<sub>2</sub>CH<sub>2</sub>CH=CHD] intermediate (Table 1): (1) the *trans*:*cis* ratio varies in a normal enthalpic manner with temperature [1.07(3):1 at 120°C, 1.225(12):1 at 25°C, 1.26(3):1 at -10°C]; (2) hydrocyclization of *cis,cis*-1,6- $d_2$ -1,5-hexadiene affords a ratio of 1.179(6):1, indicating that insertion of pendant olefin is not influenced by the geometry about its double bond; (3) *trans*-1- $d_1$ -1,5-hexadiene gives the same *trans*:*cis* ratio of 1.258(2):1 with the single deuterium partitioned equally (<sup>2</sup>H NMR) between the methyl and ring positions of the  $d_1$ -methylcyclopentane product; (4) deuterocyclization of *trans,trans*-1,6- $d_2$ -1,5-hexadiene yields tetradeutero-methylcyclopentane **C** with *trans,trans* to *cis,cis* ratio of products equal to 1.14(1):1 (Figure 3).



**Figure 3: Possible products of deuterocyclization of *trans,trans*-1,6-*d*<sub>2</sub>-1,5-hexadiene.**

Deuterocyclization of *cis,cis*-1,6-*d*<sub>2</sub>-1,5-hexadiene affords **C** with *trans,cis* to *cis,trans* ratio of products of 1.20(1):1; (5) deuterocyclization of 1,5-hexadiene yields **D** with less than 2% deuterium incorporation at the tertiary (1 position), indicating that  $\beta$  H elimination does not compete with hydrogenation of the (cyclopentylmethyl)scandium intermediate.

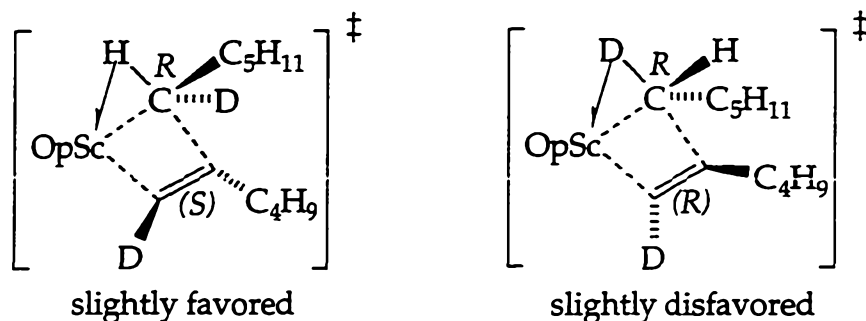
An acyclic version of Grubbs' original experiment has been performed by Brintzinger<sup>22</sup> with zirconium catalysts and by Bercaw<sup>19,20</sup> with scandium catalysts as shown in figure 4.



**Figure 4: Hydrodimerization of *trans*-1-*d*<sub>1</sub>-1-hexene.**

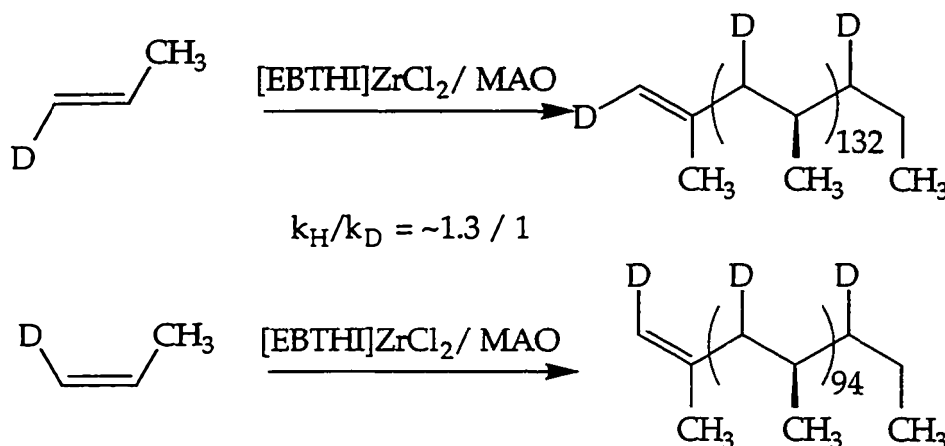
Brintzinger obtained a  $(k_H/k_D)_{max} = 1.30(3): 1$  for the hydrodimerization of *trans*-1-*d*<sub>1</sub>-1-hexene with Cp<sub>2</sub>ZrCl<sub>2</sub>/MAO to a mixture of *erythro*- and *threo*-5-methyl,6-*d*<sub>2</sub>-5-methylundecanes and Bercaw observed a similar ratio of 1.27(1):1 for the same experiment except with OpSc(PMe<sub>3</sub>)H as the catalyst. Once again, the excess stereoisomer may be rationalized on the basis of the favored transition state with H occupying the  $\alpha$ -agostic position and alkyl substituents in the sterically preferred anti arrangement,<sup>26</sup> as shown below.





**Figure 5: Transition states for *trans*-1-*d*<sub>1</sub>-1-hexene hydrodimerization.**

Brintzinger has also observed a deuterium isotope effect in the molecular weight of polypropylene obtained from the polymerization of *E* and *Z* propylene with ethylenebis(tetrahydroindenyl)zirconiumdichloride/MAO<sup>21</sup> as shown in figure 6.



**Figure 6: Isotopic perturbation of molecular weight of polypropylene.**

All of these experiments discussed above provide support for an  $\alpha$ -agostic transition state as described by the modified Green-Rooney mechanism.

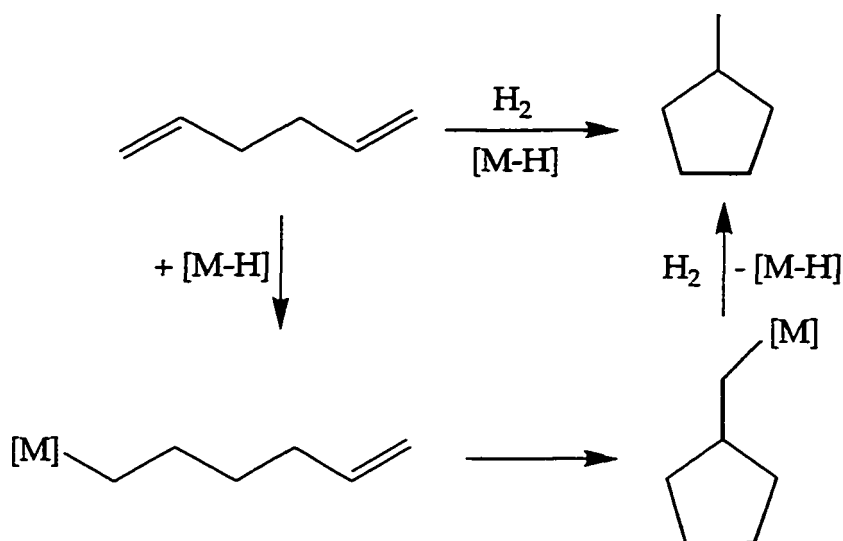
There is also substantial evidence which contradicts the notion of an  $\alpha$ -agostic transition state. In Grubbs' original report,<sup>13</sup> no isotopic perturbation of stereochemistry was observed for the Lewis-acid promoted cyclization of  $(\eta^5\text{-C}_5\text{H}_5)_2\text{Ti}(\text{Cl})(\text{CHDCH}_2\text{CH}_2\text{CH}_2\text{CH}=\text{CH}_2)$ . Also, Brintzinger has reported that no kinetic deuterium isotope effect accompanies the hydrocyclization of 1,6-*d*<sub>2</sub>-1,5-hexadiene using the zirconocene dichloride/methylaluminumoxane catalyst system.<sup>22</sup> Even those using computational methods to probe for  $\alpha$ -agostic assistance have reached differing conclusions: it is supported by some recent calculations,<sup>27-29</sup> but not others.<sup>30,31</sup>

In view of these seeming ambiguities concerning whether or not  $\alpha$ -agostic assistance is a general feature of chain propagation for Ziegler-Natta polymerization of olefins, it is clear that additional experiments are necessary. This work will be directed at further probing the generality and importance of  $\alpha$ -agostic interactions in Ziegler-Natta catalyst systems. Part 1 will describe the study of  $\alpha$ -agostic interactions in other organoscandium and organoyttrium catalysts using the stereochemical probe developed by Grubbs. Part 2 will describe the study of an isotope effect which was observed during the course of some control experiments involving the hydrogenation of labeled methylenecyclopentane with  $\text{OpSc}(\text{PMe}_3)\text{H}$ .

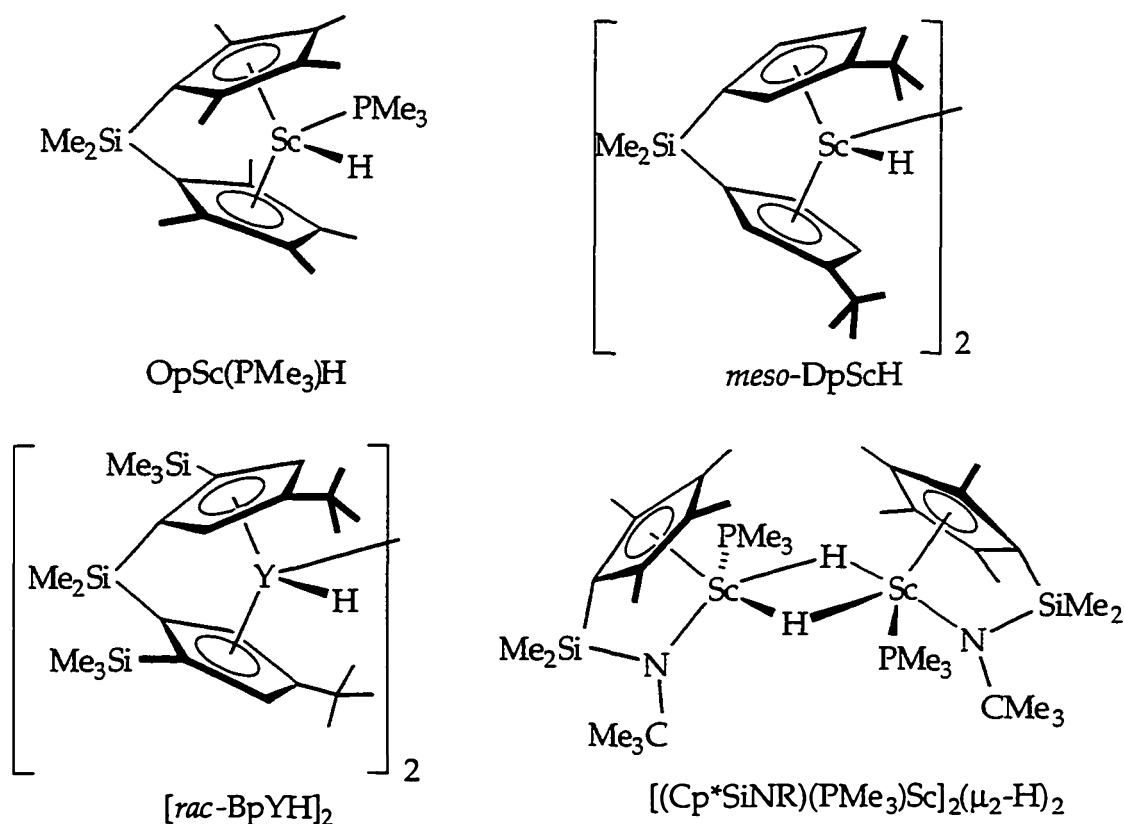
### **Part 1: $\alpha$ -Agostic Assistance in Ziegler-Natta Catalysis.**

#### **II. Results and Discussion:**

In addition to  $\text{OpSc}(\text{PMe}_3)\text{H}$ , a variety of organoscandium and organoyttrium hydrides are effective catalysts for the hydrocyclization of 1,5-hexadiene, effecting several hundred turnovers. By using *trans,trans*-1,6- $d_2$ -1,5-hexadiene as substrate and examining the *trans*:*cis* ratio of dideutero-methylcyclopentanes, *i.e.*, the stereochemical probe described by Grubbs and coworkers,<sup>13</sup> "deuterium isotopic perturbation of stereochemistry," has been adapted to the catalyst systems shown in scheme 2.



([M-H] =  $\text{OpSc}(\text{PMe}_3)\text{H}$ ,  $\text{meso-DpScH}$ ,  $[\text{BpYH}]_2$ ,  $(\text{Cp}^*\text{SiNR})(\text{PMe}_3)\text{ScH}$ )

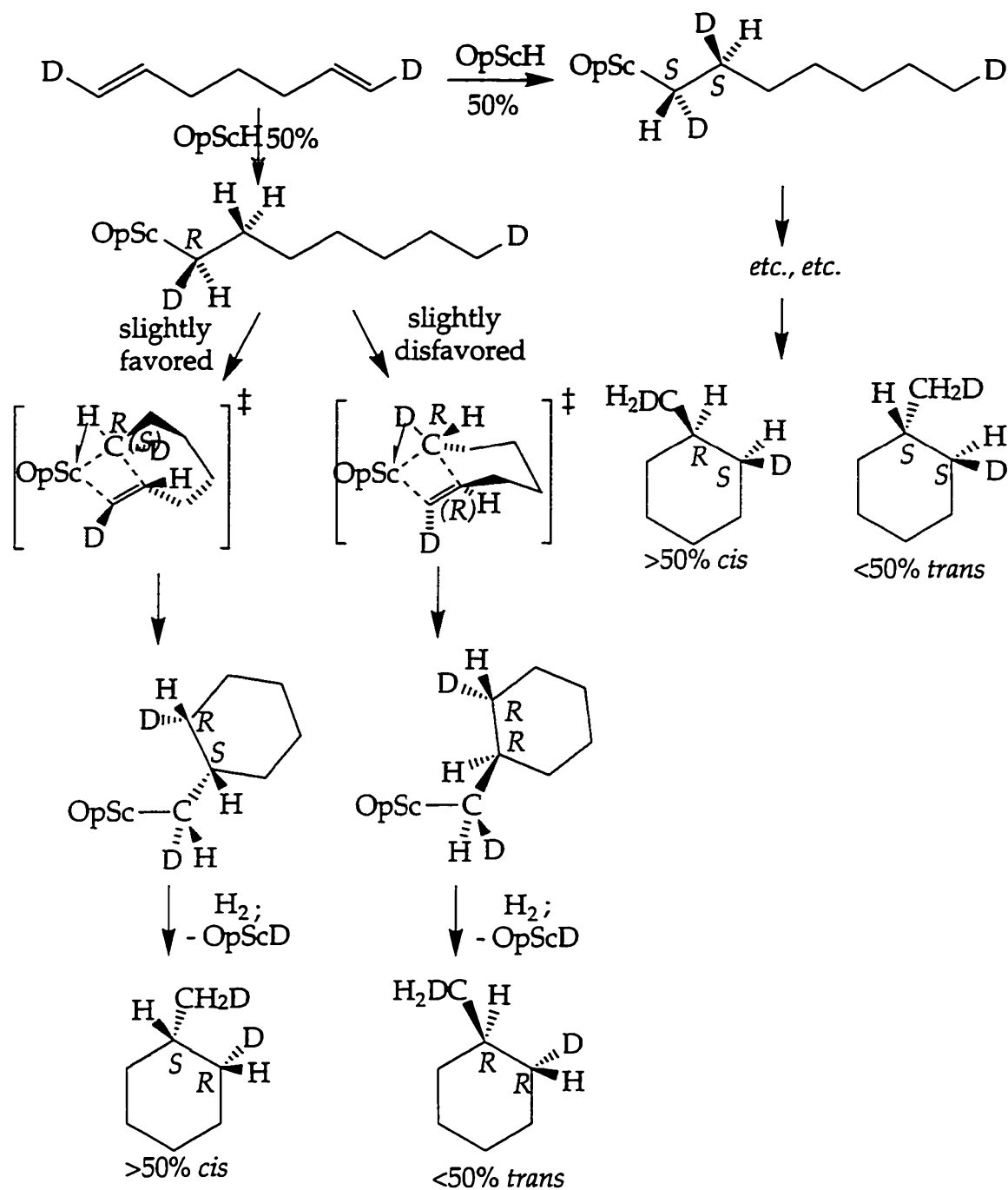


**Scheme 2: Hydrocyclization of 1,5-hexadiene with various Group III catalysts.**

Isotopic perturbation of stereochemistry, in support of an  $\alpha$ -agostic transition state, is observed for the hydrocyclization (25°C) of deuterated 1,5-hexadienes with these other catalysts as well:  $[\text{DpScH}]_2$  hydrocyclizes

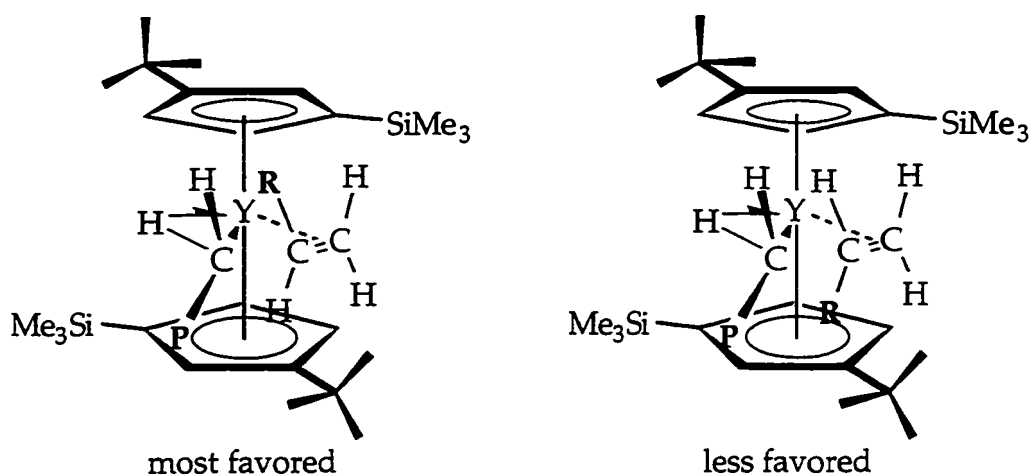
*trans,trans-1,6-d<sub>2</sub>-1,5-hexadiene* to a mixture of *trans*- and *cis-d<sub>2</sub>*-methylcyclopentanes (61%) (trans:cis = 1.203(7):1) and *1,6-d<sub>2</sub>-n-hexane* (39%),<sup>32</sup> [(Cp\*SiNR)(PMe<sub>3</sub>)Sc]<sub>2</sub>(μ-H)<sub>2</sub> produces *trans*- and *cis-d<sub>2</sub>*-methylcyclopentanes (98%) (trans:cis = 1.209(15):1) and *1,6-d<sub>2</sub>-n-hexane* (2%).

Further evidence for α-agostic assistance in the transition state for C-C bond formation with these scandium catalysts has been obtained for the related hydrocyclization of 1,6-heptadiene and for the hydrodimerization of α-olefins. Although acyclic hydrogenation competes more effectively with hydrocyclization for longer chain α,ω-dienes, reaction of *trans,trans-1,7-d<sub>2</sub>-1,6-heptadiene* with OpSc(PMe<sub>3</sub>)H under an H<sub>2</sub> atmosphere yields *1,7-d<sub>2</sub>-n-heptane* (ca. 40%) and a 1:1.12(1) mixture of *trans*- and *cis-d<sub>2</sub>*-methylcyclohexane (ca. 60%). The reversal of the trans:cis ratio for the methylcycloalkane product is consistent with the expectation that face selectivity for pendant olefin approach would be opposite to that for formation of the five-membered ring. The developing six-membered ring adopts a chair-like conformation, and the pseudo bicyclic transition state is now trans fused. Thus, as shown in scheme 3, preferential H in the α-agostic position leads to the cis isomer.



**Scheme 3: Origin of isotopic perturbation of stereochemistry in *trans, trans*-1,7-*d*<sub>2</sub>-1,6-heptadiene hydrocyclization.**

Deuterium isotopic perturbation of stereochemistry is also indicated by some preliminary experiments for the highly iso-specific catalyst system derived from  $[\text{BpY}]_2(\mu\text{-H})_2$ .<sup>33</sup> Using *rac*- $[\text{BpYH}]_2$  as catalyst, hydrocyclization of *trans,trans*-1,6-*d*<sub>2</sub>-1,5-hexadiene yields a 1:1.28(1) *trans*:*cis* ratio of *d*<sub>2</sub>-methylcyclopentanes, whereas with *cis,cis*-1,6-*d*<sub>2</sub>-1,5-hexadiene a *non*-reciprocal ratio of 1.54(1):1 is obtained. Deuterocyclization of 1,5-hexadiene with  $[\text{BpY}]_2(\mu\text{-H})_2$  yields a 1.40(1):1 ratio of *trans*:*cis* 3-*d*<sub>1</sub>-methyl-*d*<sub>1</sub>-cyclopentane, approximately the geometric mean (1.40(1)) of these *trans*:*cis* ratios. As discussed by Brintzinger and Krauledat,<sup>22</sup> such deviations from mutual reciprocity may be taken as evidence of  $\alpha$ -agostic stabilization of the transition state for C-C bond formation. Whereas application of the test for deuterium isotopic perturbation of stereochemistry for chiral catalysts is less straightforward than for achiral ones due to the simultaneous operation of enantiofacial selectivity of the ligand system and the  $\alpha$ -agostic influence, these preliminary results do suggest the  $\alpha$ -agostic transition states for the BpY-R catalysts system shown in figure 7:


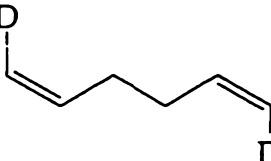
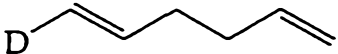

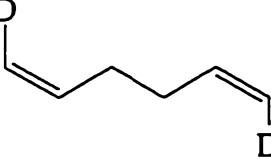
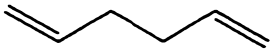









**Figure 7: Presumed  $\alpha$ -agostic assisted olefin insertion into BpY-R.**

In the case of  $C_2$  symmetric isospecific catalysts like  $[\text{BpYH}]_2$ , an  $\alpha$ -agostic interaction may serve two different roles in controlling the properties of the resulting polymers. First of all, the interaction may lower the transition energy required for olefin insertion as suggested by calculations.<sup>27-29</sup> By lowering the energy of olefin insertion relative to error mechanisms and chain termination steps such as  $\beta$ -H elimination, enantioselectivity and molecular weight may be improved. Secondly, the  $\alpha$ -agostic interaction may

serve to orient the two remaining substituents on the  $\alpha$  carbon toward the cyclopentadienyl rings. The preferred orientation should be such that the smaller hydrogen atom of the growing alkyl is directed toward the *tert*-butyl group of the upper ring, while the larger polymer fragment, P, is pointed into the open region between the *tert*-butyl and trimethylsilyl groups of the lower ring. The cooperative effects of the substitution pattern of the Bp ligand in conjunction with the  $\alpha$ -agostic interaction thus provide an attractive explanation of the remarkable iso-specificity<sup>34</sup> of the BpY-R catalyst system.

The table below summarizes the observed ratio of products for a number of different substrates with four different Group III catalysts. Each of these experiments described in table 1 shows an isotopic perturbation of stereochemistry in support of an  $\alpha$ -agostic transition state for olefin insertion.

substrate	catalyst	trans:cis ratio
	OpSc(PMe <sub>3</sub> )H/H <sub>2</sub>	1.225(12):1
	OpSc(PMe <sub>3</sub> )H/H <sub>2</sub>	1.179(6):1
	OpSc(PMe <sub>3</sub> )H/H <sub>2</sub>	1.258(2):1
	OpSc(PMe <sub>3</sub> )H/D <sub>2</sub>	1.14(1):1
	OpSc(PMe <sub>3</sub> )H/D <sub>2</sub>	1.20(1):1
	OpSc(PMe <sub>3</sub> )H/D <sub>2</sub>	1.07(2):1
	[DpScH] <sub>2</sub> /H <sub>2</sub>	1.203(7):1
	(Cp*SiNR)Sc(PMe <sub>3</sub> )H/H <sub>2</sub>	1.209(15):1
	[BpYH] <sub>2</sub> /H <sub>2</sub>	1:1.28(1)
	[BpYH] <sub>2</sub> /H <sub>2</sub>	1.54(1):1
	[BpYH] <sub>2</sub> /D <sub>2</sub>	1.40(1):1
	OpSc(PMe <sub>3</sub> )H/D <sub>2</sub>	1.27(1):1
	OpSc(PMe <sub>3</sub> )H/H <sub>2</sub>	1:1.12(1)

**Table 1: Product ratios for various substrates with Group III catalysts.**

**III. Conclusions from Part 1:** These results provide further evidence for the "modified Green-Rooney" pathway<sup>10-12</sup> for chain propagation with these Ziegler-Natta systems. Moreover, they suggest a rationale for the apparent requirement that active *bis*(cyclopentadienyl)metal catalysts be 14-electron alkyl derivatives with two vacant orbitals: one to accommodate the incoming olefin, another for the  $\alpha$ -agostic interaction. Thus, transition state



II, rather than transition state I, as shown in figure 8, is supported by our results.

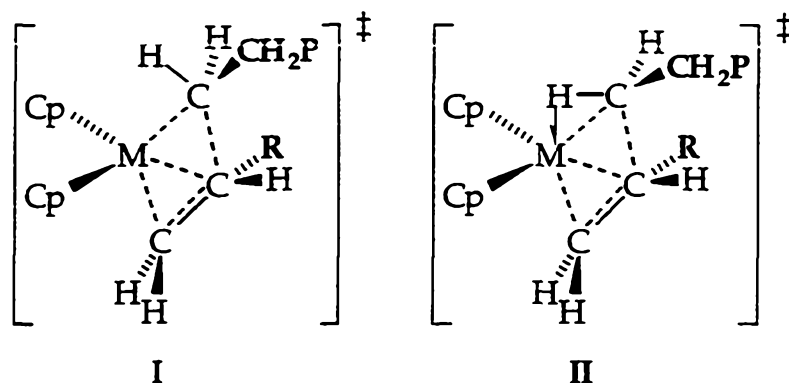


Figure 8: Two possible transition states for olefin insertion into a metal-alkyl.

The  $\alpha$ -agostic interaction in the transition state of olefin insertion may be responsible for the remarkable stereoselectivities of many Ziegler-Natta catalyst systems since it may restrict the possible orientations of the polymer chain such that it has a more significant impact on the orientation of the inserting olefin.

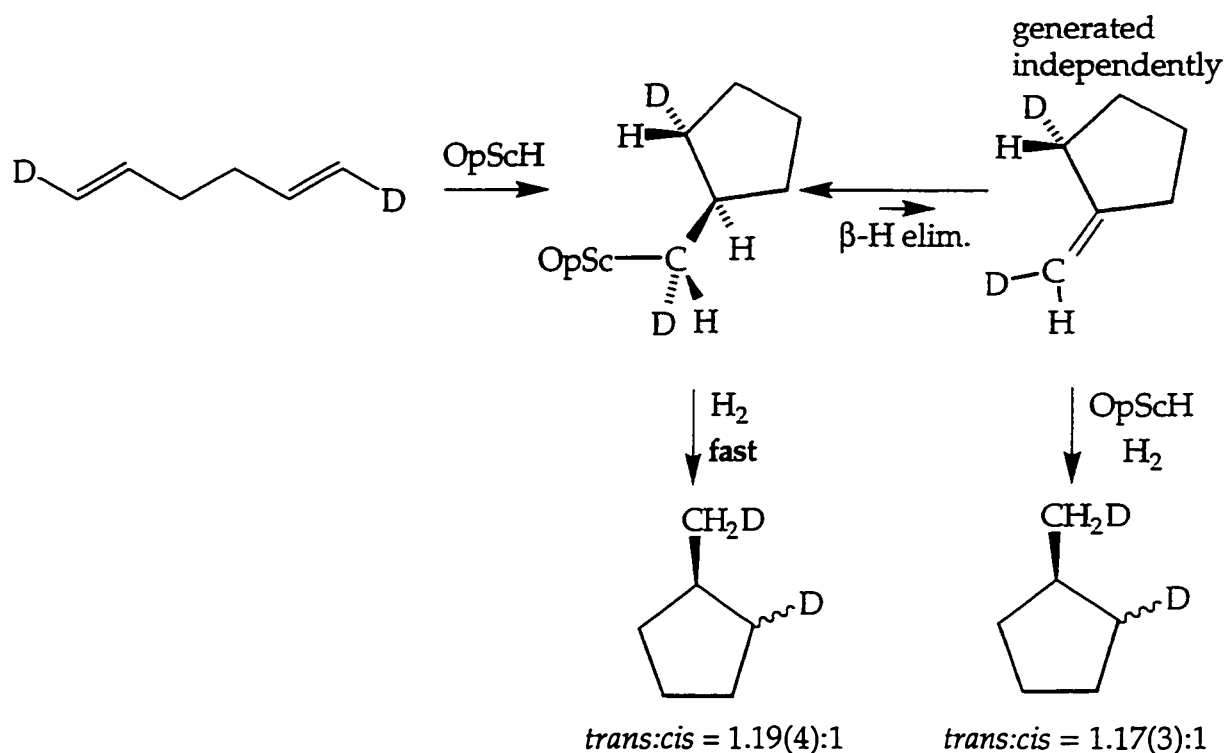
On the other hand, the stereochemical test devised by Grubbs has not always supported an  $\alpha$ -agostic transition state. Indeed, his group found no isotopic perturbation of stereochemistry for the Lewis acid-promoted cyclization of  $\text{Cp}_2\text{Ti}(\text{Cl})\text{CHDCH}_2\text{CH}_2\text{CH}_2\text{CH}=\text{CH}_2$ . Brintzinger and Krauledat likewise found a *trans*:*cis* ratio of 1.01(2):1 for the hydrocyclization of *trans,trans*-1,6- $d_2$ -1,5-hexadiene with the  $\text{Cp}_2\text{ZrCl}_2/\text{MAO}$  catalyst system. These findings could be taken as evidence that  $\alpha$ -agostic assistance is not always required for C-C bond formation and may implicate transition state I in figure 8.

## Part 2. A hyperconjugative isotope effect in the hydrogenation of methylenecycloalkanes.

### IV. Results and Discussion:

In the process of carrying out some control experiments, Köhn made an interesting discovery.<sup>20</sup> Originally it was assumed that 2,6- $d_2$ -methylenecyclopentane, the presumed product of  $\beta$ -H elimination from  $\text{OpSc}(\text{PMe}_3)\text{CHD}(\text{C}_5\text{H}_8\text{D})$ , would be hydrogenated to 2,6- $d_2$ -

methylcyclopentane without any isotope effect and thus the diastereomeric ratio of the final product mixture would not be affected significantly if  $\beta$ -H elimination occurred. It has been shown<sup>35</sup> that  $\beta$ -H elimination is not competitive with the intramolecular insertion, so this point should have limited relevance to the issue of  $\alpha$ -agostic interactions. However, the hydrogenation of 2,6- $d_2$ -methylene-cyclopentane by  $\text{OpSc}(\text{PMe}_3)\text{H}$  afforded 2,6- $d_2$ -methylcyclopentane in a *trans*:*cis* ratio of 1.17(3):1, a remarkably similar ratio to the product of the hydrocyclization of 1,6-*trans,trans*- $d_2$ -1,5-hexadiene with  $\text{OpSc}(\text{PMe}_3)\text{H}$  (*trans*:*cis* ratio = 1.225(12):1).

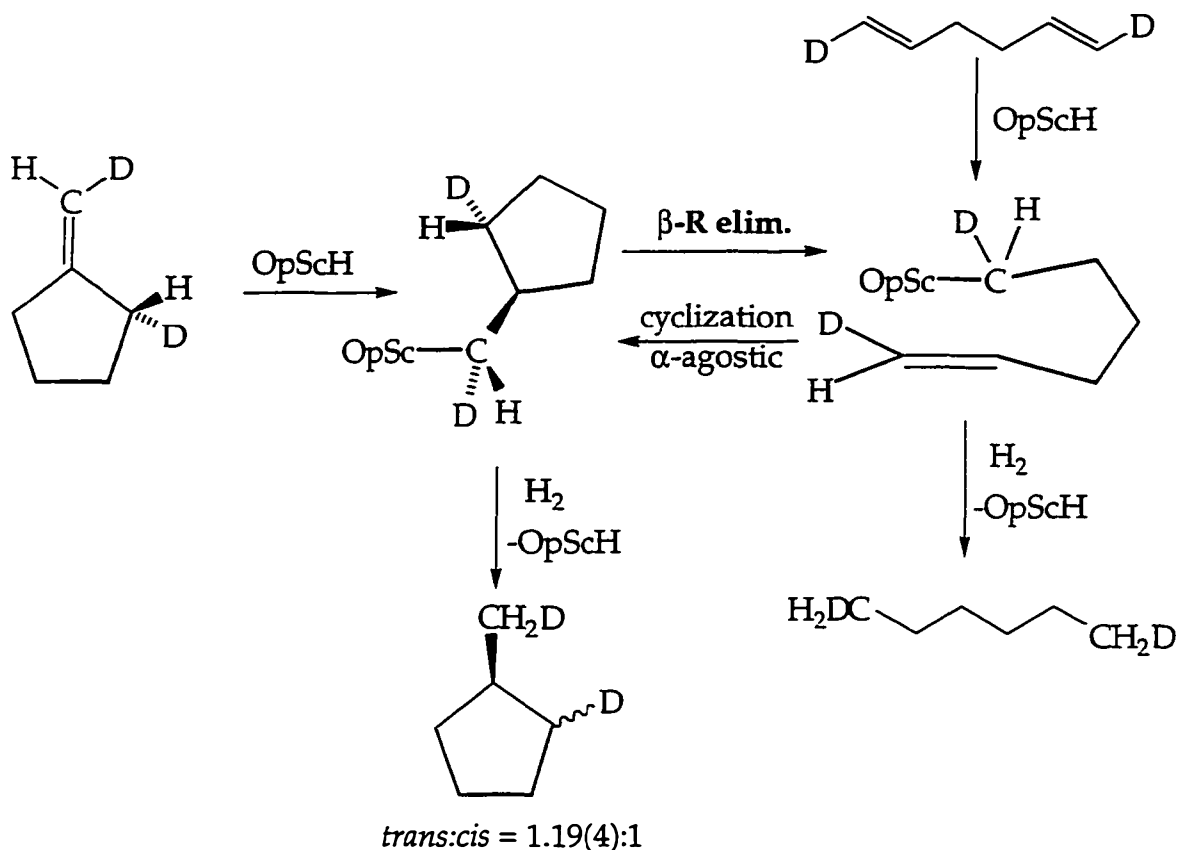


**Scheme 4: Isotopic perturbation of stereochemistry in the hydrogenation of 2,6- $d_2$ -methylcyclopentane.**

A small isotope effect is observed as well for the hydrogenation of 2,6- $d_2$ -methylene-cyclopentane with  $[\text{DpScH}]_2$  (*trans*:*cis* = 1.04(1):1). No such isotope effect is observed for the hydrogenation of 2,6- $d_2$ -methylene-cyclopentane with  $\text{Rh}(\text{PPh}_3)_3\text{Cl}$  (*trans*:*cis* = 0.99(1):1) or with  $\text{Cp}_2\text{ZrHCl}$  (*trans*:*cis* = 1.01(1):1).

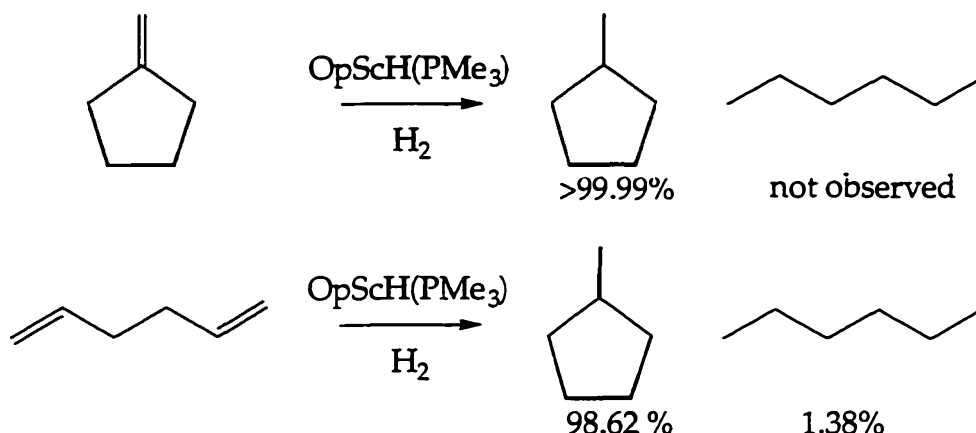
One possibility was that the scandium-methylcyclopentyl complex, formed by insertion of methylene-cyclopentane into a Sc-H bond, could  $\beta$ -alkyl

eliminate to form a scandium alkenyl complex. Insertion of the alkene into the scandium alkyl could then go through an  $\alpha$ -agostic transition state with the same isotope effect as that for hydrocyclization as shown below.



Scheme 5:  $\beta$ -alkyl elimination?

An experiment to test this hypothesis was devised based on the fact that hydrocyclization of 1,5-hexadiene was found to produce a small amount of n-hexane as well as methylcyclopentane. Therefore, if the hexenyl complex was formed in significant quantities in the hydrogenation of methylenecyclopentane, some n-hexane should be formed in addition to the methylcyclopentane. The hydrocyclization of 1,5-hexadiene and the hydrogenation of methylenecyclopentane, both with  $\text{OpSc}(\text{PMe}_3)\text{H}$ , were performed under identical conditions and the products were analyzed by G. C. as shown below.<sup>36</sup>

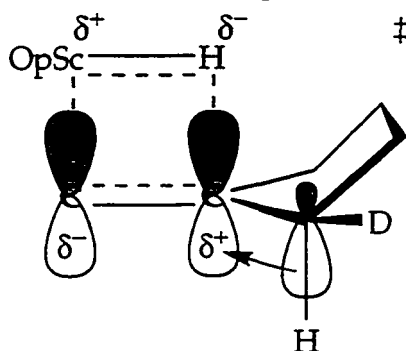


**Figure 9: G. C. analysis of hydrogenation of methylenecyclopentane and hydrocyclization of 1,5-hexadiene.**

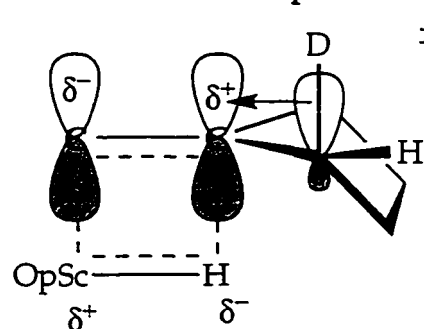
Since no hexane forms during methylenecyclopentane hydrogenation, the hexenyl species is ruled out as an intermediate in this reaction. Therefore, it is assumed that ring opening via  $\beta$ -alkyl elimination does not occur to a significant extent and is thus not responsible for the isotope effect observed in the hydrogenation of 2,6- $\text{d}_2$ -methylenecyclopentane with  $\text{OpSc(PMe}_3\text{)H}$ .

To explain the observed isotope effect for methylenecyclopentane insertion into the Sc-H bond, a  $\beta$ -hyperconjugative transition state is proposed. The effect is observed for scandium presumably due to the positive charge buildup at the  $\beta$ -carbon of the inserted olefin.<sup>14</sup> This positive charge can be stabilized by hyperconjugative donation from the  $\beta$  C-H orbital to the  $\beta$ -C  $\pi$  orbital as shown below.

**I. Favored: *trans* product**



**II. Disfavored: *cis* product**

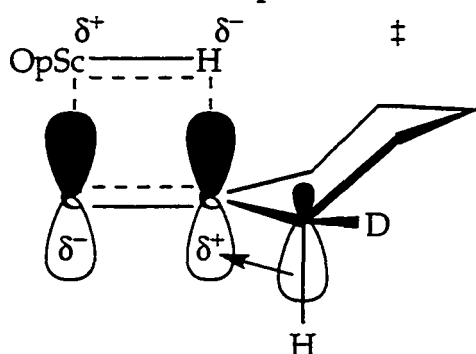


**Figure 10: Hyperconjugative transition state for methylenecyclopentane hydrogenation.**

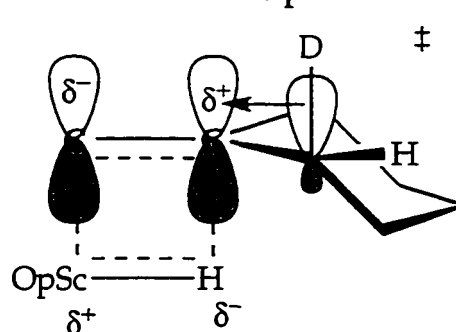
The C-H bond is predicted to stabilize the transition state more than the C-D bond resulting in a preference for transition state I above. Wilkinson's catalyst does not show an effect presumably due to the less polar nature of the transition state of olefin insertion for rhodium.<sup>37</sup> The fact that  $\text{Cp}_2\text{ZrClH}$  is a  $16 e^-$  complex, which may be less polar than the presumed  $14 e^-$   $\text{OpScH}$ , may be the reason that no effect is observed in that case.

Further support for a  $\beta$ -hyperconjugative mechanism in the hydrogenation of methylenecycloalkane hydrogenation is provided by the hydrogenation of  $2,7-d_2$ -methylene cyclohexane with  $\text{OpSc}(\text{PMe}_3)\text{H}$ . Based on our proposed  $\alpha$ -agostic and  $\beta$ -hyperconjugative transition states,  $2,7-d_2$ -methylene cyclohexane hydrogenation with  $\text{OpSc}(\text{PMe}_3)\text{H}$  is predicted to yield the opposite ratio of diastereomers than *trans,trans*- $1,7-d_2$ - $1,6$ -heptadiene hydrocyclization. As predicted for a  $\beta$ -hyperconjugative transition state, the hydrogenation of  $2,7-d_2$ -methylene cyclohexane with  $\text{OpSc}(\text{PMe}_3)\text{H}$  yielded  $1,7-d_2$ -methylcyclohexane with an excess of the *trans* diastereomer (*trans*:*cis* = 1.078(4):1) which is in contrast to the *trans*:*cis* ratio of 1:1.12(1) observed for *trans,trans*- $1,7-d_2$ - $1,6$ -heptadiene hydrocyclization with  $\text{OpSc}(\text{PMe}_3)\text{H}$ .

### I. Favored: *trans* product



### II. Disfavored: *cis* product



**Figure 11: Hyperconjugative transition state for methylenecyclohexane hydrogenation.**

Again, the favored transition state has a  $\beta$  C-H bond available for hyperconjugative donation to the  $\beta$ -C of the inserting olefin. Since the observed effect for methylenecyclohexane hydrogenation is the opposite of the effect for  $1,6$ -heptadiene hydrocyclization, we conclude that this  $\beta$ -hyperconjugative effect is different than the  $\alpha$ -agostic isotope effects. In the case of *5-methylene,6,12-d\_2*-undecane hydrogenation with  $\text{OpSc}(\text{PMe}_3)\text{H}$ , no isotopic perturbation of stereochemistry is observed. This also is in contrast

to the hydrodimerization of 1-*d*<sub>1</sub>-1-hexene with  $\text{OpSc}(\text{PMe}_3)\text{H}$  to form 5-methyl,6,12-*d*<sub>2</sub>-undecane in which there is a erythro:threo ratio of 1.27:1. The magnitude of the observed  $\beta$ -hyperconjugative effect appears to correlate with the rigidity of the ring system. In the case of methylenecyclopentane, the 5 membered ring must fix the orbitals in such a way to provide good overlap. With less strained rings and with acyclic systems, the  $\beta$ -C will be increasingly free to rotate such that the 6 membered ring of methylenecyclohexane has only a small effect and the acyclic case, 5-methylenundecane, results in no observable isotope effect. A table of methylenecycloalkane hydrogenation with different catalysts is shown below.

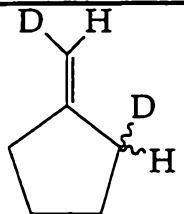
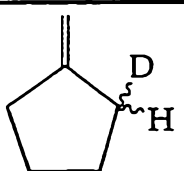
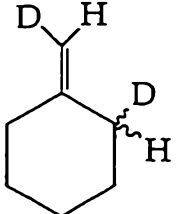
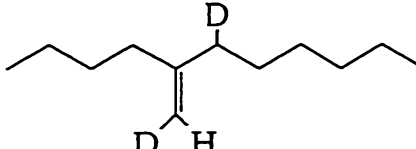
Substrate	catalyst	trans:cis ratio
	$\text{OpSc}(\text{PMe}_3)\text{H}/\text{H}_2$	1.17(3)
" "	$[\text{DpScH}]_2/\text{H}_2$	1.04(1):1
" "	$(\text{PPh}_3)_3\text{RhCl}/\text{H}_2$	0.99(1):1
" "	$\text{Cp}_2\text{ZrHCl}/\text{HCl}$	1.01(1):1
	$\text{OpSc}(\text{PMe}_3)\text{H}/\text{H}_2$	1.22(3)
	$\text{OpSc}(\text{PMe}_3)\text{H}/\text{H}_2$	1.078(4):1
	$\text{OpSc}(\text{PMe}_3)\text{H}/\text{H}_2$	erythro:threo 1.03(1):1

Table 2: Product ratios for methylenecycloalkane hydrogenation with various catalysts.

**V. Conclusions from Part 2:**

The observed isotope effect for the hydrogenation of labelled methylenecycloalkanes with  $\text{OpSc}(\text{PMe}_3)\text{H}$  is presumed to arise from a  $\beta$ -hyperconjugative transition state and supports the idea that the transition state in these catalyst systems are polarized with positive charge buildup at the  $\beta$ -carbon of the transition state for olefin insertion. The fact that the observed effect for methylenecyclohexane hydrogenation is opposite of the effect for 1,6-heptadiene hydrocyclization shows that this  $\beta$ -hyperconjugative effect is different than the observed  $\alpha$ -agostic effects.

### Experimental Section

All air or moisture sensitive chemistry was performed using standard high vacuum line, Schlenk, or drybox techniques<sup>38</sup> under a nitrogen or argon atmosphere. All gases were purified with MnO on vermiculite and activated molecular sieves. Solvents were stored in vacuum transfer flasks over titanocene<sup>39</sup> or sodium benzophenone ketyl. CH<sub>2</sub>Cl<sub>2</sub> was stored over CaH<sub>2</sub>. All olefins were dried over molecular sieves and stored over CaH<sub>2</sub> or sodium sand. OpSc(PMe<sub>3</sub>)H,<sup>40</sup> [(Cp\*SiNR)Sc(PMe<sub>3</sub>)H]<sub>2</sub>,<sup>41</sup> and [BpYH]<sub>2</sub><sup>42</sup> were prepared as described previously. Unless otherwise mentioned, all chemicals were purchased from Aldrich and used as received.

[DpScCl]<sub>2</sub>. Toluene (100 ml) is vacuum transferred onto Li<sub>2</sub>Dp<sup>42</sup> (6.438 g, 20.57 mmol) and ScCl<sub>3</sub>·3THF (7.56 g, 20.57 mmol) in a 250 ml R.B.F. attached to a reflux condenser and Teflon needle valve. The reaction is refluxed under argon for 36 hours resulting in a cloudy white suspension. The volatiles are removed under vacuum and the flask is switched to a swivel frit assembly. Et<sub>2</sub>O (100 ml) is vacuum transferred onto the solid and the product is extracted with 3 X 100 ml Et<sub>2</sub>O at 25°C. All volatiles are removed under vacuum and the white solid is washed with 3 X 50 ml petroleum ether; 5.75 g (73.9%). <sup>1</sup>H NMR (CD<sub>2</sub>Cl<sub>2</sub>) .5 s (3H), .8 s (3H), 1.2 s (18H), 6.3 m (2H), 6.5 m (2H), 6.7 m (2H).

DpSc(CH<sub>2</sub>SiMe<sub>3</sub>). Toluene (100 ml) is vacuum transferred onto [DpScCl]<sub>2</sub> (4.75 g, 12.55 mmol) and sublimed LiCH<sub>2</sub>SiMe<sub>3</sub> (1.20 g, 12.55 mmol) in a swivel frit assembly. The reaction is stirred at RT for 40 hours. Volatiles are removed under vacuum and the product is extracted with petroleum ether (75 ml x 3). The product was cooled to -78°C to precipitate the product as yellow crystals; 3.12 g (58%). <sup>1</sup>H NMR (C<sub>6</sub>D<sub>6</sub>) .3 s (3H), .5 s (3H), .8 m (2H), 1.1 s (18H), 1.0 s (9H), 5.3 m (2H), 5.8 m (2H), 7.0 m (2H).

[DpScH]<sub>2</sub>.<sup>43</sup> A thick walled glass reactor was charged with DpSc(CH<sub>2</sub>SiMe<sub>3</sub>) (0.500 g, 1.16 mmol) and petroleum ether (10 ml). The reactor was evacuated at 77° K and filled with H<sub>2</sub> (1 atm). The reactor was warmed to 25°C and is stirred at 25°C for 12 hours resulting in a white suspension. The suspension is transferred to a frit assembly and the white solid is filtered, washed with



cold petroleum ether and dried; 0.24 g (60%).  $^1\text{H}$  NMR ( $\text{C}_6\text{D}_6$ ) .2 s (3H), .8 s (3H), 1.2 s (18H), 6.3 m (2H), 6.7 m (2H), 7.3 m (2H).

**1,6- $d_2$ -1,5-hexadiyne.** A mixture of 1,5-hexadiyne (3.0 g, 38 mmol),  $\text{K}_2\text{CO}_3$  (2.3 g, 17 mmol),  $\text{D}_2\text{O}$  (20 g, 1 mol), and diglyme (20 mL) was stirred for 20 hours at 25°C. The organic layer was separated. All > 10 mm Hg volatiles were condensed onto mol sieves (4 A) and then transferred to a  $\text{CaH}_2$  vacuum transfer flask; 2.6 g (86%), 96% isotopic purity.

***trans,trans*-1,6- $d_2$ -1,5-hexadiene.**<sup>40</sup> 1,5-hexadiyne (Lancaster) (24.8 mL, 256 mmoles) was vacuum transferred onto a stirred solution of  $\text{Cp}_2\text{ZrHCl}^{44}$  (132.5 g, 512 mmoles) in  $\text{CH}_2\text{Cl}_2$  (600 mL). The reaction was warmed to 0°C in an ice water bath and the resulting suspension was stirred for 2 hours at 0°C forming an orange solution. All volatiles were removed at 25°C and high vacuum. 500 mL of diglyme were added forming a yellow suspension. About 20 mL of diglyme were removed at high vacuum to remove traces of  $\text{CH}_2\text{Cl}_2$ . A solution of  $\text{D}_2\text{O}$  (11g, 549 mmoles) in diglyme (100 mL) was added over 20 minutes via syringe forming a white suspension. 40 mLs of solution are vacuum transferred to a cold trap. 5 torr of Ar are admitted and all RT volatiles are vacuum transferred to mol sieves. The clear colorless liquid is distilled from  $\text{CaH}_2$  into a vacuum transfer flask with LAH; 24.3 g (80%).

***trans-trans*-1,7- $d_2$ -1,6-heptadiene** was prepared analogously with 1,6-heptadiyne (Lancaster),  $\text{Cp}_2\text{ZrHCl}$  (2 equivalents) and hydrolysis with  $\text{D}_2\text{O}$  (2.1 equivalents).

***cis-cis*-1,6- $d_2$ -1,5-hexadiene** was prepared analogously with 1,6- $d_2$ -1,5-hexadiyne,  $\text{Cp}_2\text{ZrHCl}$  (2 equivalents) and hydrolysis with  $\text{H}_2\text{O}$  (2.1 equivalents).

***trans*-1,6- $d_1$ -1-hexene** was prepared analogously with 1,6-hexyne,  $\text{Cp}_2\text{ZrHCl}$  (1 equivalent) and hydrolysis with  $\text{D}_2\text{O}$  (1.05 equivalents).

**2,6- $d_2$ -methylenecyclopentane.** Dry *trans,trans*-1,6- $d_2$ -1,5-hexadiene (8.4g, 100 mmol) was condensed onto  $\text{OpSc}(\text{PMe}_3)\text{H}$  (20 mg, 0.044 mmol) and stirred at 25°C for 24 hours. All volatiles were vacuum transferred to a  $\text{CaH}_2$  pot.

**2,7-*d*<sub>2</sub>-methylene cyclohexane** was obtained analogously from *trans,trans*-1,7-*d*<sub>2</sub>-1,6-heptadiene and OpSc(PMe<sub>3</sub>)H.

**Hydrogenation of methylene cycloalkanes with OpSc(PMe<sub>3</sub>)H or [DpScH]<sub>2</sub>.** In a dry box, approximately 10 mg of OpSc(PMe<sub>3</sub>)H or [DpScH]<sub>2</sub> were placed in a ~100 ml thick walled glass bomb with a Teflon needle valve attached to a standard taper joint. ~100 equivalents of olefin were added by vacuum transfer at 77°K. Hydrogen gas (1 atmosphere) was then admitted into the bomb and allowed to cool to 77°. The bomb was rapidly warmed to 25°C, resulting in a H<sub>2</sub> pressure of ~4 atm., while being physically agitated. After several hours, the bomb was again cooled to 77°C and degassed after which all volatile products were removed by distillation and analyzed by NMR and G. C. for purity. If necessary, the products were further purified by preparative G.C.

**Hydrogenation of 2,6-*d*<sub>2</sub>-methylene cyclopentane with RhCl(PPh<sub>3</sub>)<sub>3</sub>.** Hydrogenation was carried out in benzene as described previously.<sup>45</sup> Volatile products were removed by distillation and analyzed by NMR.

**Hydrogenation of 2,6-*d*<sub>2</sub>-methylene cyclopentane with Cp<sub>2</sub>ZrHCl.** CH<sub>2</sub>Cl<sub>2</sub> (10 ml) is vacuum transferred into a 50 mL schlenk flask containing Cp<sub>2</sub>ZrHCl (1.196 g, 4.6 mmol) and the solution is warmed to RT, 2,6-*d*<sub>2</sub>-methylene cyclopentane (.5 mL, .46 mmol) is added, and the solution is stirred at RT for 10 hours. All volatiles are removed from the resulting yellow solution and 10 mL of diglyme are added via cannula. HCl (1 ml, 50%(aq)) is added at RT and the reaction is stirred for 20 minutes. H<sub>2</sub>O (10 mL) is added and the organic layer is separated. Under 5 torr Ar, the volatiles are vacuum transferred to a cold trap. Yield = 0.4 ml.

<sup>1</sup>H NMR spectra were recorded on a Bruker AM500 (500.13 MHz) spectrometer, a Joel GX-400 (399.7 MHz) spectrometer, and a G.E. QE300 spectrometer.

<sup>2</sup>H{<sup>1</sup>H} NMR spectra<sup>46,47</sup> were recorded exclusively on the Bruker AM500 (76.774 MHz) spectrometer using a 10mm broadband probe. Approximately

10 $\mu$ L of C<sub>6</sub>D<sub>6</sub> was used to lock and shim. By locking and shimming on the sample before accumulation, excellent resolution was obtained. The natural field drift was corrected by watching the change in chemical shift of a standard over a ten minute period and iteratively changing the drift correct setting until the chemical shift remained unchanged after a period as long as 30 minutes. By using concentrated samples, shimming on the actual sample, and correcting for drift, excellent spectra with very narrow line widths were obtained. Integrations were taken a number of different times for each of several different accumulations. The T<sub>1</sub>'s were on the order of 2 seconds so 13 seconds between pulses was sufficient to obtain integrable spectra.

**Gas Chromatography.** All analytical G.C. data was obtained on a Perkin Elmer Model #8410 gas chromatograph with a Flame Ionization Detector and a RSL-150 (Alltech) column. Preparative G.C. was performed on a Varian 920 gas chromatograph with a Thermal Conductivity Detector and a 80/100 mesh carbowax column at 70°C. All G.C. standards were purchased from Aldrich.

**References and notes:**

- 1) Boor, J. *Ziegler-Natta Catalysts and Polymerizations*; Academic Press: New York, 1979.
- 2) Pino, P.; Mulhaupt, R. *Angew. Chem. Intl. Ed. Engl.* **1980**, *19*, 857.
- 3) Sinn, H.; Kaminsky, W. *Adv. Organomet. Chem.* **1980**, *18*, 99.
- 4) Tait, P. J. T.; Watkins, N. D. *Comprehensive Polymer Science*; Pergamon Press: Oxford, 1989 Chapter 1, 2.
- 5) Brintzinger, H. H.; Fischer, D.; Mulhaupt, R.; Rieger, B.; Waymouth, R. M. *Angew. Chem. Intl. Ed. Engl.* **1995**, *34*, 1143-1170. and references therein.
- 6) Shapiro, P. J.; Cotter, W. D.; Schaefer, W. P.; Labinger, J. A.; Bercaw, J. E. *J. Am. Chem. Soc.* **1994**, *116*, 4623-4640. presents evidence that the linked Cp-amido catalysts operate via a  $12e^-$  active species.
- 7) A new class of catalysts with a cyclopentadienyl ligand linked to an amido have been developed. The active species for these catalysts with Group IV metals are  $12e^-$  cations which are incredibly active for the polymerization of olefins.
- 8) Waymouth, R.; Pino, P. *J. Am. Chem. Soc.* **1990**, *112*, 4911.
- 9) Pino, P.; Galimberti, M. *J. Organomet. Chem.* **1989**, *370*, 1.
- 10) Brookhart, M.; Green, M. L. H.; Wong, L. *Prog. Inorg. Chem.* **1988**, *36*, 1.
- 11) Brookhart, M.; Green, M. L. H. *J. Organomet. Chem.* **1983**, *250*, 395.
- 12) Laverty, D. T.; Rooney, J. J. *J. Chem. Soc., Faraday Trans.* **1983**, *79*, 869.
- 13) Clawson, L.; Soto, J.; Buchwald, S. L.; Steigerwald, M. L.; Grubbs, R. H. *J. Amer. Chem. Soc.* **1985**, *107*, 3377.
- 14) Burger, B. J.; Thompson, M. E.; Cotter, W. D.; Bercaw, J. E. *J. Am. Chem. Soc.* **1990**, *112*, 1566-1577.
- 15) Thompson, M. E.; Baxter, S. M.; Bulls, A. R.; Burger, B. J.; Nolan, M. C.; Santarsiero, B. D.; Schaefer, W. P.; Bercaw, J. E. *J. Am. Chem. Soc.* **1987**, *109*, 203.
- 16) Calvert, R. B.; Shapley, J. R. *J. Am. Chem. Soc.* **1978**, *100*, 7726.
- 17) Melander, L.; Saunders, J. W. H. "Reaction Rates of Isotopic Molecules," Robert E. Krieger Publishing Co., Malabar, Florida, 1987, section 6.1.2.
- 18) Grubbs, R. H.; Coates, G. W. *Acc. Chem. Res.* **1996**, *29*, 85-93.
- 19) Piers, W. E.; Bercaw, J. E. *J. Am. Chem. Soc.* **1990**, *112*, 9406.
- 20) Piers, W. E.; Köhn, R. D.; Herzog, T. A.; Bercaw, J. E. Manuscript in preparation.
- 21) Leclerc, M. K.; Brintzinger, H. H. *J. Am. Chem. Soc.* **1995**, *117*, 1651-1652.

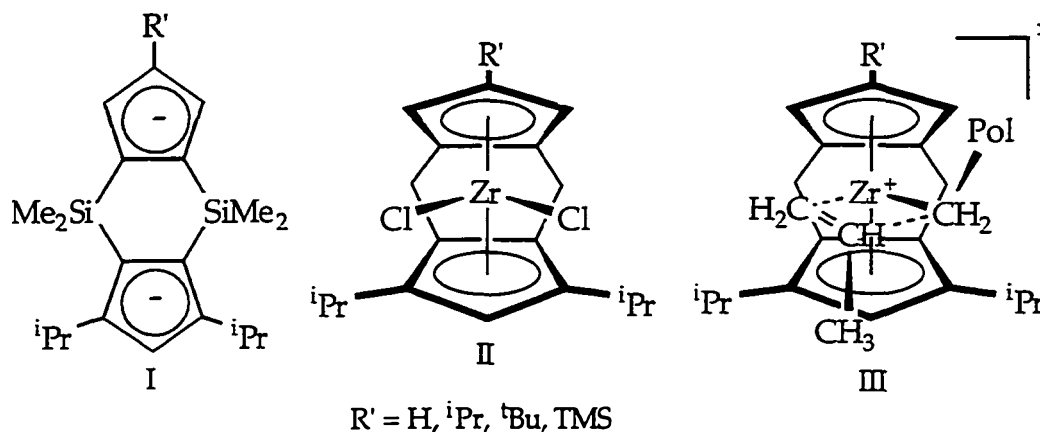
- 22) Brintzinger, H. H.; Krauledat, H. *Angew. Chem. Int. Ed. Engl* **1990**, *29*, 1412.
- 23) Barta, N. S.; Kirk, B. A.; Stille, J. R. *J. Am. Chem. Soc.* **1994**, *116*, 8912-8919.
- 24) Mueller, E.G.; Bercaw, J. E. Manuscript in preparation.
- 25) Fuchs, B. *Top. Stereochem.* **1978**, *10*, 1.
- 26) Gilchrist, J. C.; Bercaw, J. E. Manuscript in preparation.
- 27) Janiak, C. *J. Organomet. Chem.* **1993**, *452*, 63.
- 28) Prosenc, M. H.; Janiak, C.; Brintzinger, H. H. *Organometallics* **1992**, *11*, 4036.
- 29) Kawamura-Kuribayashi, H.; Koga, N.; Morokuma, K. *J. Am. Chem. Soc.* **1992**, *114*, 8687.
- 30) Castonguay, L. A.; Rappé, A. K. *J. Am. Chem. Soc.* **1992**, *114*.
- 31) Jolly, C. A.; Marynick, D. S. *J. Am. Chem. Soc.* **1989**, *111*, 7986.
- 32) The higher proportion of acyclic hydrogenation to n-hexane observed with the meso DpScH catalyst is likely due to the increased steric crowding associated with the cyclization step for the meso [DpScCHDCH<sub>2</sub>CH<sub>2</sub>CH<sub>2</sub>CH=CHD] intermediate. The hexenyl group undoubtedly resides in the less crowded side of the wedge, forcing the pendant olefin to coordinate from the side blocked by the two tert-butyl substituents of the cyclopentadienyl ligands. Hence, bimolecular hydrogenation to 1-hexene, which is undoubtedly less sensitive to steric effects, competes more effectively for this catalyst.
- 33) Coughlin, E. B.; Bercaw, J. E. *J. Am. Chem. Soc.* **1992**, *114*, 7606-7607.
- 34) <sup>13</sup>C NMR analysis of polypropylene produced by BpY-R is greater than 99% [mmmm].
- 35) Köhn, R. D. Personal Communication: If β-H elimination to form methylenecyclopentane did occur, then the deuterocyclization of 1,5-hexadiene would result in scrambling of D to the 1-ring position. Since <sup>2</sup>H NMR revealed no such scrambling, β-H elimination is not competitive with hydrogenolysis of the OpSc(methylcyclopentyl) intermediate.
- 36) A similar experiment was performed with 1,6-heptadiene and methylenecyclohexane with OpSc(PMe<sub>3</sub>)H. Hydrocyclization of 1,6-heptadiene gave 50.3%/49.7% cyclized/uncyclized products while hydrogenation of methylenecyclohexane gave 99.9%/0.1% cyclized/uncyclized products. This again shows that ring opening via beta-alkyl elimination is not competitive at the reaction conditions.

- 37) Halpern, J.; Okamoto, T. *Inorg. Chim. Acta.* **1984**, *89*, L53-L54.
- 38) Burger, B. J.; Bercaw, J. E. *New Developments in the Synthesis, Manipulation, and Characterization of Organometallic Compounds*, **1987**; Vol. 357. ACS Symposium Series.
- 39) Marvich, R. H.; Brintzinger, H. H. *J. Am. Chem. Soc.* **1971**, *93*, 203.
- 40) Piers, W. E.; Shapiro, P. J.; Bunel, E. E.; Bercaw, J. E. *Synlett* **1990**, *2*, 74.
- 41) Shapiro, P. J.; Bunel, E. E.; Schaefer, W. P.; Bercaw, J. E. *Organometallics* **1990**, *9*, 867-869.
- 42) Mitchell, J. P.; Hajela, S.; Brookhart, S. K.; Hardcastle, K. L.; Henling, L. M.; Bercaw, J. E. *J. Am. Chem. Soc.* **1996**, *118*, 1045-1053.
- 43) Bunel, E. E.; Ph.D. Thesis, Caltech, Pasadena, CA, **1989**.
- 44) Buchwald, S. L.; LaMaire, S. J.; Nielson, R. B.; Watson, B. T.; King, S. M. *Tetrahedron Letters* **1987**, *28*, 3895-3898.
- 45) *Organic Reactions*, *20*, 1-50.
- 46) Elvidge, J. A. *Isotopes: Essential Chemistry and Applications*; The Chemical Society: London, **1979**.
- 47) McDade, C.; Green, J. C.; Bercaw, J. E. *Organometallics* **1982**, *1*, 1629. The integration is not effected by nuclear Overhauser enhancement.

**CHAPTER 2**  
**THE DEVELOPMENT OF NEW C<sub>s</sub> SYMMETRIC CATALYSTS FOR**  
**THE SYNDIOSPECIFIC POLYMERIZATION OF  $\alpha$ -OLEFINS.**

**Abstract:**

A new class of Group IV metallocene catalysts is presented for the syndiospecific polymerization of propylene. These catalysts incorporate what are thought to be the key characteristics of syndiospecific metallocene catalysts: C<sub>s</sub> symmetry and rigidly linked cyclopentadienyls of greatly differing size. However, preliminary attempts to develop new syndiospecific catalysts have suggested another important characteristic: a pocket in the larger moiety to avoid undesirable steric interactions between the ligand framework and coordinated olefin. In order to accommodate this constraint, a doubly bridged ligand system with a 1,3-dialkylcyclopentadienyl was chosen. The ligand system (I), the catalyst precursor (II), and the proposed transition state for olefin insertion (III) are shown below.



These metallocenes, in the presence of a cocatalyst (MAO), react rapidly with neat propylene to form highly syndiotactic polypropylene. This is the first example of a stereospecific doubly bridged olefin polymerization catalyst and is the first example of a highly syndiospecific polymerization catalyst not based on a fluorenyl like ligand. This catalyst system is also very versatile since straightforward changes at R' and in the reaction conditions lead to dramatic changes in the polymer microstructure. For example, in the case of R' = CH(Me)(<sup>t</sup>Bu), highly isotactic polypropylene is obtained at low propylene concentration. These catalysts should provide an excellent platform for mechanistic study and may be important industrially.

I. Introduction.....	35
Part 1. Transition state analogs for syndiospecific catalysts.	
II. Results and Discussion.....	46
III. Conclusions from Part 1.....	57
Part 2. A hyperconjugative isotope effect in the hydrogenation of methylenecycloalkanes.	
IV. Results and Discussion.....	58
V. Conclusions from Part 2.....	79
Experimental Section.....	81
References and Notes.....	99
Appendix A: Table of $^1\text{H}$ NMR data.....	104
Appendix B: Crystal Structure Data for $\text{HpZrCl}_2$ .....	120
Appendix C: Crystal Structure Data for $^i\text{PrThpZrCl}_2$ .....	128



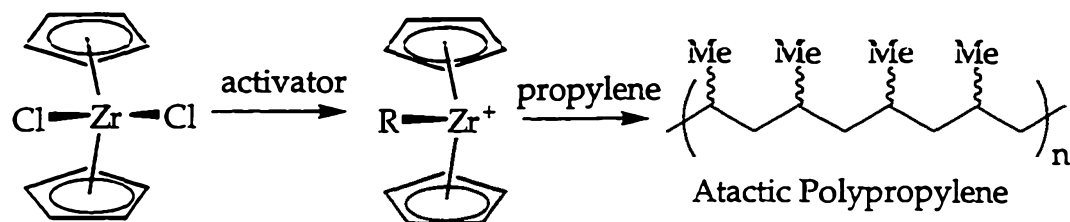
## I. Introduction:

The polymerization of olefins using homogeneous Ziegler-Natta catalysts has created tremendous interest in the past 15 years.<sup>1-4</sup> Industrially, this interest has arisen from the very high activity and productivity of these systems as well as the favorable economics of transforming inexpensive olefins, such as ethylene and propylene, into useful polymers. To the organometallic chemist, however, the most interesting aspects of Ziegler-Natta catalysis are the relationship between a catalyst's structure and its function, the mechanism of polymerization, and the mechanism by which errors occur. Despite a broad and intense effort, the design of new catalysts is still largely trial and error, and a number of mechanistic questions remain unanswered.

Historically, the best Ziegler-Natta catalysts were multi-component heterogeneous mixtures of transition metal halides, alkyl aluminums and Lewis bases. As a result of the ill defined nature of these systems, the development of new heterogeneous catalysts has proceeded with limited understanding of the mechanism of operation of the catalysts. The discovery of homogeneous catalysts based on metallocenes<sup>5</sup> has allowed for a much better understanding of the mechanism of these important reactions and for a more rational development of new catalysts. The active catalyst species for Ziegler-Natta polymerization all share the trait of having at least two vacant orbitals as discussed in chapter 1. In the case of early transition metal metallocenes, the active species is a 14 e<sup>-</sup>, d<sup>0</sup> alkyl. For the catalysts based on a linked Cp/ amido ligand, the active species is believed to be a 12 e<sup>-</sup>, d<sup>0</sup> alkyl. The group IV catalysts are typically cationic<sup>6</sup> while the Group III metallocene catalysts are typically neutral.<sup>7</sup> The Group IV cations require a noncoordinating anion such as methylaluminoxane (MAO)<sup>5,8</sup> or perfluorophenylborates<sup>9,10</sup> to be active polymerization catalysts. Catalysts with Group IV metals are often extremely active<sup>1</sup> and are therefore very important industrially. The Group III neutral catalysts are much less active<sup>11</sup> than their group IV counterparts, but they do not require a cocatalyst and are thus well suited to mechanistic studies.<sup>12,13</sup>

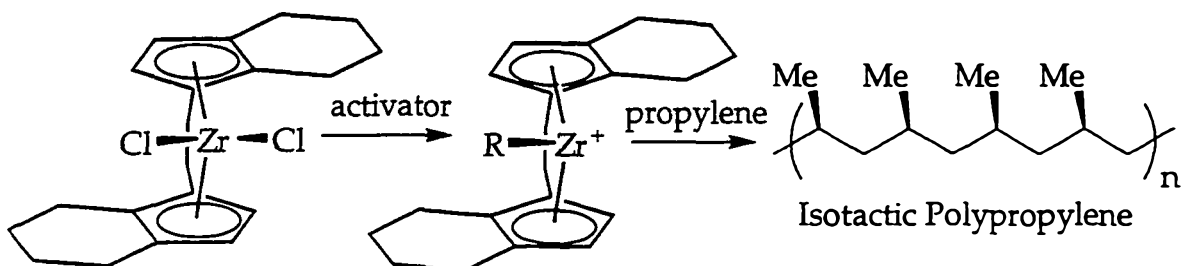
There is a clear relationship between the structure and function of Ziegler-Natta metallocene catalysts for olefin polymerization.<sup>9</sup> For example, most achiral catalysts, such as zirconocene dichloride, in the presence of an

activating species, such as MAO, react with propylene to form atactic polypropylene, an amorphous solid with few uses.<sup>1</sup>



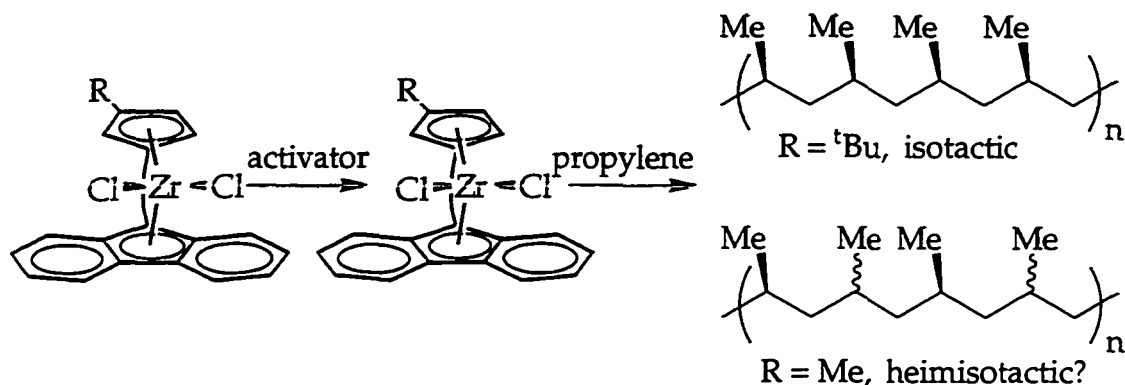
**Figure 1: Aspecific polymerization with  $C_{2v}$  symmetric metallocenes.**

Most  $C_2$  symmetric metallocenes<sup>14,15</sup> react with propylene to form isotactic polypropylene which is a hard translucent material with numerous applications. The prototypical example of a  $C_2$  symmetric, isospecific catalyst is the ethylene linked bis(tetrahydroindenyl)zirconium dichloride catalyst<sup>16</sup> as shown in figure 2. The degree of isospecificity of these catalysts depends on a number of factors. The origins of deviation from purely isotactic polymer formation are poorly understood since there are a variety of possible error mechanisms which will be discussed later in detail.



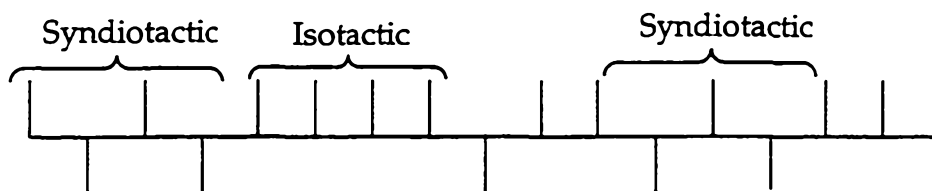
**Figure 2: Isospecific polymerization with  $C_2$  symmetric metallocenes.**

A number of  $C_1$  symmetric metallocenes<sup>17-21</sup> have been prepared. Several of these chiral catalysts react with propylene to form isotactic polypropylene. A few  $C_1$  symmetric catalysts react with propylene to make a material which does not fit the definition of purely atactic, isotactic or syndiotactic.<sup>22</sup> The microstructure of these polymers has been described as hemi-isotactic indicating that it is like isotactic polymer except that every other methyl group is randomly oriented.<sup>23</sup>



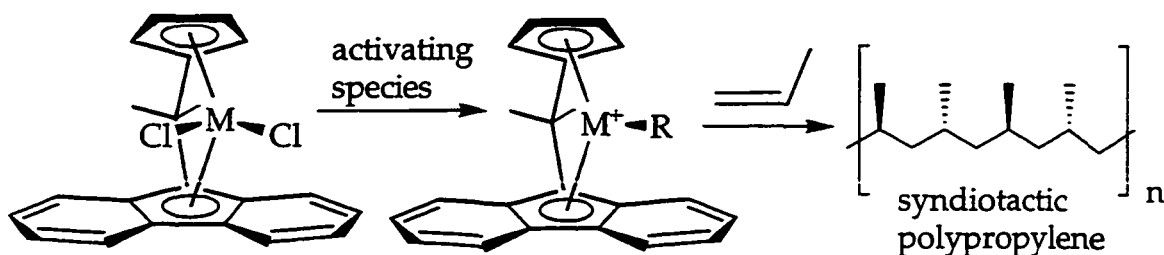
**Figure 3: Polymerization with  $C_1$  symmetric catalysts.**

This assignment is currently in dispute, however, and Razavi<sup>24</sup> has proposed an alternative assignment of very short stereoblocks of syndiotactic and isotactic polypropylene as shown in figure 4.



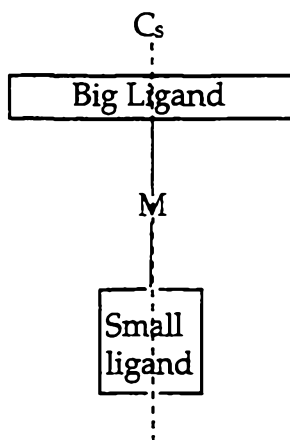
**Figure 4: Microstructure of polymer from some  $C_1$  symmetric catalysts.**

A number of  $C_s$  symmetric catalysts have been prepared as well although far fewer than the  $C_2$  symmetric catalysts. The prototypical syndiospecific polymerization catalyst is the  $C_s$  symmetric, isopropylidene linked fluorenyl cyclopentadienyl ligand ( $^i\text{PrFlCp}$ ) developed by Ewen and Razavi.<sup>10</sup> Catalysts based on this ligand, with Group IV metals and a suitable activating species, generate highly syndiotactic polypropylene which is a hard, transparent material. Syndiotactic polypropylene had not been used extensively due to processing difficulties, but has recently been produced on a large scale and used as a blend with isotactic polypropylene.<sup>25</sup>



**Figure 5: Syndiospecific polymerization with  $C_5$  symmetric metallocenes.**

Despite the apparent simplicity of these fluorenyl based ligands, the development of new syndiospecific catalysts not based on fluorenyl has been unsuccessful. The two obvious characteristics of the current successful syndiospecific catalysts are  $C_5$  symmetry and ligands of greatly differing size as shown schematically in figure 6.



**Figure 6: Generic features of syndiospecific systems.**

A number of different metallocenes have been prepared in the past which would seem to be suitable catalysts for syndiospecific polymerization as they are  $C_5$  symmetric and have ligands of greatly differing size. A table of catalysts that fit these apparent criteria for syndiospecificity is given below; the catalysts that are relatively syndiospecific are labeled with an ✖.

(E)(L<sup>1</sup>)(L<sup>2</sup>)MCl<sub>2</sub> (M = Ti, Zr, Hf) / MAO + propylene → polypropylene

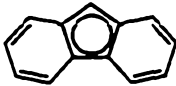
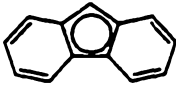
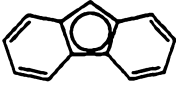
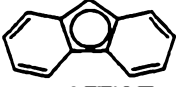
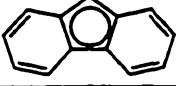







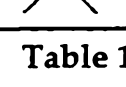
	Big ligand L <sup>1</sup>	Small ligand (L <sup>2</sup> )	Linking group (E)	<sup>13</sup> C NMR <sup>26</sup>	Reference
*		Cp	Me <sub>2</sub> C	[rrrr] = 86% [r] = 96%	10
*		Cp	Ph <sub>2</sub> C	[r] = 97.5%	27
*		Cp	Me <sub>2</sub> Si	[rr] = 76.18%	28
*		Cp	Ph <sub>2</sub> Si	[rr] = 74.45%	28
*		Cp	Me <sub>2</sub> Ge	[rr] = 65.46%	28
*		Cp	Me <sub>2</sub> Si	[rr] = 64.95%	28
		tBuN	Me <sub>2</sub> Si	[r] = .641	29
		Cp	none	atactic	30
		MeCp	none	[rrrr] = 11.2% [r] = 58.2	31
*		Cp	Ph <sub>2</sub> C	[rrrr] = 58%	25
*		Cp	Ph <sub>2</sub> C	[rrrr] = 93.5%	25
		Cp	Me <sub>2</sub> Si	[r] = 62.3%	32
		Cp	H <sub>2</sub> C	[r] = 72.1%	32

Table 1: Some C<sub>s</sub> symmetric polymerization catalysts.

As shown in table 1, the only syndiospecific homogeneous catalysts to date are those that contain a fluorenyl like moiety linked to a smaller moiety. The important distinctions between these syndiospecific catalysts and the many

aspecific catalysts has yet to be fully established. A better mechanistic understanding of this system is therefore essential in order to shed light on the structural features of syndiospecific polymerization.

The questions associated with the mechanism of syndiospecific systems can best be understood by a comparison with  $C_2$  symmetric isospecific systems which have been studied more thoroughly. In both cases, the key interactions are believed to involve the relative positions of the polymer chain, the olefin, and the ligand framework. The proposed transition state for isospecific polymerization is shown in figure 7:

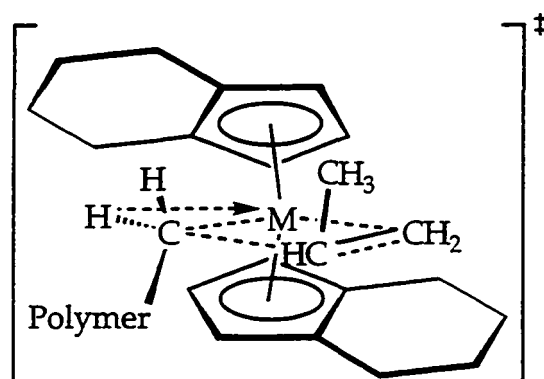
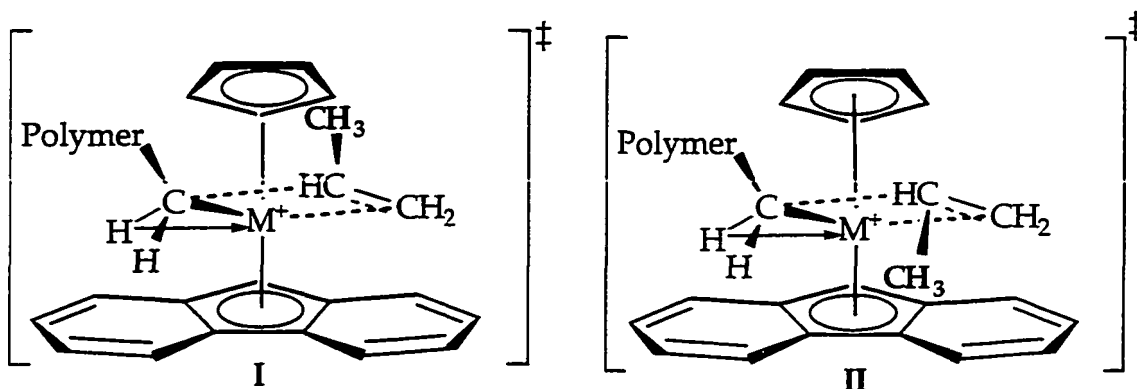


Figure 7: Transition state for olefin insertion in isospecific systems.

In a  $C_2$  symmetric catalyst, olefin insertion will occur with the same stereochemistry whether the polymer chain is on the left or right side of the metallocene wedge. An  $\alpha$ -agostic interaction<sup>12</sup> and the ligand framework work together to orient the polymer chain such that it is down and away from the top tetrahydroindenyl group. The inserting olefin approaches such that the methyl group of propylene is directed up and away from the bottom tetrahydroindenyl ligand and is in an anti orientation to the polymer chain across the forming C-C single bond.<sup>33,34</sup> Both the polymer chain and the ligand environment, therefore, work together to direct the methyl group of the inserting olefin.

In syndiospecific systems, the key interactions are basically the same. However, due to the  $C_s$  symmetry of the ligand framework, there are two likely transition states for olefin insertion as shown in figure 8.



**Figure 8: Possible transition states for olefin insertion in syndiospecific systems.**

In both I and II, the  $\alpha$ -agostic interactions and the sterics of the ligand system work together to orient the polymer up and away from the fluorenyl in the same manner as for the  $C_2$  symmetric metallocenes. However, the methyl group of the inserting olefin can either be directed up and away from the fluorenyl in a syn orientation to the polymer chain (I) or down toward the fluorenyl in an anti orientation to the polymer chain (II). These interactions are contradictory so the actual transition state for olefin insertion is difficult to establish. Calculations<sup>35</sup> and experiment<sup>33,34</sup> seem to support the idea that the most important interaction is that between the polymer chain and the methyl group of the inserting olefin. This would tend to favor transition state II and disfavor transition state I. However, this remains an open question.

Regardless of the transition state, it appears obvious that a requirement for syndioselectivity with these catalysts is that the olefin insert from alternating sides of the metallocene wedge. The mechanism by which this alternation occurs has also yet to be established, but two possibilities will be presented herein. The first mechanism is essentially the same as that which was originally proposed by Ewen.<sup>10</sup> It simply involves a migratory insertion mechanism in which the olefin inserts before the pendant alkyl has a chance to change sides. This mechanism is shown in figure 9.

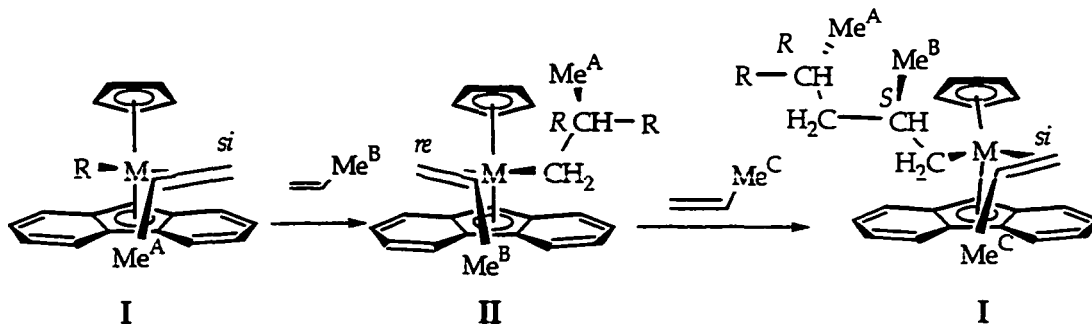
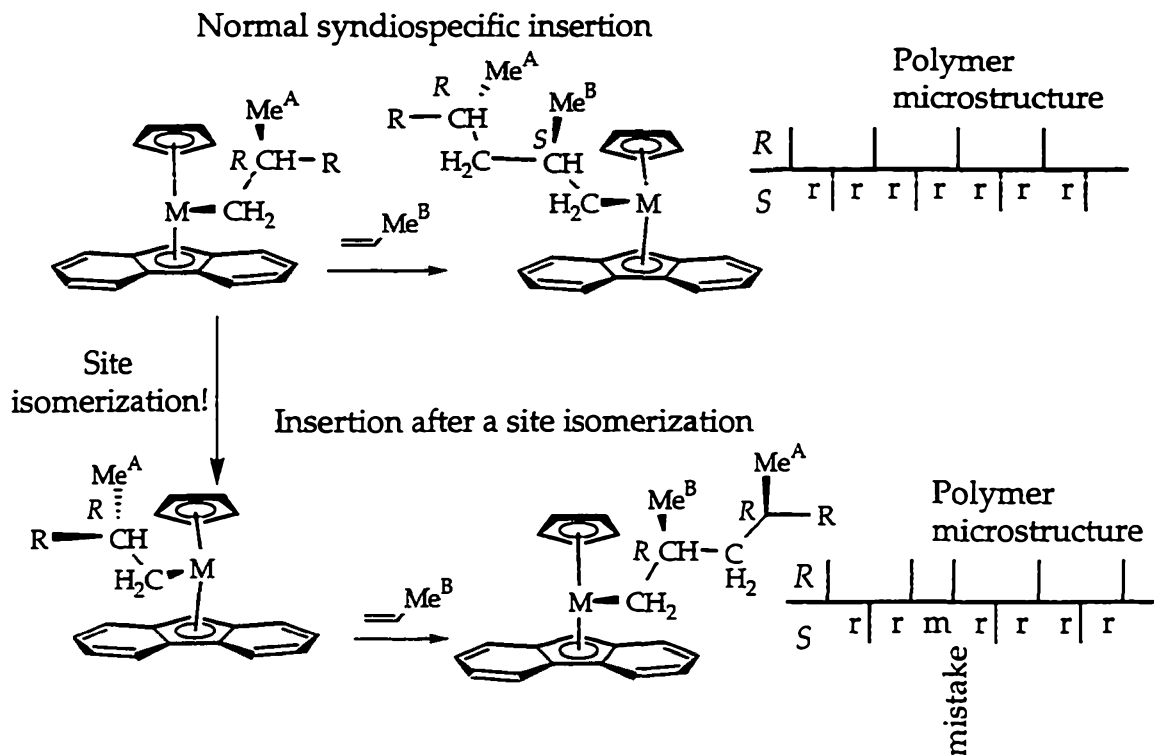


Figure 9: Ewen's migratory insertion mechanism.

Due to the  $C_s$  symmetry of the metallocene, insertion of propylene on the right side of the wedge, as in I, generates an *R* stereocenter while addition of propylene on the left side of the wedge, as in II, generates an *S* stereocenter. The alkyl is presumed to switch sides after every insertion since the forming M-C bond is always on the opposite side of the wedge from the breaking M-C bond. The  $C_s$  symmetry of the metallocene and the fact that the olefin insertion occurs at alternating sites work together to make syndiotactic polypropylene. A potential source of errors in this system is site isomerization, a process by which the stereochemistry of the metal center is scrambled by a migration of the polymer chain in the absence of olefin insertion. A single site isomerization would result in two identical insertions in a row as shown in figure 10.





**Figure 10: Mechanism of site isomerization.**

An alternative mechanism for syndiospecific polymerization is based on the realization that the  $\beta$ -carbon of the polymer chain is chiral. Since the metallocene is  $C_s$  symmetric, placing the same chiral group on either side of the metallocene wedge will result in diastereomers which, by definition, are different in energy. Therefore, A and B, as shown in figure 11, will be of different energy since the *S* stereocenter is on opposite sides of the ligand mirror plane.

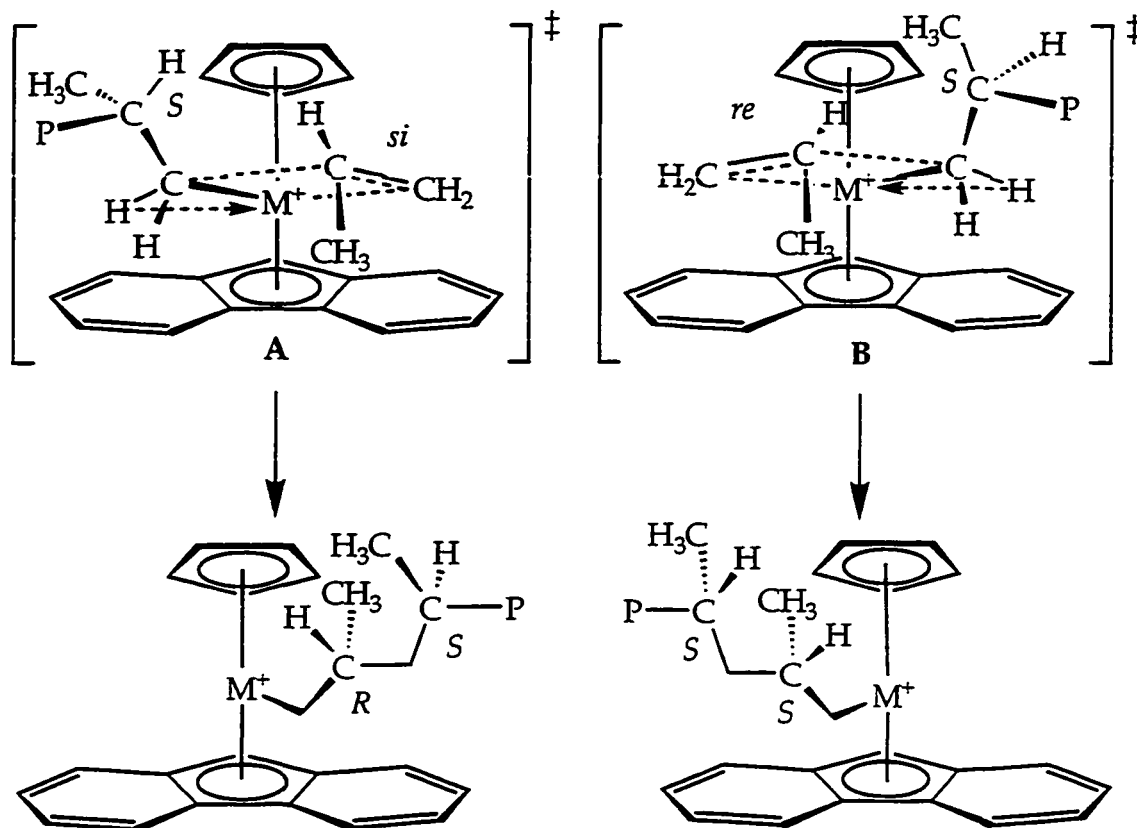


Figure 11: Importance of chirality at the polymer  $\beta$ -C.

If site isomerization is rapid, then the selectivity of the catalyst will be related to the relative energies of the two diastereomeric transition states. In order for this mechanism to produce syndiotactic polymer, the transition state for a *si* insertion into an *S* alkyl (A) must be significantly favored over the transition state for a *re* insertion into an *S* alkyl (B) and vice versa for insertion into an *R* alkyl.

Another potential source of errors in both mechanisms is epimerization. Epimerization is a process, facilitated by  $\beta$ -H elimination, by which the stereochemistry at the  $\beta$ -C of the polymer chain is scrambled. Epimerization has been implicated by Brintzinger and Busico as an important mechanism of stereoerrors in isospecific polymerizations at low monomer concentrations<sup>36,37</sup> as shown in figure 12.

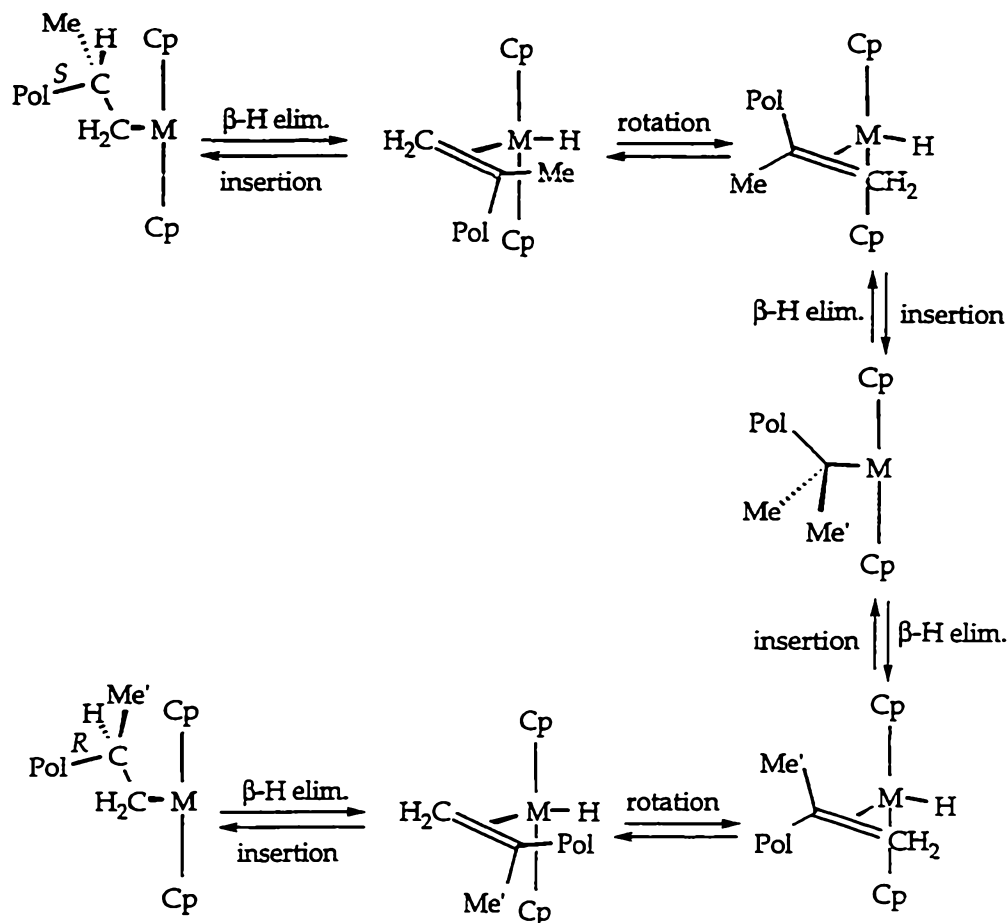


Figure 12: Epimerization mechanism.

For clarity, this chapter is divided into two parts, both of which involve syndiospecific Ziegler-Natta catalysts. Part 1 will present the attempted synthesis of transition state analogs of syndiospecific catalysts using Group III metallocenes. These complexes could be useful to both study the importance of the alkyl group stereochemistry on determining the selectivity of these catalysts and to probe the usefulness of Group III complexes as syndiospecific catalysts.<sup>38</sup> Part 2 will present the development and synthesis of a new family of syndiospecific catalysts that incorporate a double silicon bridge. These catalysts show remarkable stereospecificity which can be tuned by modifications of the ligand framework and by the reaction conditions.

## Part 1: Transition state analogs for syndiospecific catalysts.

### II. Results and Discussion:

The <sup>i</sup>PrFlCp ligand was chosen as the ligand for the preparation of transition state analogs with Group III metals. The initial target complex for this study was to be a scandium or yttrium complex of <sup>i</sup>PrFlCp with a chiral alkyl and a Lewis base such as PMe<sub>3</sub>. The chiral alkyl group would have its chiral center at the β-carbon to simulate a growing polymer chain and the Lewis base would serve as a model for a bound olefin. If there is a significant difference in the energy of the possible diastereomers **A** and **B** as shown in figure 11, this would be reflected by a nonstoichiometric product distribution as shown in figure 13. Since the products would be diastereomers of each other, the product distribution could be measured by NMR.

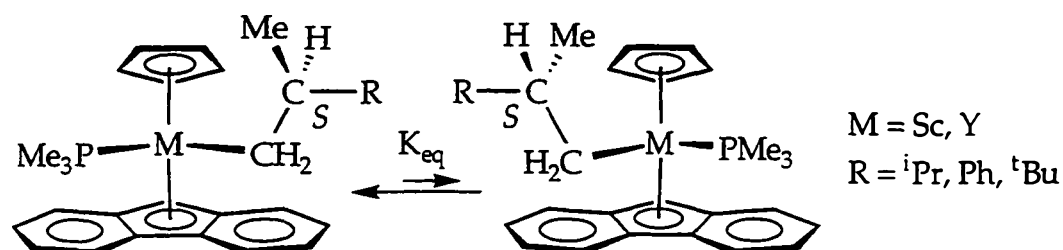
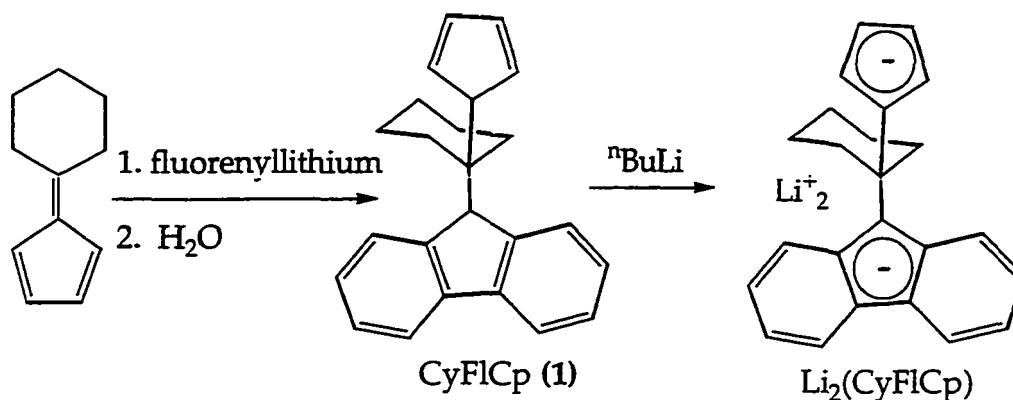


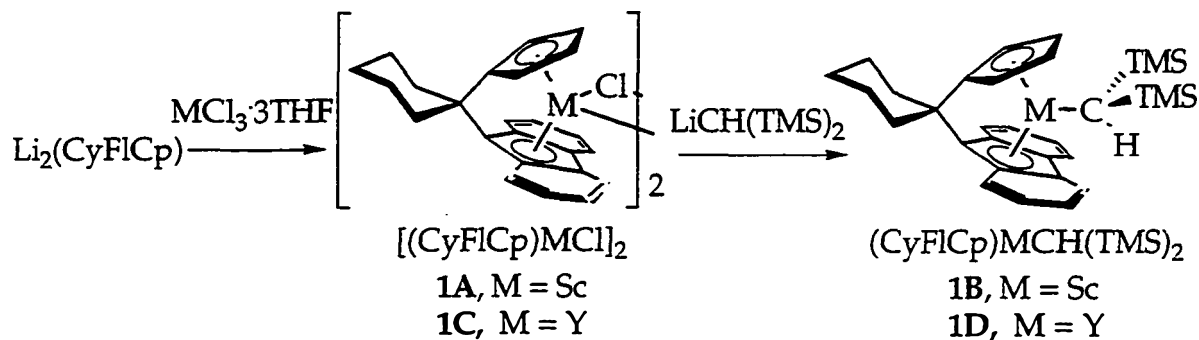
Figure 13: Target complexes.

Reaction of a hydride complex such as [(<sup>i</sup>PrFlCp)M-H]<sub>2</sub> (M= Sc, Y) with a prochiral olefin such as α-methylstyrene in the presence of PMe<sub>3</sub> was expected to be a useful route to these model complexes. Unfortunately, attempts to synthesize [<sup>i</sup>PrFlCp]ScH and [<sup>i</sup>PrFlCp]YH were eventually aborted due to very poor solubility and subsequent poor reactivity of the key starting materials, [<sup>i</sup>PrFlCpScCl]<sub>n</sub> and [<sup>i</sup>PrFlCpYCl]<sub>n</sub>. The solubility problems with this ligand on Group III metals led us to develop a more soluble ligand with a cyclohexylidene linker. Using Ewen's approach to the ligand synthesis<sup>39</sup> with the substitution of pentamethylenefulvene for 6,6-dimethylfulvene, a cyclohexyl linked ligand (CyFlCp) was prepared on a large scale as shown in figure 14.



**Figure 14: CyFlCp (1) synthesis.**

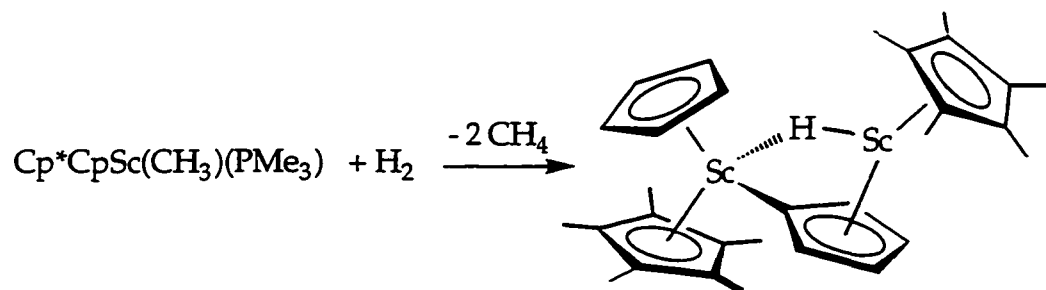
Reaction of  $\text{Li}_2(\text{CyFlCp})$  with  $\text{MCl}_3 \cdot 3\text{THF}$  ( $\text{M}=\text{Sc}, \text{Y}$ ) in toluene yields  $(\text{CyFlCp})\text{MCl}(\text{THF})_n$  which can be isolated as a base free dimer by dissolving the solid in toluene and removing solvent in vacuo three times. Both  $[(\text{CyFlCp})\text{ScCl}]_2$  and  $[(\text{CyFlCp})\text{YCl}]_2$  are soluble in benzene and can be alkylated readily by reaction with  $\text{LiCH}(\text{SiMe}_3)_2$  in toluene to yield  $(\text{CyFlCp})\text{M}-\text{CH}(\text{SiMe}_3)_2$ .



**Figure 15: Synthesis of  $(\text{CyFlCp})\text{M}-\text{R}$  (1B, 1D).**

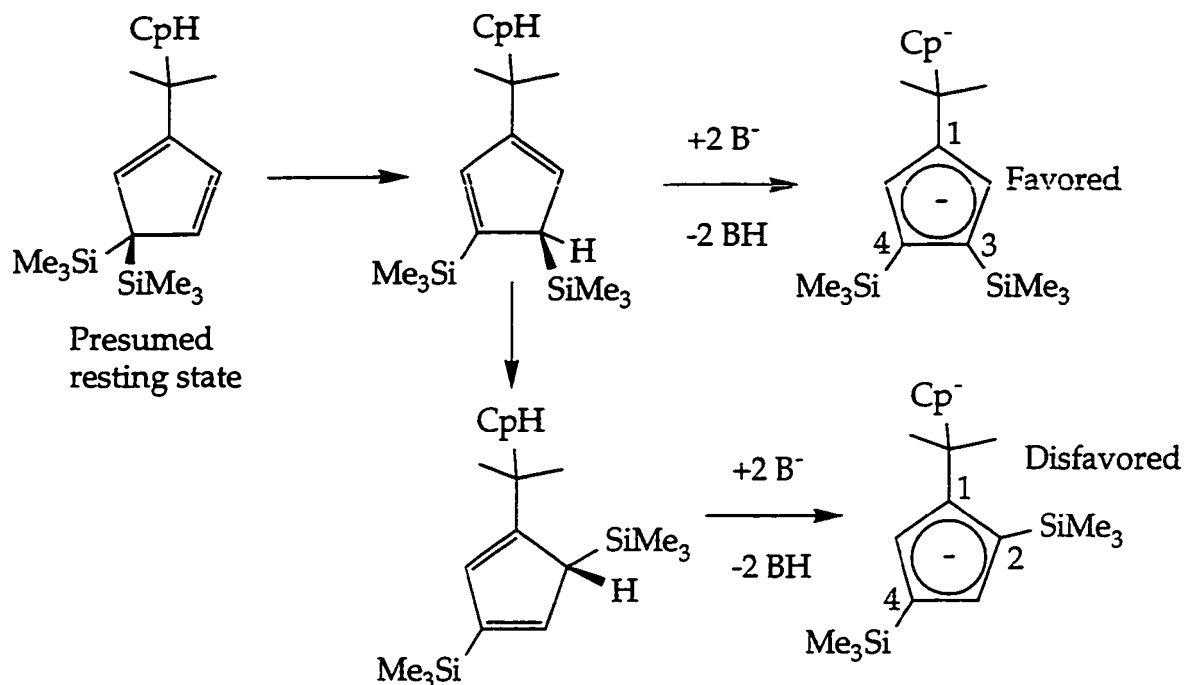
Both  $(\text{CyFlCp})\text{Sc}-\text{CH}(\text{SiMe}_3)_2$  and  $(\text{CyFlCp})\text{Y}-\text{CH}(\text{SiMe}_3)_2$  are active catalysts for ethylene polymerization, but neither initiate propylene polymerization. Numerous attempts to hydrogenate these catalysts to form a more active hydride species under several different conditions resulted only in decomposition. Also, attempts to synthesize other alkyl derivatives from the  $[(\text{CyFlCp})\text{M}-\text{Cl}]_2$  dimers also resulted in decomposition. One explanation for the decomposition of the hydride species is that the aromatic C-H groups of the fluorenyl or cyclopentadienyl ligand are activated by the highly Lewis acidic metal centers. A precedent for this type of reaction is provided by the

hydrogenation of  $\text{Cp}^*\text{CpSc}(\text{CH}_3)(\text{PMe}_3)^{40}$  in which intermolecular C-H activation of the ring occurs as shown in figure 16.



**Figure 16: Reaction of Sc-R with unprotected Cp-H bonds.**

Despite the failure of these  $(\text{CyFlCp})\text{Sc-R}$  and  $(\text{CyFlCp})\text{Y-R}$  complexes to act as models for syndiospecific polymerization, insight can be gained toward the design of new  $\text{C}_5$  symmetric ligands for Group III model complexes. Future catalysts must avoid easily activated aromatic C-H bonds and must have enough steric bulk to prevent intermolecular attack of the cyclopentadienyl ligands. Since all homogeneous syndiospecific catalysts to date have incorporated a fluorenyl ligand, in order to avoid aromatic C-H bonds a new ligand not based on fluorenyl was needed. With these new criteria in mind, a target molecule was chosen that incorporated a bis(trimethylsilyl)cyclopentadienyl (BTCp) ligand as the bulky Cp moiety linked to an unsubstituted Cp. The original strategy was to use an isopropylidene linker since the isopropylidene-Cp group was expected to be effectively larger than the TMS groups<sup>11</sup> resulting in exclusively the 1,3,4 isomer as shown in figure 17. The 1,3,4 isomer would result in a  $\text{C}_5$  symmetric complex while the 1,2,4 isomer would result in a  $\text{C}_1$  symmetric complex. The presumed resting states of the protonated ligands would have both silicon groups on the same ring carbon atom.<sup>41</sup>



**Figure 17: Proposed BTCp ligands.**

Unfortunately, the synthesis of these ligands proved exceedingly difficult, so a silicon bridged approach was chosen instead of the isopropylidene bridged approach. The deprotonation of BTCp and subsequent reaction with R<sub>2</sub>SiCl<sub>2</sub> (R = Me, Et, <sup>i</sup>Pr) was carried out as shown in figure 18 yielding mixtures of isomers I and II.

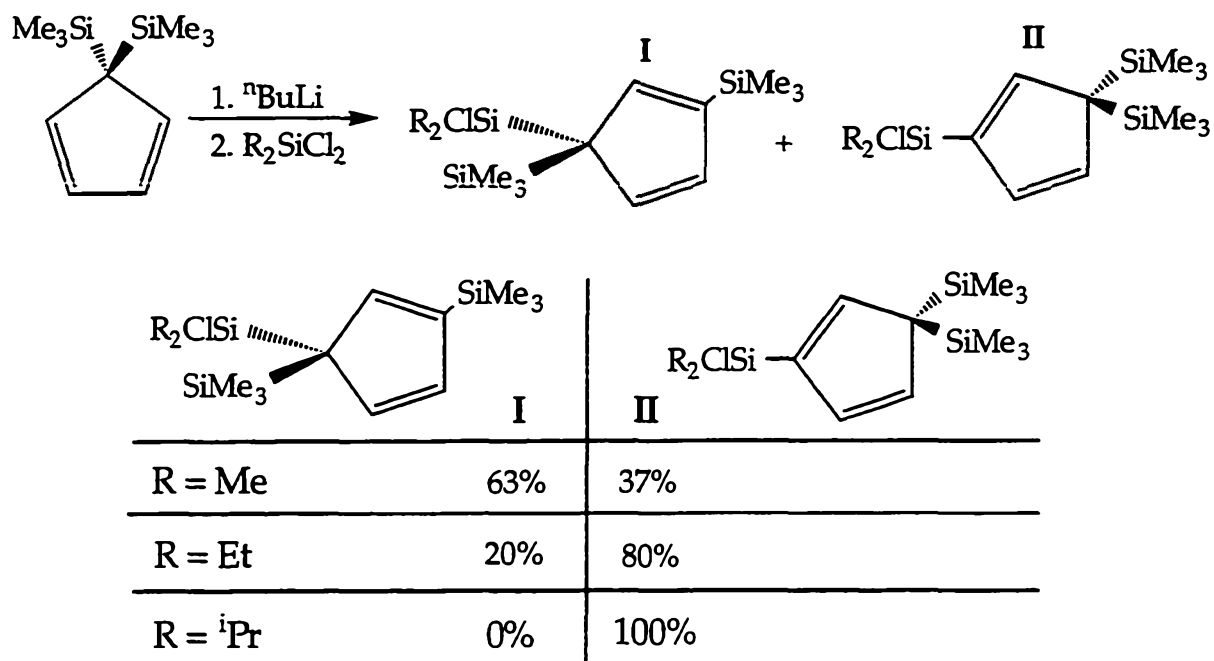


Figure 18: Distribution of isomers in (BTCp) $R_2SiCl$ .

An increase in the size of the alkyl groups on silicon increases the ratio of II/I. Since a silicon has to migrate in order to generate an acidic proton,<sup>41,42</sup> the  $Me_3Si$  group of isomer I is expected to migrate to the 2 position relative to the linking group while the  $Me_3Si$  group of isomer II is expected to migrate to the 3 position relative to the linking group as shown in figure 19.

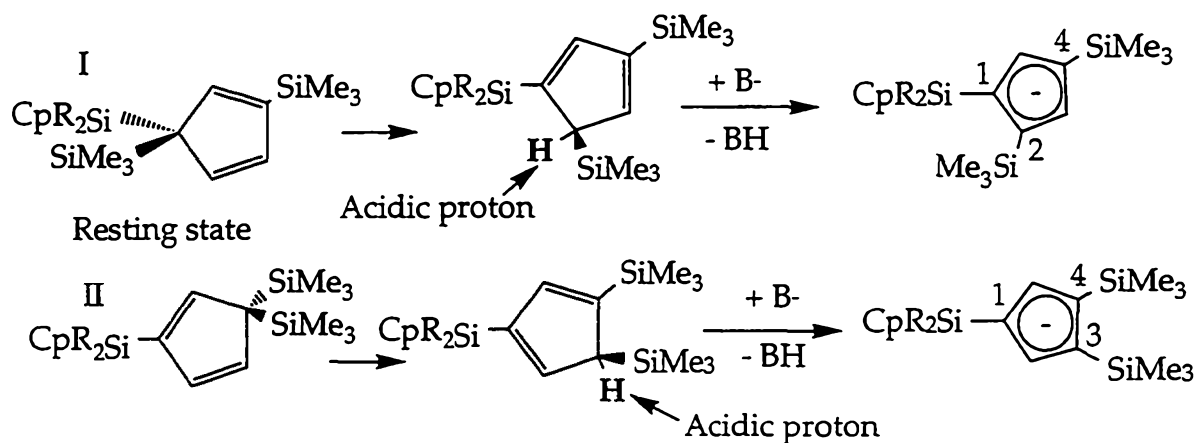


Figure 19:  $SiMe_3$  migrations in deprotonation reactions.<sup>43</sup>

Therefore, since isomer II generates a 1,3,4 and thus  $C_5$  symmetric substitution pattern on the bulky ring,  $^iPr_2Si$  is the best choice for a linking group.



Reaction of  $(\text{BTCp})\text{iPr}_2\text{SiCl}$  with  $\text{NaCp}$  and subsequent double deprotonation with  $\text{KN}(\text{TMS})_2$  yields exclusively the 1,3,4 isomer of the  $(\text{BTCp})\text{iPr}_2\text{SiCp}$  ligand. This ligand has been given the trivial name "Hp."

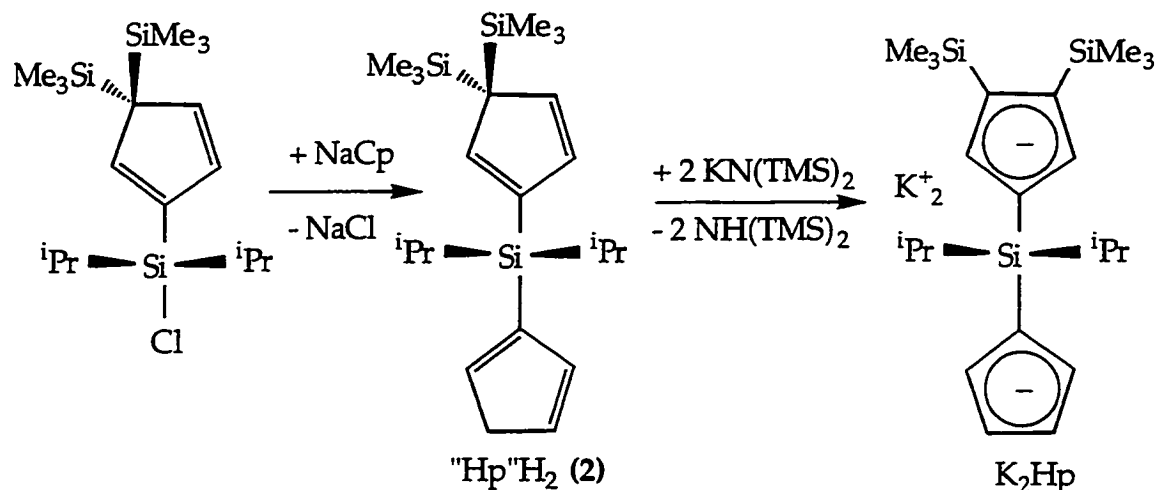


Figure 20: Synthesis of HpH<sub>2</sub> (2) and K<sub>2</sub>Hp.

The reaction of K<sub>2</sub>Hp with YCl<sub>3</sub>·3.5THF in tetrahydrofuran and subsequent workup in ether and petroleum ether yields HpYCl which is presumed to be a chloride bridged dimer.

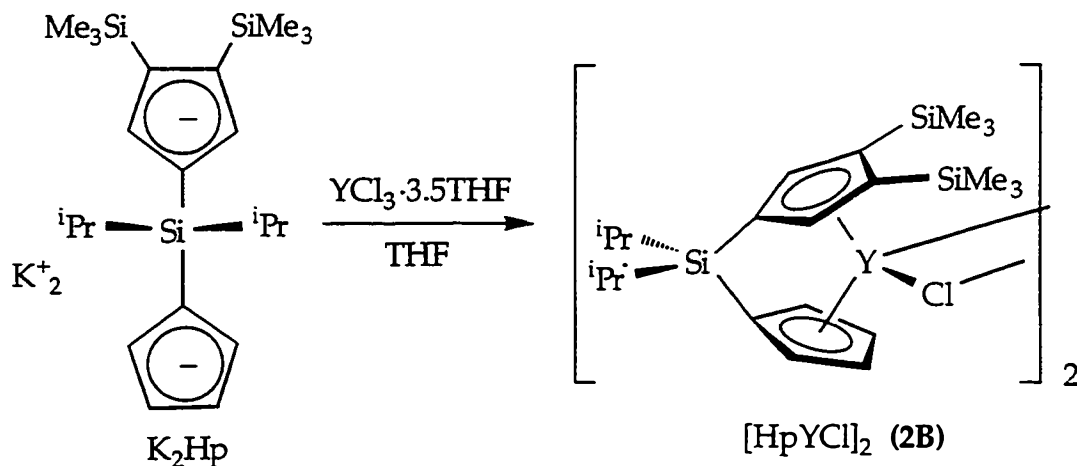
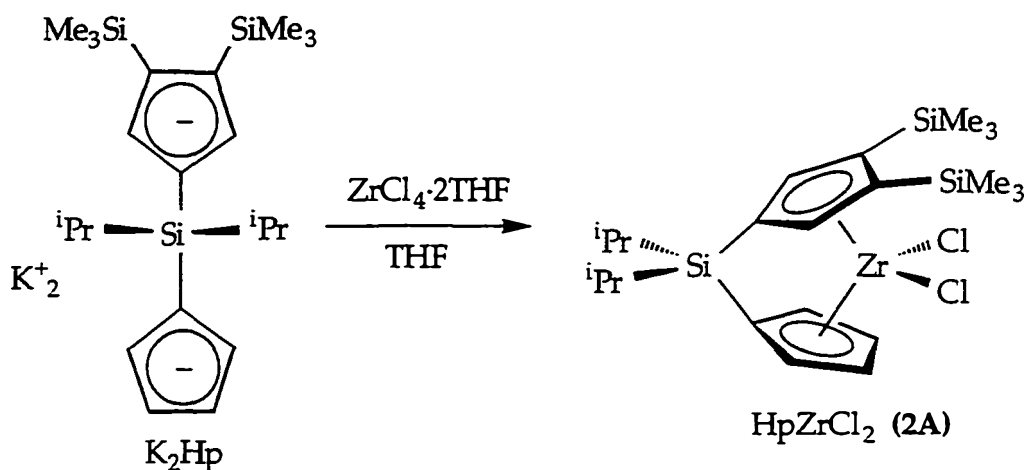


Figure 21: Synthesis of [HpYCl]<sub>2</sub> (2B).

The reaction of [HpYCl]<sub>2</sub> and  $\text{LiCH}(\text{SiMe}_3)_2$  in benzene yields  $\text{HpYCH}(\text{SiMe}_3)_2$ . Some preliminary alkene polymerization studies were carried out and showed that  $\text{HpYCH}(\text{SiMe}_3)_2$  is a very slow catalyst for the polymerization of ethylene and is unreactive with  $\alpha$ -olefins. Hydrogenation

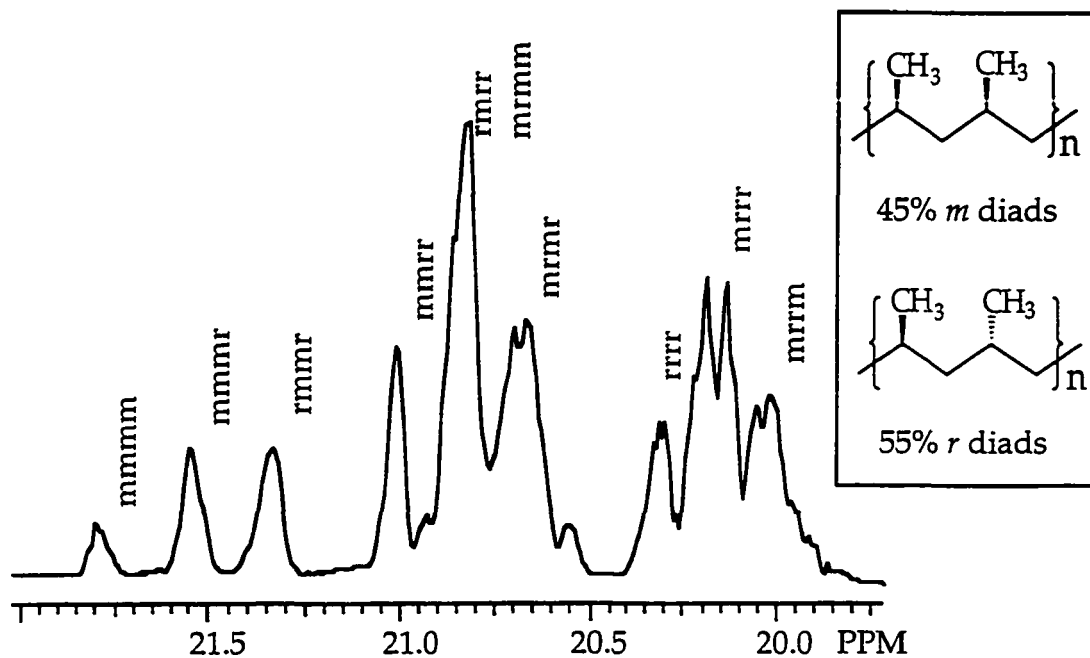
of  $\text{HpYCH}(\text{SiMe}_3)_2$  in  $\text{C}_6\text{D}_{12}$  yields  $[\text{HpYH}]_2$  which is clearly a hydride bridged dimer as shown by a triplet<sup>11</sup> at 2.40 ppm with  $J_{\text{Y-H}} = 33$  Hz in the  $^1\text{H}$  NMR. Unfortunately, preliminary studies show that  $[\text{HpYH}]_2$  does not catalyze  $\alpha$ -olefin polymerization.

In order to determine if further studies with Hp Group III complexes would be relevant to the mechanism of syndiospecific polymerizations, Group IV complexes with the Hp ligand were prepared. Since Group IV complexes are typically more reactive than Group III complexes for  $\alpha$ -olefin polymerization, it was thought that the polymerization of  $\alpha$ -olefins with  $\text{HpZrCl}_2/\text{MAO}$  should be relatively straightforward. Therefore,  $\text{HpZrCl}_2$  was synthesized by the reaction of  $\text{K}_2\text{Hp}$  and  $\text{ZrCl}_4 \cdot 2\text{THF}$  in tetrahydrofuran.



**Figure 22: Synthesis of  $\text{HpZrCl}_2$  (2A).**

Despite the fact that  $\text{HpZrCl}_2$  appears to fit the key criteria for a syndiospecific catalysts as mentioned previously, the polymerization of propylene with  $\text{HpZrCl}_2/\text{MAO}$  yields mostly atactic polypropylene. The  $^{13}\text{C}$  NMR spectrum of the polymer obtained is shown below.



**Figure 23:**  $^{13}\text{C}$  NMR of atactic polypropylene (2a) from  $\text{HpZrCl}_2$  (2A)/ MAO.

X-ray quality crystals of  $\text{HpZrCl}_2$  were obtained by recrystallization from hot methylcyclohexane and the structure was determined by Larry Henling of the Caltech X-Ray Crystallographic Laboratory. Two different views of  $\text{HpZrCl}_2$  are shown in figures 24 and 25 and key bond distances and angles are given in table 2.

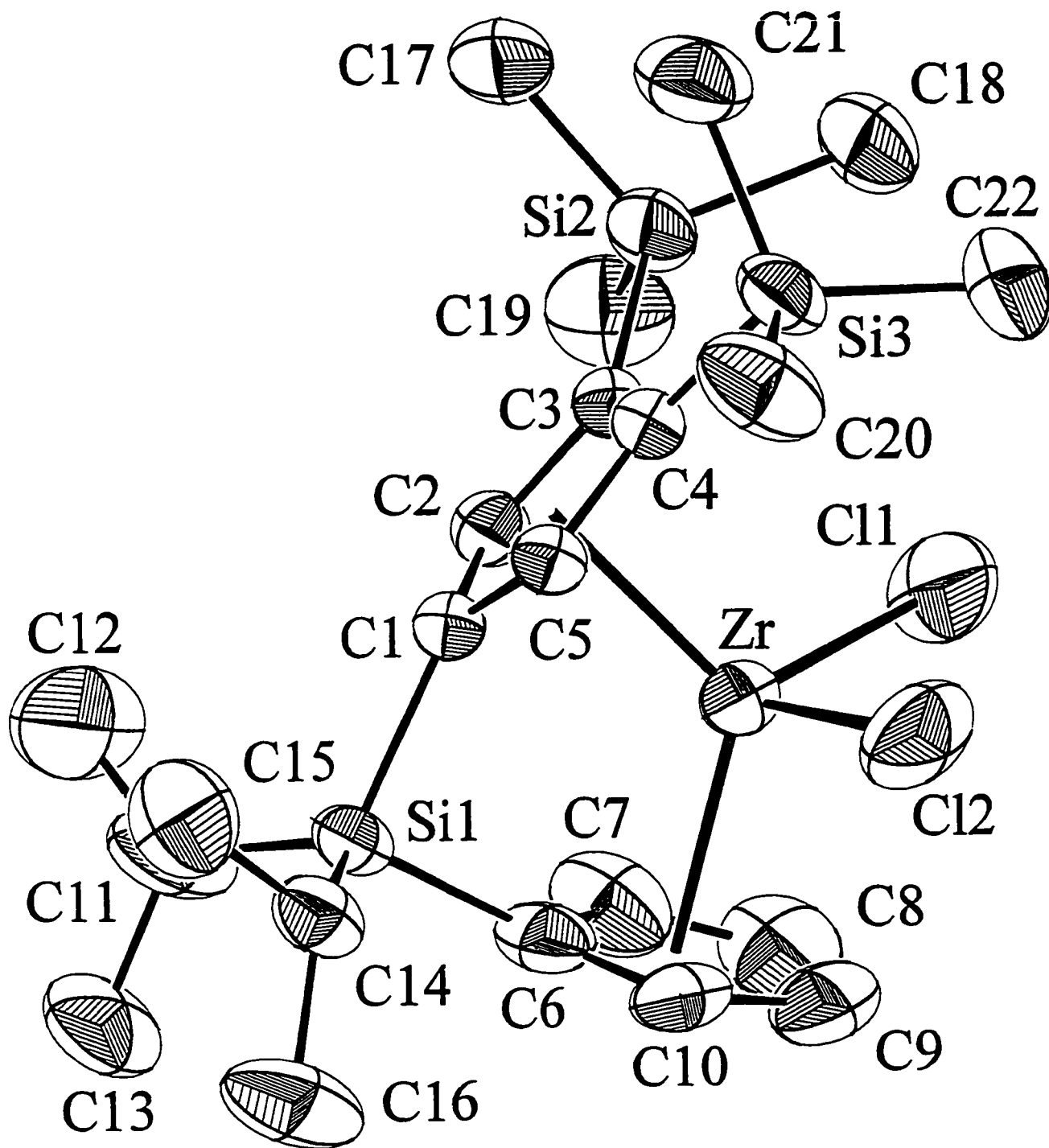


Figure 24: An ORTEP drawing of HpZrCl<sub>2</sub> (2A) with 50% probability ellipsoids showing the numbering system. Hydrogen atoms are not shown.

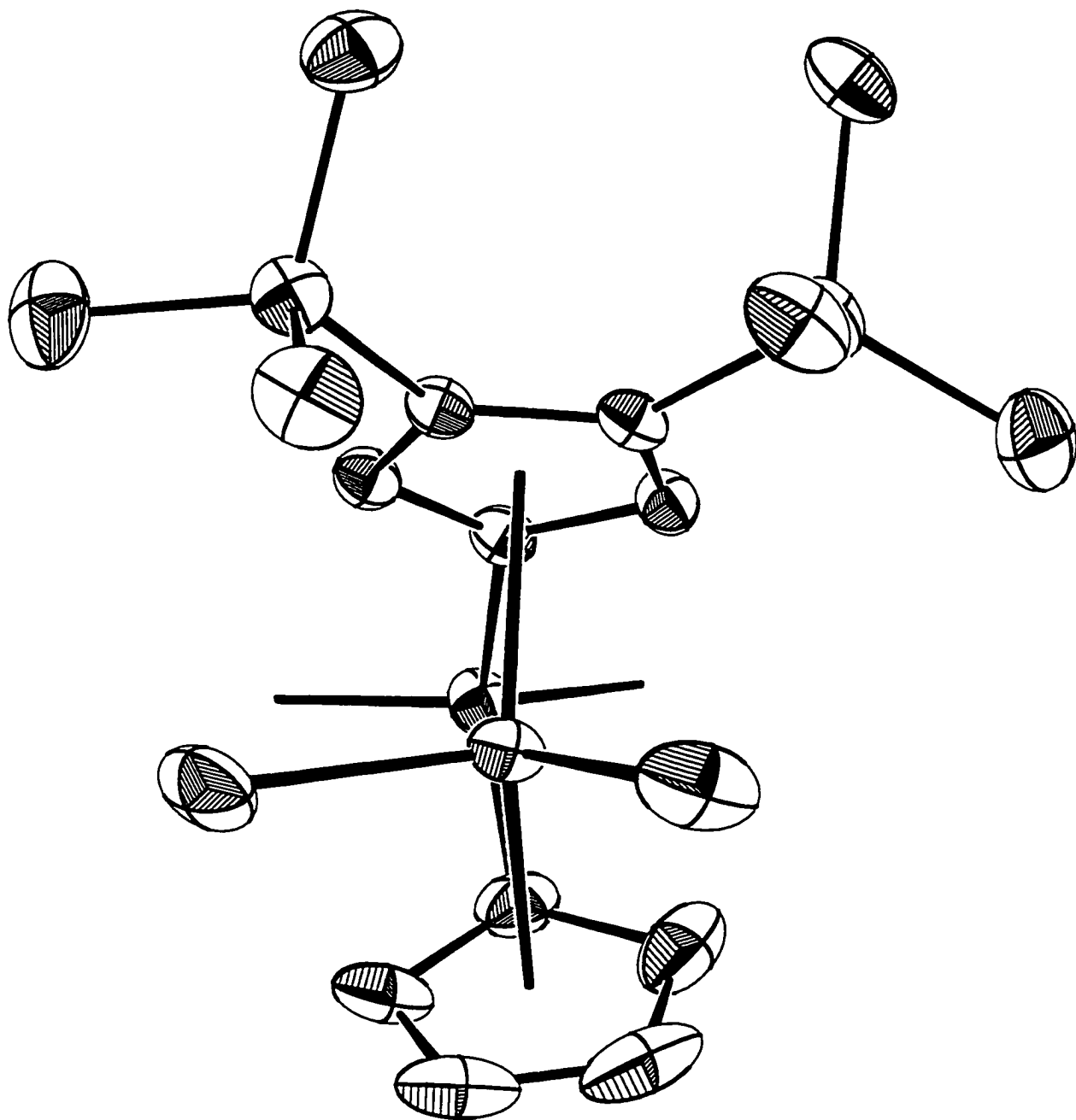


Figure 25: An ORTEP drawing of  $\text{HpZrCl}_2$  (2A) with 50% ellipsoids showing the asymmetry of the chlorine atoms. Isopropyl groups are not shown.

	Distance(Å)		Angle(°)
Zr-Cl1	2.412(1)	CpA-Zr-CpB	122.5
Zr-Cl2	2.435(1)	CpA-CpB dihedral	119.0(2)
Zr-CpA(centroid)	2.217	Cl1-Zr-Cl2	100.5(0)
Zr-CpB(centroid)	2.211	CpA-Zr-Cl1	111.0
Zr-C1	2.471(3)	CpA-Zr-Cl2	107.0
Zr-C2	2.486(3)	CpB-Zr-Cl1	110.2
Zr-C3	2.608(3)	CpB-Zr-Cl2	103.0
Zr-C4	2.587(3)	C6-Si1-C1	93.7(1)
Zr-C5	2.483(3)	C2-C1-Si1	124.1(2)
Zr-C6	2.484(4)	C5-C1-Si1	127.2(2)
Zr-C7	2.473(4)	C7-C6-Si1	125.7(3)
Zr-C8	2.557(5)	C10-C6-Si1	125.3(3)
Zr-C9	2.553(5)	C2-C3-Si2	119.6(2)
ZrC-10	2.498(4)	C4-C3-Si2	133.0(2)
Si1-C1	1.880(3)	C3-C4-Si3	131.4(2)
Si1-C6	1.872(4)	C5-C4-Si3	121.9(2)
Si1-C11	1.865(5)		
Si1-C14	1.865(3)		
Si2-C3	1.890(3)		
Si3-C4	1.898(3)		
C4-C9	5.055		
C3-C8	4.774		
C5-C10	3.823		
C2-C7	3.302		

**Table 2: Selected bond distances and angles for HpZrCl<sub>2</sub> (2A)  
(a complete table is provided in Appendix B).**

The most notable feature of this crystal structure is the strong interaction between the two trimethylsilyl groups as evidenced by the  $\sim 10^\circ$  difference between the C2-C3-Si2 and C5-C4-Si3 bond angles and the C4-C3-Si2 and C3-C4-Si3 bond angles. The Cp rings are also twisted out of plane such that the distance between opposite carbons on CpA and CpB vary dramatically. In a typical ansa metallocene, the C4-C9 bond distance should be very similar to the C3-C8 bond distance and likewise for C5-C10 and C2-C7. However, in

$\text{HpZrCl}_2$ , these distances differ by as much as  $0.5\text{\AA}$ . This is likely due to non-bonding interactions between the chlorines and the trimethylsilyl groups. Another result of these interactions are the non- $C_s$  symmetric orientation of the trimethylsilyl groups as shown in figure 25.

Comparison of the crystal structures of  $[\text{CyFlCp}]\text{ZrCl}_2$ <sup>44</sup> and  $\text{HpZrCl}_2$  sheds some light on the difference in selectivity of the two catalysts. The fluorenyl moiety is a flat group which extends out in a plane with a small pocket in the center of the front of the ligand while the trimethylsilyl groups of bis(trimethylsilyl)cyclopentadienyl extend above and below the plane of the cyclopentadienyl ligand completely filling the so called "pocket" that is present in the fluorenyl.

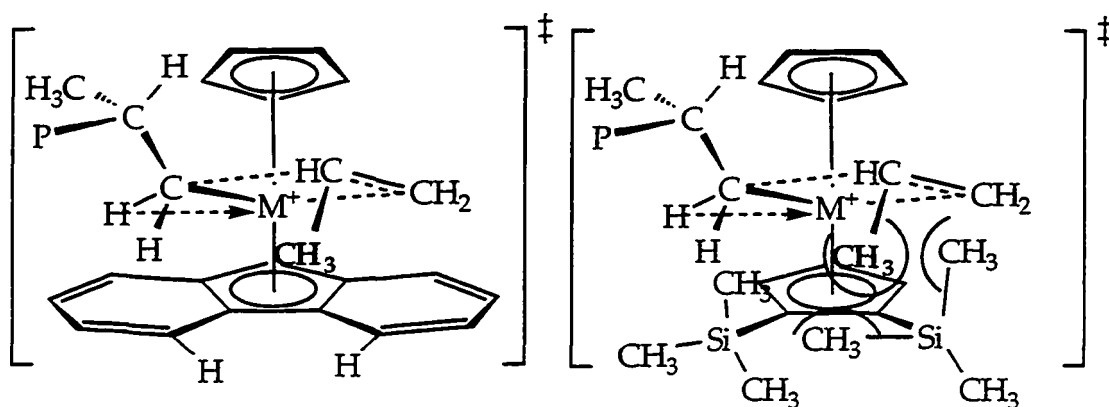


Figure 26: Comparison between "pocket" of fluorene and  $(\text{TMS})_2\text{Cp}$ .

Thus, the insertion of olefin with the methyl group toward the larger ligand would either be blocked or would be disfavored in the case of  $\text{HpZrCl}_2$ . Assuming, therefore, that the insertion of olefins into  $\text{HpZr}^+\text{R}$  is relatively high in energy, error mechanisms such as epimerization or site isomerization could now be competitive with olefin insertion, resulting in essentially atactic polypropylene.

### III. Conclusions from Part 1:

The apparent reactivity of the  $\text{CyFlCp}$  ligand with Group III alkyls and hydrides is presumed to make it unacceptable in these highly Lewis acidic Group III complexes. The  $\text{Hp}$  ligand is certainly more suitable in terms of the stability of hydride species but  $[\text{HpYH}]_2$  unfortunately does not catalyze the polymerization of  $\alpha$ -olefins. Polymerization studies with  $\text{HpZrCl}_2/\text{MAO}$

gave only atactic polypropylene. Therefore, further studies with the yttrium analogs were not carried out. The major conclusion to be drawn from this work is that a new ligand system is necessary to carry out these kinds of studies with group III metals. An additional criterion for syndiospecificity of a pocket in the larger Cp is proposed to explain the aspecific polymerization of  $\text{HpZrCl}_2$ .

## Part 2: Development, synthesis, and reactivity of a new family of syndiospecific catalysts.

### IV. Results and Discussion:

Based on the results of part 1, a new catalyst system was sought for syndiospecific polymerization of  $\alpha$ -olefins. Due to the increased likelihood of obtaining active catalysts with Group IV complexes, Group IV syndiospecific catalysts were chosen as the preliminary goal. The target ligand would have to incorporate a "pocket" in the larger ligand in addition to the previous requirements of  $C_s$  symmetry and Cp ligands of greatly differing size. After considering a number of disubstituted ligands, it became clear that it would be difficult to find a 1,2 disubstituted Cp ligand with a pocket bigger than that of fluorenyl. A 1,3 disubstituted cyclopentadienyl should therefore be preferable since it provides a large pocket for the methyl group of an inserting propylene. In order to maintain  $C_s$  symmetry with a 1,3-dialkylcyclopentadienyl moiety, a double bridge is required as shown below.

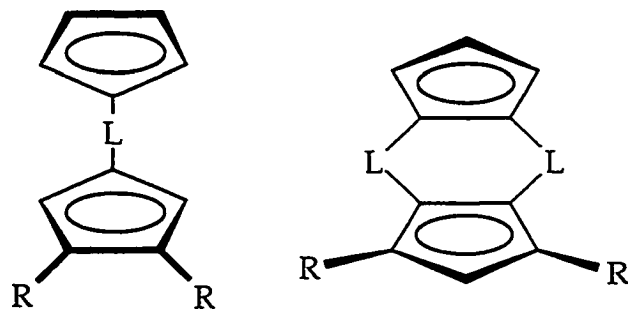
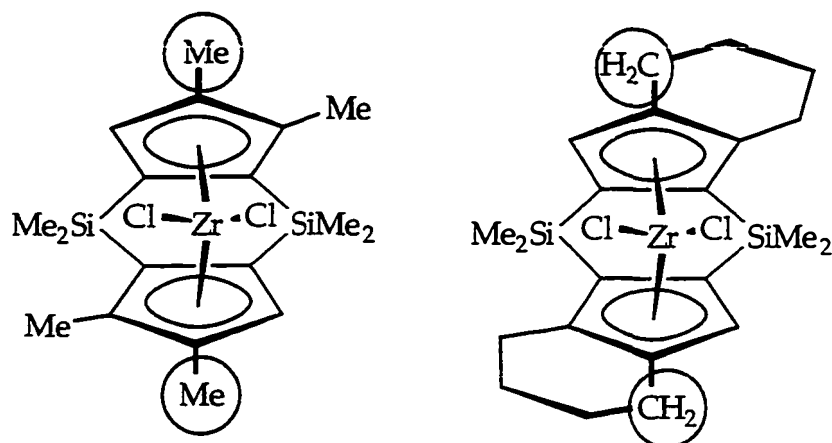


Figure 27: 1,2-disubstituted vs. 1,3 disubstituted Cp ligands.

A number of doubly bridged Group IV metallocenes have been prepared in the literature.<sup>45-47</sup> All of these complexes have had either  $C_{2v}$  or  $C_2$



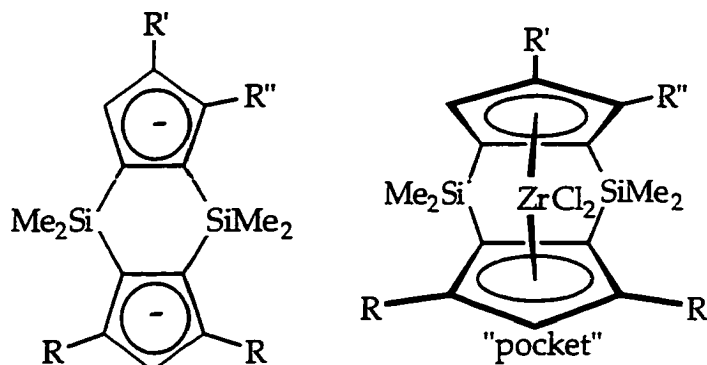
symmetry. Brintzinger has prepared two different  $C_2$  symmetric complexes as shown below.



**Figure 28: Brintzinger's doubly bridged metallocenes.<sup>47</sup>**

Both of these complexes are active catalysts for the polymerization of ethylene, but both have extremely low activity for propylene polymerization. Brintzinger attributes this to bad steric interactions between the methyl groups of propylene and the circled groups in figure 28.<sup>1</sup> This result supports the idea that a pocket is required for propylene insertion since there is no pocket in either of Brintzinger's doubly bridged complexes.

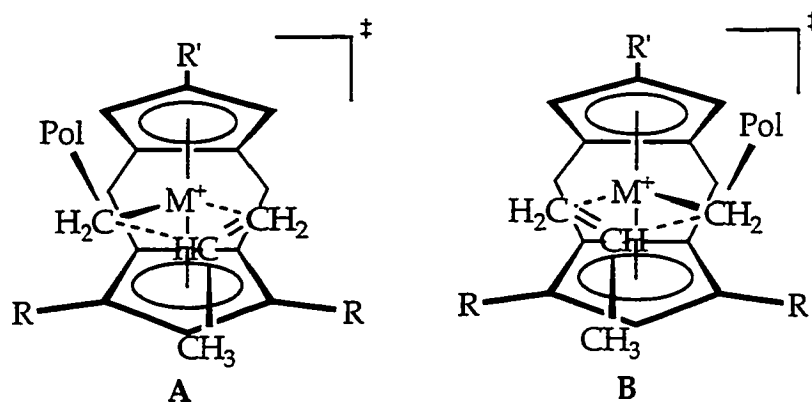
With this in mind, a new catalyst system was designed. The two key design criteria were the presence of a "pocket" in the larger moiety, which was accomplished by using a 1,3-dialkylcyclopentadienyl, and an easily varied alkyl group, which is R' in figure 29. A double dimethylsilyl bridge was incorporated to maintain  $C_s$  symmetry. The general ligand and metallocene design is shown below.



**Figure 29: New ligand design.**

Careful substitutions at R and R' were expected to increase the enantiofacial selectivity of olefin insertion and prevent site isomerization.  $C_1$  symmetric metallocenes would also be available by the use of a chiral group at R' or by alkyl groups other than H for R."

The  $C_s$  symmetric versions of these catalysts where R' is an achiral alkyl group and R'' is H are well suited to syndiospecific polymerization since alternating between transition states A and B,<sup>48</sup> as shown in figure 9, should yield alternating stereochemistry on the backbone of the resulting polymer chain.

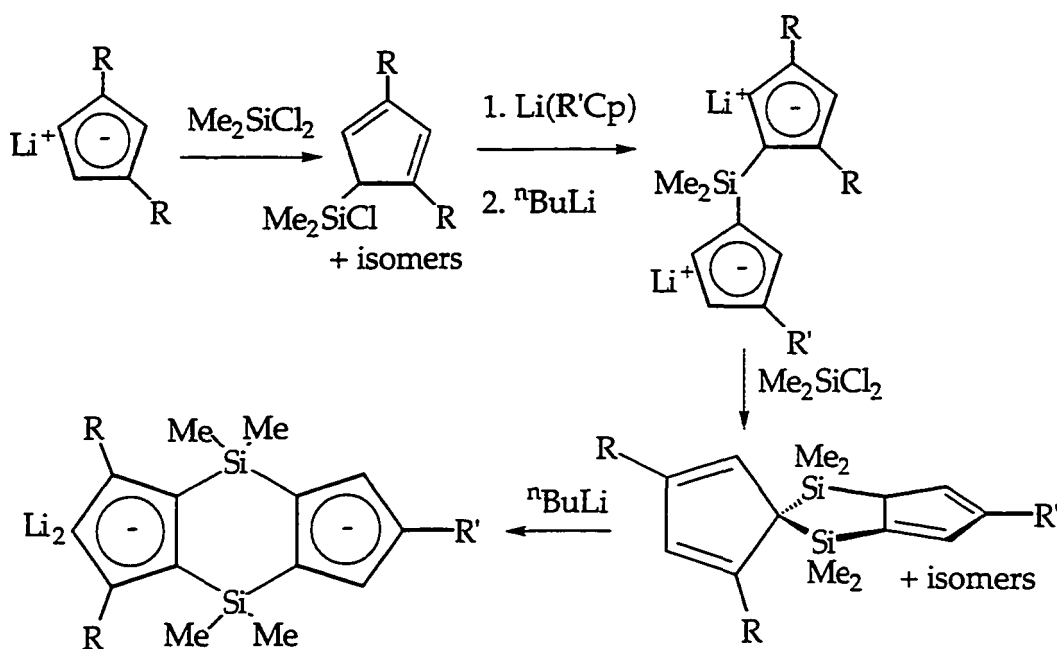


**Figure 30: Proposed transition states for olefin insertion with  $C_s$  symmetric catalysts.**

The key features of the proposed transition states for propylene insertion are the following: the polymer chain is directed up and away from one of the R groups and the methyl group of the inserting olefin is directed anti to the  $\beta$ -C of the polymer chain as well as being directed down and away from the R'

group.<sup>33,34</sup> These interactions were expected to work in concert resulting in highly syndioselective olefin polymerization.

**Synthesis:** The synthetic approach used to prepare these complexes is very similar to that developed by Bulls<sup>49</sup> and Brintzinger<sup>47</sup> where a singly bridged dianionic ligand is treated with dimethylsilyldichloride to form the doubly bridged protonated ligand. The key difference is in the synthesis of the asymmetric singly linked ligand. The basic approach is shown below.

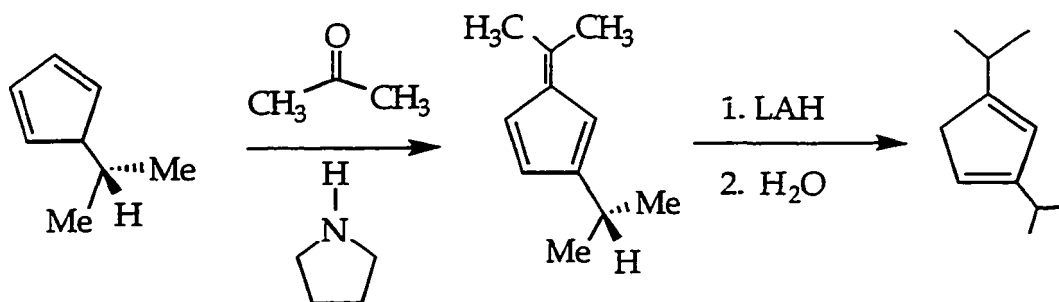


**Figure 31: Synthetic scheme for doubly bridged ligands.**

The first step in the synthesis of these types of catalysts is the synthesis of 1,3-dialkylcyclopentadienes. 1,3-di(*tert*-butyl)cyclopentadiene has been prepared by Casserly<sup>50</sup> so it was a straightforward starting point. Using this synthetic scheme, singly bridged dianionic ligands were prepared, but the second linking reaction was never successful despite considerable effort. After a molecular modeling analysis of the expected structure, it was determined that the *tert*-butyl groups were too bulky to allow for the second linking group. For comparison, it is exceedingly difficult to prepare other bulky tetrasubstituted cyclopentadienyls.<sup>41</sup>

Therefore, 1,3-diisopropylcyclopentadiene was selected as the starting point for the synthesis. Unfortunately, the reported syntheses of 1,3-

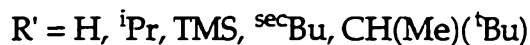
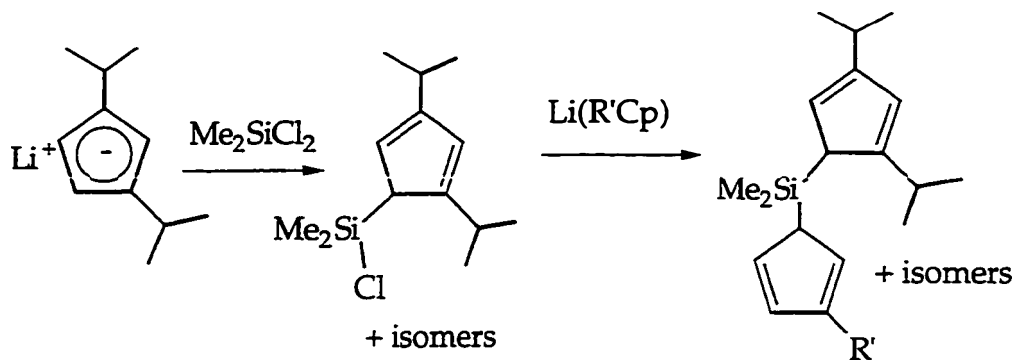
diisopropylcyclopentadiene<sup>51</sup> gave low yields since the final step was always separation of the 1,3 product from the 1,2 product. A more selective method was found by extension of work by Nile<sup>52-54</sup> in which he prepared a number of 1,3 disubstituted cyclopentadienes using a fulvene route. Using this method, reaction of isopropylcyclopentadiene with acetone catalyzed by pyrrolidine gave the 3-isopropyl-6,6-dimethylfulvene. Subsequent reduction of the fulvene with LAH and hydrolysis provided 1,3-diisopropylcyclopentadiene, "*i*Pr<sub>2</sub>Cp."



**Figure 32: Preparation of 1,3-diisopropylcyclopentadiene.**

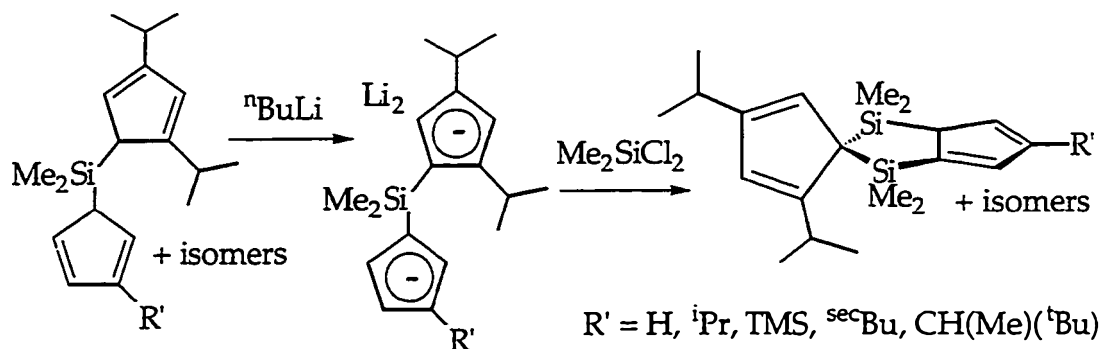
This synthesis is amenable to large scales and has been used to prepare over 400 g of 1,3-diisopropylcyclopentadiene in a single prep in 74% yield from isopropylcyclopentadiene.<sup>55</sup>

1,3-diisopropylcyclopentadiene is easily deprotonated with <sup>n</sup>BuLi in pentane to yield lithium(1,3-diisopropylcyclopentadienylyde) "Li(*i*Pr<sub>2</sub>Cp)" in high yield. Following the route in figure 31, the reaction of Li(*i*Pr<sub>2</sub>Cp) with excess dichlorodimethylsilane in tetrahydrofuran at -78°C yields (*i*Pr<sub>2</sub>Cp)Me<sub>2</sub>SiCl in over 90% yield as a yellow oil. Reaction of (*i*Pr<sub>2</sub>Cp)Me<sub>2</sub>SiCl with the lithium salt of R'Cp {R' = H, *i*Pr, TMS, <sup>sec</sup>Bu, or CH(Me)(<sup>t</sup>Bu)} yields the singly bridged ligand, "(*i*Pr<sub>2</sub>Cp)Me<sub>2</sub>Si(R'Cp)," as yellow oils which can be kugel-röhr distilled at high vacuum at 90- 120°C.



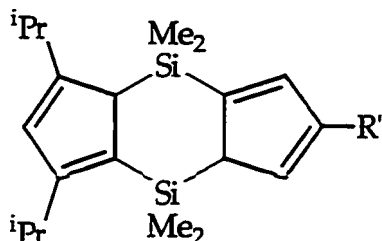
**Figure 33: Synthesis of singly bridged ligands.**

Deprotonation of  $(\text{}^i\text{Pr}_2\text{Cp})\text{Me}_2\text{Si}(\text{R}'\text{Cp})$  with  ${}^n\text{BuLi}$  in ether yields the singly bridged dianions,  $\text{Li}_2[(\text{}^i\text{Pr}_2\text{Cp})\text{Me}_2\text{Si}(\text{R}'\text{Cp})]$ , as fine white solids. Reaction of  $\text{Li}_2[(\text{}^i\text{Pr}_2\text{Cp})\text{Me}_2\text{Si}(\text{R}'\text{Cp})]$  with  $\text{Me}_2\text{SiCl}_2$  in tetrahydrofuran at  $-78^\circ\text{C}$  yields the doubly bridged ligands,  $(\text{}^i\text{Pr}_2\text{Cp})(\mu\text{-Me}_2\text{Si})_2(\text{R}'\text{Cp})$ , as shown below.<sup>56</sup>



**Figure 34: Synthesis of doubly bridged ligands, R'Thp (3-7).**

The doubly bridged ligands are kugel-röhr distilled at high vacuum and  $90$ – $130^\circ\text{C}$ . The overall yields of these reactions are typically in excess of 50% overall based on  $\text{}^i\text{Pr}_2\text{Cp}$ . These ligands have been given the trivial names R'Thp as shown in figure 35.



	R'	ligand name
3	-H	Thp
4	-CHMe <sub>2</sub>	<sup>i</sup> PrThp
5	-SiMe <sub>3</sub>	TMSThp
6	-CH(Me)(Et)	<sup>s</sup> BuThp
7	-CH(Me)( <sup>t</sup> Bu)	MNThp

Figure 35: Ligand 3-7 names.

These R'Thp ligands can be deprotonated with either  $\text{LiCH}_2(\text{SiMe}_3)$ ,  $^n\text{BuLi}$  or  $\text{KO}^t\text{Bu}$  to yield the  $C_5$  symmetric dianionic ligands for Thp and TMSThp and  $C_1$  symmetric dianionic ligands for <sup>s</sup>BuThp and MNThp.

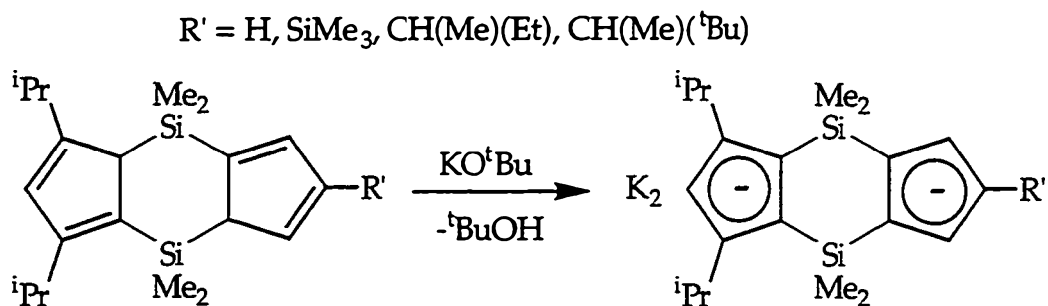


Figure 36: Deprotonation of R'Thp (3, 5, 6, and 7).

The only exception among the five different ligands presented above is the deprotonation of <sup>i</sup>PrThp. Reaction of <sup>i</sup>PrThp with either  $\text{LiCH}_2\text{SiMe}_3$  or  $\text{KO}^t\text{Bu}$  yields a mixture of the  $C_5$  symmetric 1,2,4 and the  $C_1$  symmetric 1,2,3 isomers shown below.

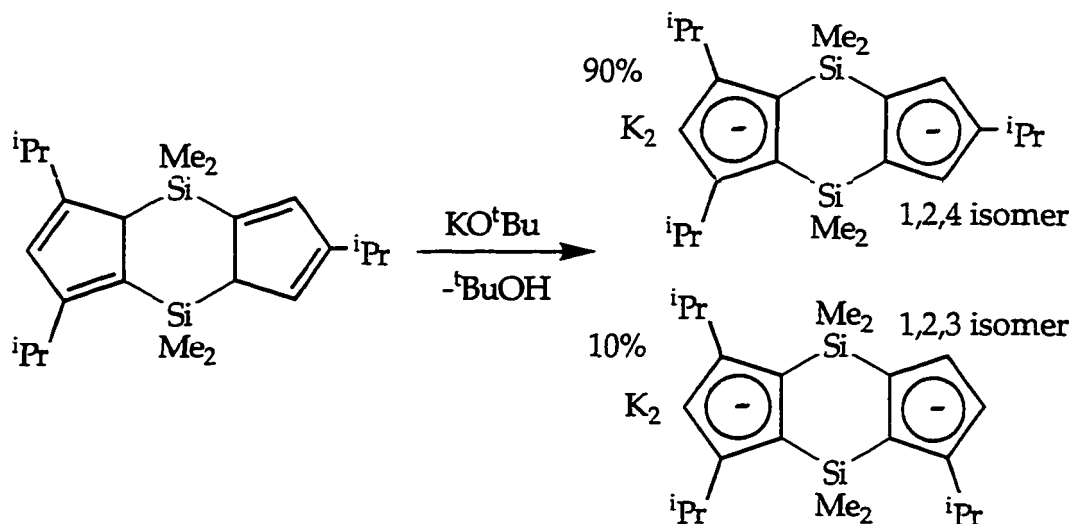
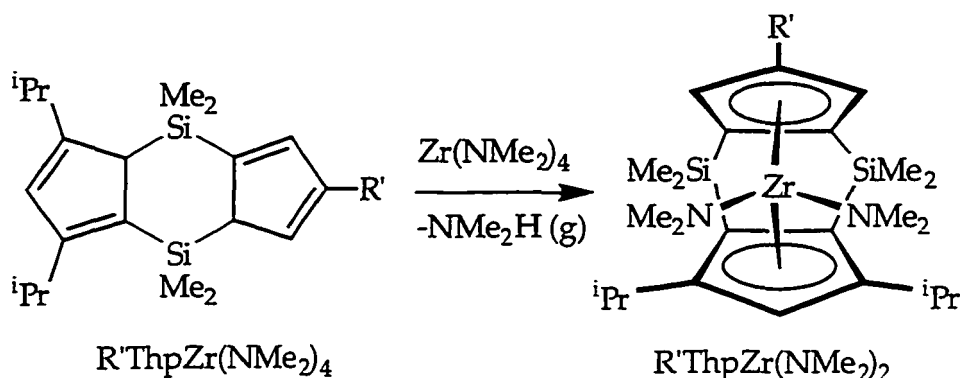


Figure 37: Deprotonation of *i*PrThp (4).

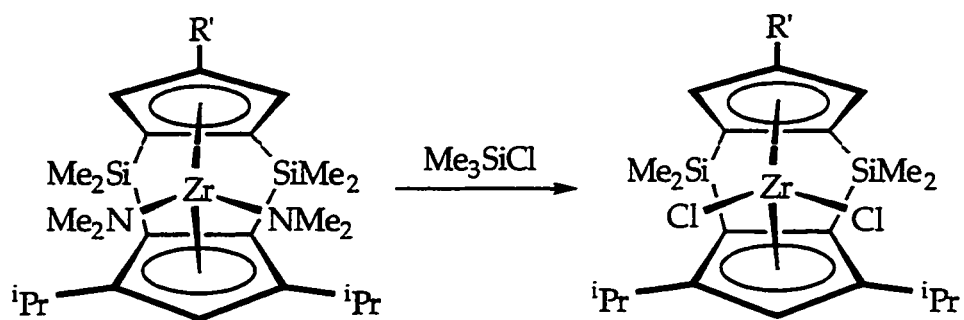
Fortunately, this problem with *i*PrThp deprotonation was solved by a one step deprotonation and metallation. Metallation of all of these ligands is carried out using an amine elimination route<sup>20,57,58</sup> in which the protonated R'Thp ligands are treated with  $\text{Zr}(\text{NMe}_2)_4$  in refluxing xylenes with a strong argon purge. The strong purge is necessary to remove dimethylamine gas from the reaction as it forms and thus drives the reaction to completion. Reaction of R'Thp, including *i*PrThp, with  $\text{Zr}(\text{NMe}_2)_4$  yields exclusively the 1,2,4 isomer of  $\text{R'ThpZr}(\text{NMe}_2)_2$ .<sup>59</sup>



R' = H (3A), *i*Pr (4A),  $\text{SiMe}_3$  (5A),  $\text{CH}(\text{Me})(\text{Et})$  (6A),  $\text{CH}(\text{Me})(^t\text{Bu})$  (7A)

Figure 38: Metallation of R'Thp (3-7) to form 3A-7A.

Reaction of  $\text{R'ThpZr}(\text{NMe}_2)_2$  with excess trimethylsilylchloride<sup>60</sup> in toluene results in rapid formation of  $\text{Me}_3\text{Si}(\text{NMe}_2)$  and  $\text{R'ThpZrCl}_2$ .



$\text{R}' = \text{H}$  (**3B**),  $i\text{Pr}$  (**4B**),  $\text{SiMe}_3$  (**5B**),  $\text{CH}(\text{Me})(\text{Et})$  (**6B**),  $\text{CH}(\text{Me})(i\text{Bu})$  (**7B**)

**Figure 39: Synthesis of  $\text{R}'\text{ThpZrCl}_2$  (**3B** - **7B**).**

This synthetic scheme has proven to be an effective means of producing a variety of  $\text{C}_s$  and  $\text{C}_1$  symmetric complexes.<sup>61</sup>

**Structure:** A crystal structure of  $i\text{PrThpZrCl}_2$  (**4B**) has been obtained by recrystallisation from hot methylcyclohexane. Two different views are provided in figures 40 and 41 and selected bond distances and angles are provided in table 3.



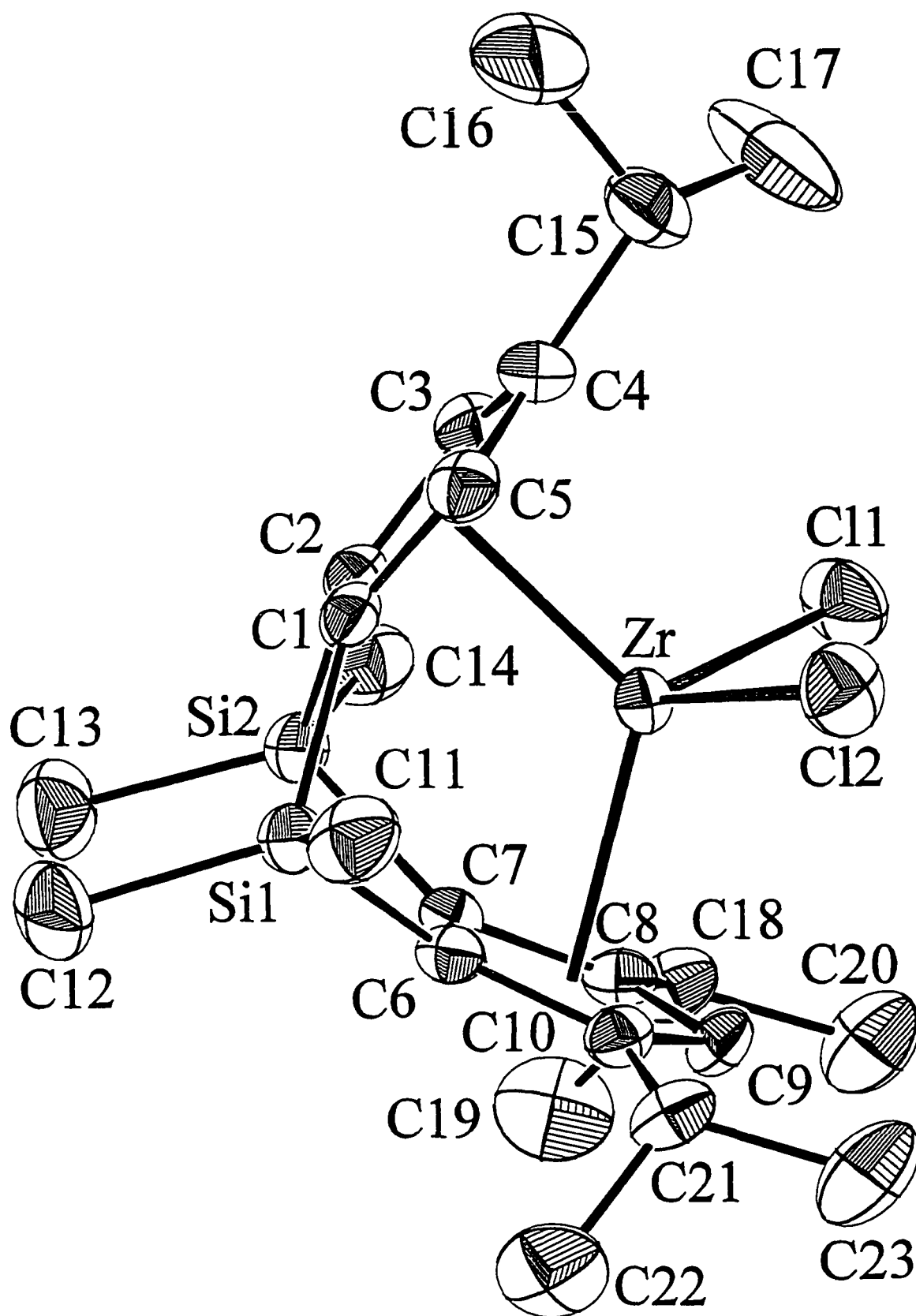


Figure 40: An ORTEP drawing of  $i\text{PrThpZrCl}_2$  (4B) with 50% probability ellipsoids showing the numbering system. Hydrogen atoms are not shown.

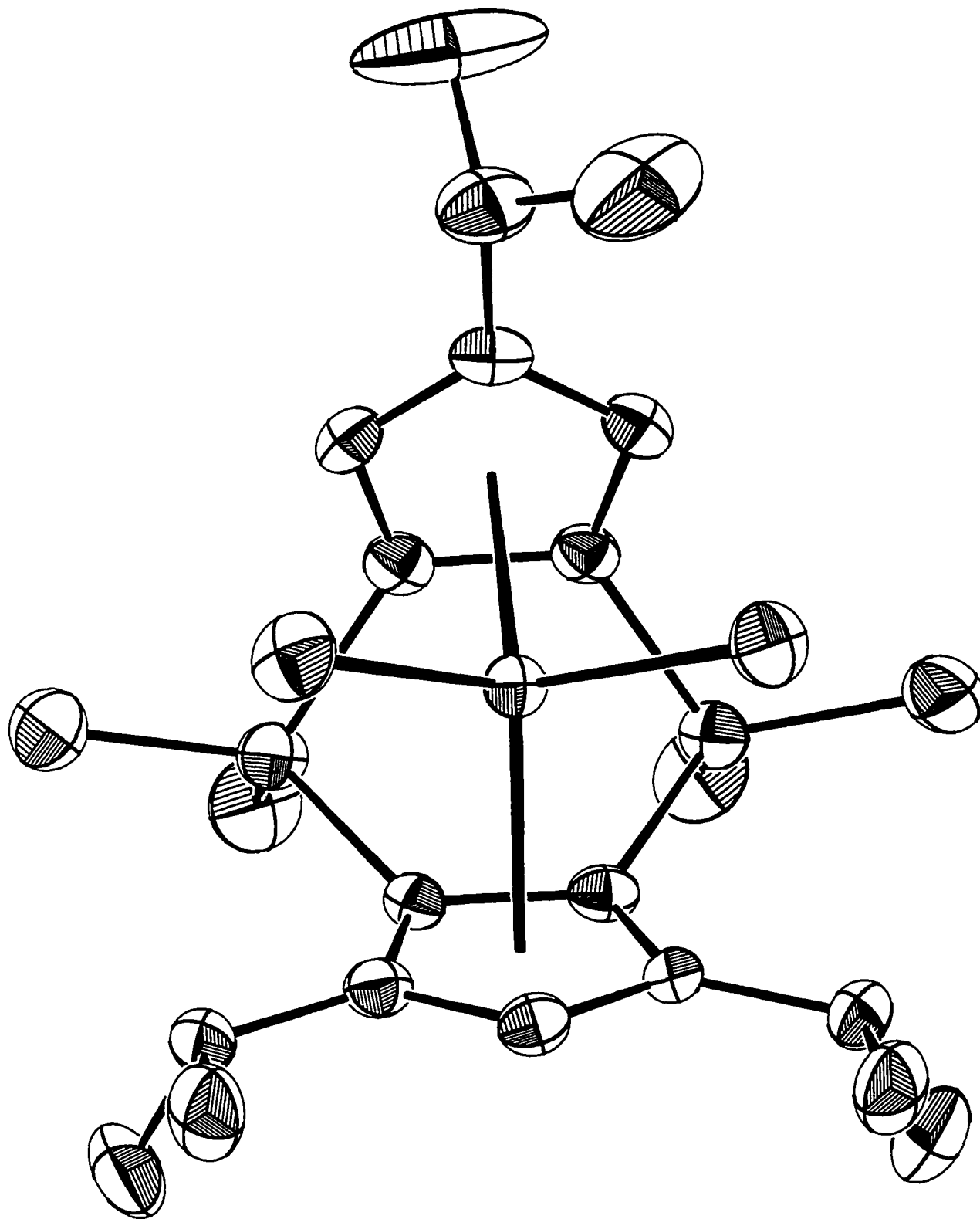


Figure 41: An ORTEP drawing of  $i\text{PrThpZrCl}_2$  (4B) with 50% probability ellipsoids. Hydrogen atoms are not shown.

	Distance(Å)		Angle(°)
Zr-Cl1	2.432(2)	CpA-Zr-CpB	120.3
Zr-Cl2	2.424(2)	CpA-CpB dihedral	73.9(2)
Zr-CpA(centroid)	2.217	Cl1-Zr-Cl2	100.4(1)
Zr-CpB(centroid)	2.240	CpA-Zr-Cl1	109.1
Zr-C1	2.441(5)	CpA-Zr-Cl2	108.1
Zr-C2	2.428(5)	CpB-Zr-Cl1	107.7
Zr-C3	2.550(5)	CpB-Zr-Cl2	109.5
Zr-C4	2.652(5)	C6-Si1-C1	91.6(2)
Zr-C5	2.565(5)	C7-Si2-C2	92.1(2)
Zr-C6	2.415(5)	C5-C1-Si1	125.2(4)
Zr-C7	2.418(5)	C3-C2-Si2	127.4(4)
Zr-C8	2.624(5)	C10-C6-Si1	128.0(4)
Zr-C9	2.673(5)	C8-C7-Si2	127.2(4)
Zr-C10	2.617(5)		
Si1-C1	1.875(5)		
Si1-C6	1.888(5)		
Si2-C2	1.870(5)		
Si2-C7	1.887(5)		
C4-C15	1.518(8)		
C8-C18	1.514(7)		
C10-C21	1.517(7)		

**Table 3: Selected bond distances and angles for  $i\text{PrThpZrCl}_2$  (4B).**  
(A complete table is provided in Appendix C.)

The most dramatic feature of this structure is the  $73.9^\circ$  dihedral angle between the two Cp planes which is similar to other double bridged zirconium metallocenes.<sup>47</sup> For comparison, a typical single silicon bridged zirconium metallocene<sup>62</sup> has a  $62.6^\circ$  dihedral angle and most unbridged zirconium metallocenes have a  $\sim 50^\circ$  dihedral angle.<sup>63</sup> Thus, introducing a second linking group increases the openness of the wedge which may result in a less crowded active site for polymerization and the high activity of these catalysts. The orientation of the isopropyl group in the R' position seems to break the  $C_s$  symmetry, but rotation about the C4-C15 bond is fast on the NMR time scale since only one doublet is observed for the methyl groups (C16 and C17)

by  $^1\text{H}$  NMR. For all three isopropyl groups, the face of the tetrahedron made up of the methine carbon atom, the methine proton, one of the methyl groups, and the adjacent Cp-carbon atom is directed towards the metal.

In structural terms, this complex meets all of the criteria that were presented as goals for this research. The two Cp ligands are of greatly differing size and shape, since the steric bulk of  $^i\text{Pr}_2\text{Cp}$  extends out to the sides while the steric bulk of  $^i\text{PrCp}$  extends out to the front along the plane of symmetry. Finally, there is a pocket in the  $^i\text{Pr}_2\text{Cp}$  moiety to allow for the methyl group of the inserting olefin. The isopropyl group of  $^i\text{PrCp}$  may serve two beneficial roles in that it may prevent misinsertion of olefin and/or block site isomerization.

**Polymerization:** In order to explore the reactivity of these new catalysts and to determine the effect of substitutions at R' on stereospecificity, a number of polymerizations were run. The 16 e<sup>-</sup> zirconium catalysts, R'ThpZrCl<sub>2</sub> (3B-7B), when activated by methylaluminoxane (MAO), initiate rapid polymerization of  $\alpha$ -olefins to form polyolefins. The presumed initiating species for this type of reaction is a 14 e<sup>-</sup>, d<sup>0</sup> cationic metal alkyl<sup>6,8,64</sup> as shown below.

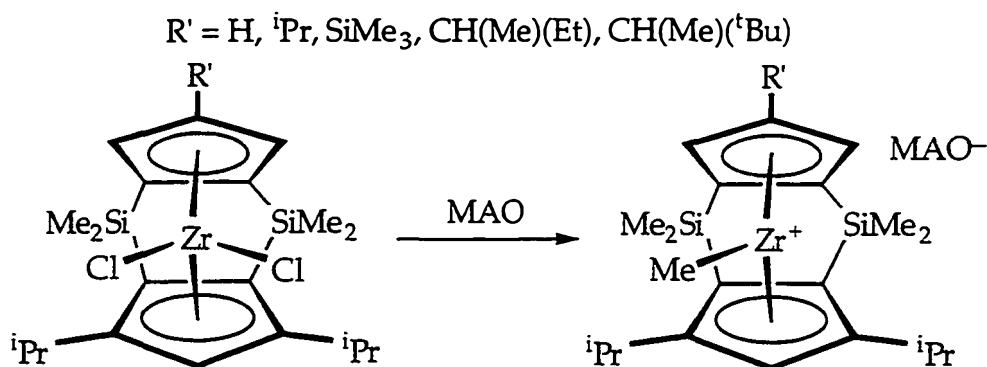
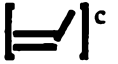


Figure 42: Activation of R'ThpZrCl<sub>2</sub> (3B - 7B) with MAO.

A table of propylene polymerization data is included below:

Entry	Cat <sup>a</sup>	R'	T °C	 <sup>c</sup>	Activity <sup>d</sup>	[r <sup>4</sup> ] <sup>e</sup>	[m <sup>4</sup> ] <sup>e</sup>	[r] <sup>f</sup>	[m] <sup>g</sup>
3a	3B	H	0°	neat	2160	83.7	0.0	94.0	6.0
3b	(C <sub>s</sub> ) <sup>b</sup>	H	25°	40 psig	300	27.3	~0	74.1	25.9
3c		H	60°	neat	74,200	76.0	0.1	92.6	12.6
4a	4B	iPr	0°	neat	1750	98.9	0	99.6	0.4
4b	(C <sub>s</sub> ) <sup>b</sup>	iPr	25°	40 psig	230	38.8	~0	75.6	24.3
5a	5B	TMS	0°	neat	1730	95.9	0	99.0	1.0
5b	(C <sub>s</sub> ) <sup>b</sup>	TMS	25°	40 psig	230	33.9	~0	75.2	24.8
6a	6B	<sup>s</sup> Bu	0°	neat	1500	83.1	0.0	94.4	5.6
6b	(C <sub>1</sub> ) <sup>b</sup>	<sup>s</sup> Bu	25°	40 psig	200	20.0	4.8	62.0	38.0
7a	7B	MN	0°	neat	930	41.8	5.6	73.5	26.5
7b	(C <sub>1</sub> ) <sup>b</sup>	MN	25°	40 psig	156	0	61.2	14.6	85.4
7d		MN	25°	10 psig	110	0	58.5	17.6	82.4

**Table 4 Polymerization data for catalysts 3B-7B.**

<sup>a</sup>Complete data in experimental section. <sup>b</sup>Symmetry of catalyst. <sup>c</sup>Except for those in neat propylene (50 ml), samples were run in toluene (35 ml).

<sup>d</sup>Grams of polymer isolated /g catalyst/ hour (activity numbers are approximate at best). <sup>e</sup>% of [r r r r] and [m m m m] pentad by <sup>13</sup>C NMR (complete data in table 6). <sup>f</sup>[r] = [rr] + .5[mr]. <sup>g</sup>[m] = [mm] + .5[mr].

Run 3c was performed under more industrially relevant conditions by Terry Burkhardt at the Exxon Chemical Company in Baytown, Texas. The properties of the resulting polymer were measured in comparison to the prototypical (<sup>i</sup>PrFlCp)ZrCl<sub>2</sub>/MAO catalyst system and are shown in table 5.

catalyst	ThpZrCl <sub>2</sub>	( <sup>i</sup> PrFlCp)ZrCl <sub>2</sub>
melting point	131.2°C	138°C
M <sub>w</sub>	109,200	88,000
PDI	3.1	1.9
[rr]	87.5 %	88.2 %
activity(g/ g/ hr.)	74,200	30,300
polymerization temp	~60°C	60°C

**Table 5: Comparison of polypropylene 3c (from ThpZrCl<sub>2</sub>, (3B)/ MAO) with polypropylene from (<sup>i</sup>PrFlCp)ZrCl<sub>2</sub> / MAO.**

Despite the slightly higher molecular weight and comparable stereoselectivity of 3c to the polymer from (<sup>i</sup>PrFlCp)ZrCl<sub>2</sub> under identical conditions, the larger PDI of 3c presumably results in the lower melting point of 3c. The high PDI may arise from poor temperature control in the polymerization reaction.

**C<sub>s</sub> symmetric catalysts:** ThpZrCl<sub>2</sub> (3B), <sup>i</sup>PrThpZrCl<sub>2</sub> (4B), and TMSThpZrCl<sub>2</sub> (5B), activated by MAO, all react with neat propylene at 0°C to form highly syndiotactic polypropylene as shown in table 6 in entries 3a, 4a, and 5a.

Entry	R'	mmmm (%)	mmmr	rmmr	mmrr	mrmm rmrr	mrmr	rrrr	mrrr	mrrm
3a	H	0.0	0.0	1.7	4.0	3.0	1.6	83.7	6.0	0.0
3b	H	0.0	2.0	3.7	6.9	21.8	11.6	27.3	19.1	7.5
3c	H	0.1	0.4	1.7	3.4	6.0	1.0	76.0	10.3	1.1
4a	<sup>i</sup> Pr	0.0	0.0	0.1	0.3	0.5	0.0	98.9	0.3	0.0
4b	<sup>i</sup> Pr	0.0	3.6	4.1	7.6	21.7	3.9	38.8	17.6	2.6
5a	TMS	0.0	0.0	0.0	0.0	2.0	0.0	95.9	2.2	0.0
5b	TMS	0.0	3.1	3.8	6.6	22.7	6.4	33.9	19.9	3.6
6a	<sup>s</sup> Bu	0.0	0.4	1.5	3.0	4.6	0.0	83.1	7.5	0.0
6b	<sup>s</sup> Bu	4.8	8.2	5.1	12.3	20.4	7.1	20.0	15.6	6.5
7a	MN	5.6	6.8	3.7	13.9	6.6	0.37	41.8	17.0	4.3
7b	MN	61.2	15.5	0.0	14.3	2.9	0.0	0.3	0.4	5.3
7d	MN	58.5	14.8	0.0	14.4	4.0	0.0	0.2	0.5	6.2

**Table 6: <sup>13</sup>C NMR data for polymers 3a-7d.**

The polymer is obtained as a white powder, but it can be melted and cooled to obtain a hard transparent material. The fact that all of these  $C_5$  symmetric metallocenes are highly syndiospecific is consistent with the proposed transition state for olefin insertion. A useful comparison is between Brintzinger's  $C_2$  symmetric doubly bridged metallocene<sup>47</sup> and  $iPrThpZrCl_2$ . As stated previously, Brintzinger found that his complexes did not polymerize propylene, but they did polymerize ethylene. The proposed transition state for  $iPrThpZrCl_2$  and the transition state necessary for propylene insertion into Brintzinger's complex are shown below.

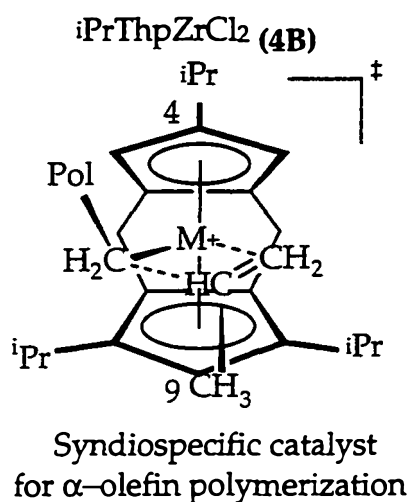


Figure 43

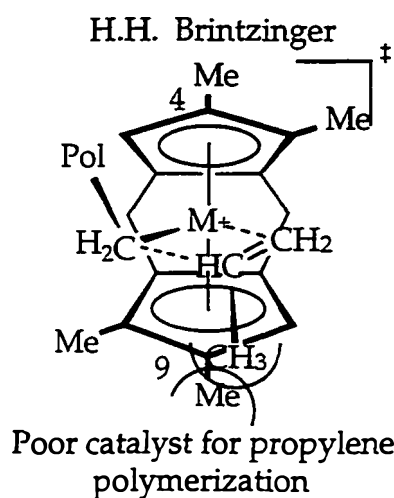
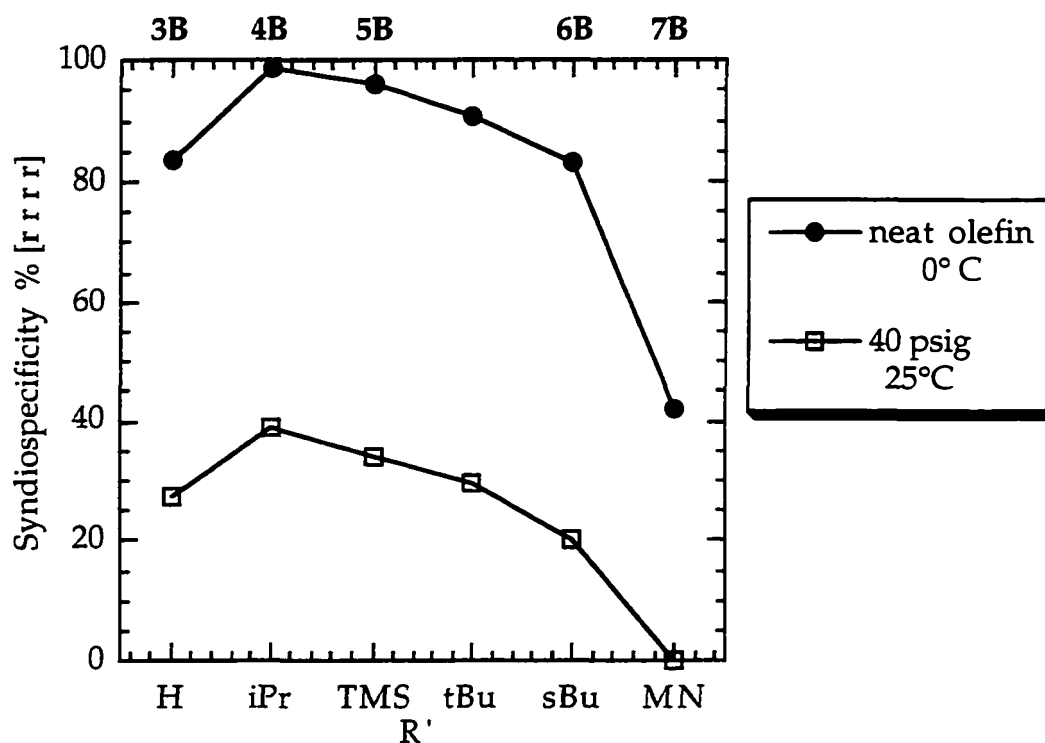


Figure 44

Brintzinger states that there is a bad interaction as shown in figure 44 between the methyl group of propylene and the methyl groups on the 4 or 9 ring positions that effectively blocks olefin insertion. In the case of  $iPrThpZrCl_2$  (**4B**), the isopropyl group in the 4 position of **4B** should block olefin insertions in which the methyl group of propylene is pointed up and thus should only insert in the manner shown above in figure 43 since there is no group in the 9 ring position.

The activity of these catalysts decreases as the size of  $R'$  increases, but it is only a modest decrease from 2160 g pol/g cat/hour for  $ThpZrCl_2$  (**3B**) to 1730 g pol/g cat/hour for  $TMSThpZrCl_2$  (**5B**). In addition to the slight decrease in activity, the syndioselectivity of the catalysts is clearly a function of the  $R'$  group. Of the  $C_5$  symmetric catalysts, the syndiospecificity is highest for

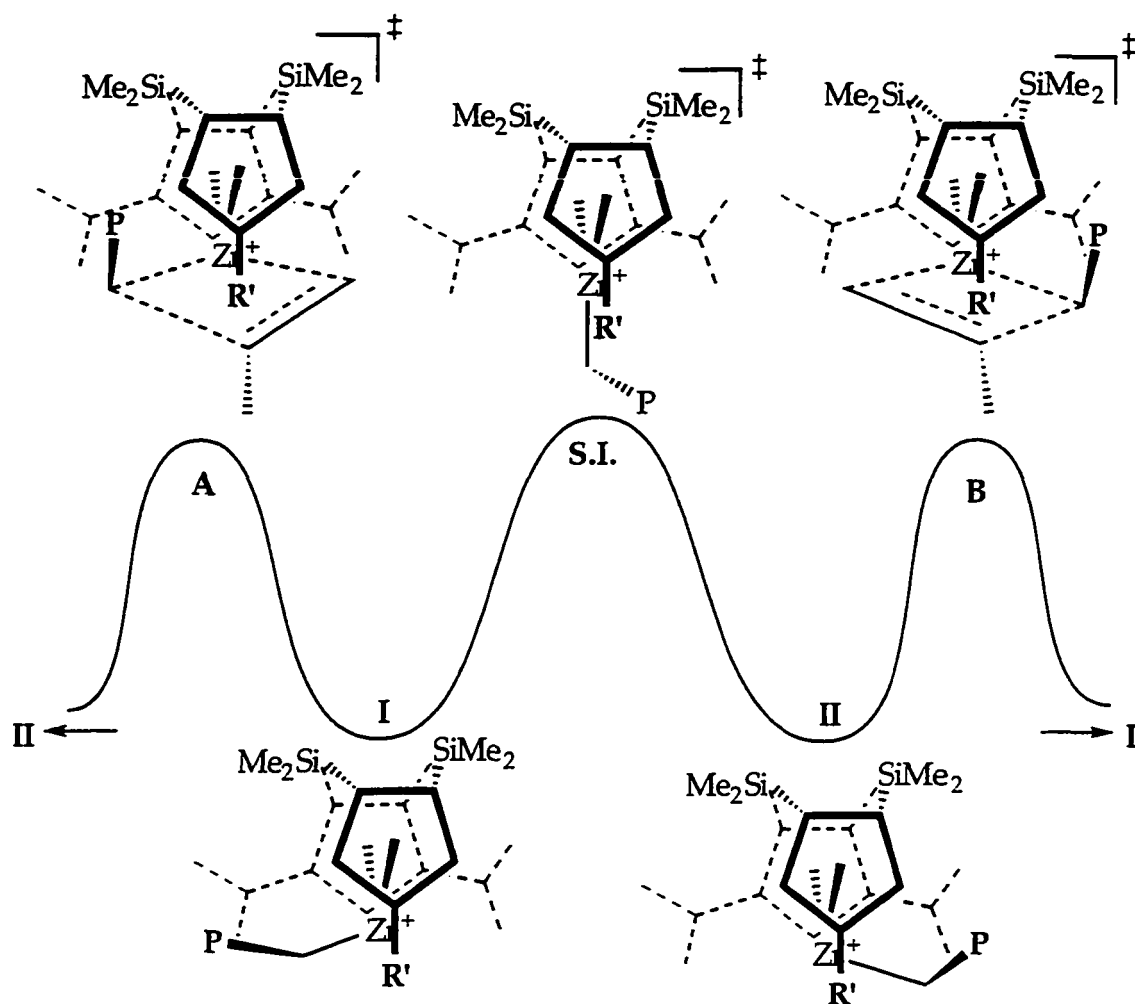
$i\text{PrThpZrCl}_2$  (**4B**) and the lowest for  $\text{ThpZrCl}_2$  (**3B**) as shown below.  $t\text{BuThpZrCl}_2$  is also included for comparison.<sup>61</sup>



**Figure 45: Effect of R' on the syndiospecificity of R'ThpZrCl<sub>2</sub>/MAO.**

This study also shows that the syndioselectivity of the C<sub>5</sub> symmetric catalysts (R' = H, iPr, TMS, and tBu) is dependent on the concentration of olefin. An energy profile for the C<sub>5</sub> symmetric catalysts is proposed based on the assumption that the primary error mechanism in these systems is site isomerization.



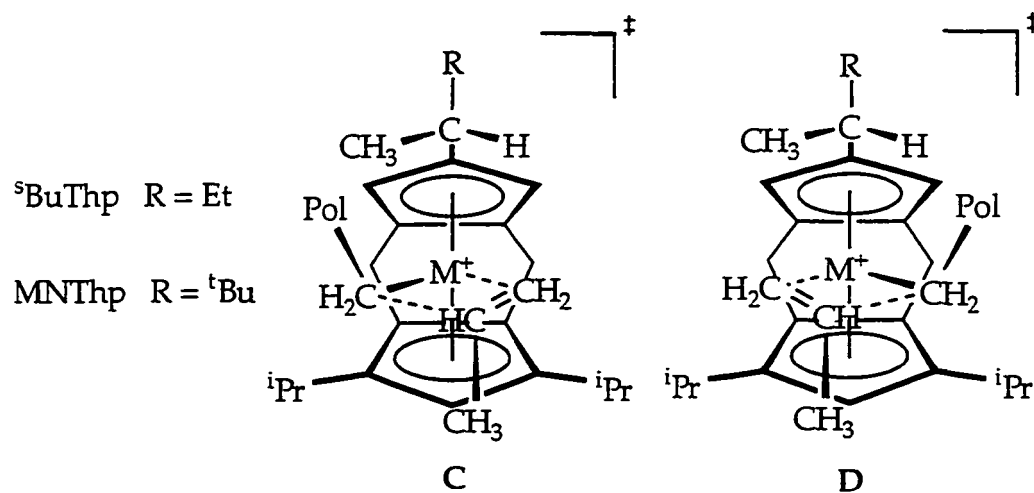


**Figure 46: Proposed energy profile for  $C_5$  symmetric catalysts**  
 ( $R' = H, iPr, TMS, tBu$ ).  
 (The relative energy levels are arbitrary.)

For the  $C_5$  symmetric catalysts, transition states **A** and **B** are enantiomers of each other and thus are the same energy.<sup>48</sup> Since site isomerization (**S.I.**) is a unimolecular process, its rate is expected to be independent of olefin concentration. Olefin insertion through transition states **A** and **B**, however, is a bimolecular process and thus the rate of olefin insertion should depend on the concentration of olefin. In neat olefin, these catalysts are all very syndioselective indicating that the rate of olefin insertion through both **A** and **B** is much faster than the rate of site isomerization. At lower olefin concentrations, however, the loss of syndiospecificity could indicate that site isomerization is now competitive with olefin insertion. The effect of  $R'$  on these systems can also be rationalized using this picture. Increasing the size of

R' was expected to increase the energy of S.I. and thus increase the syndiospecificity of these systems. However, substitutions at R' could also increase the energy of olefin insertion which should decrease the syndiospecificity of the catalyst since site isomerization could then become important. There seems to be a balance between these two effects since syndiospecificity is maximized with R' = *i*Pr and then decreases with the larger alkyl groups TMS and *tert*-butyl as shown in figure 45.

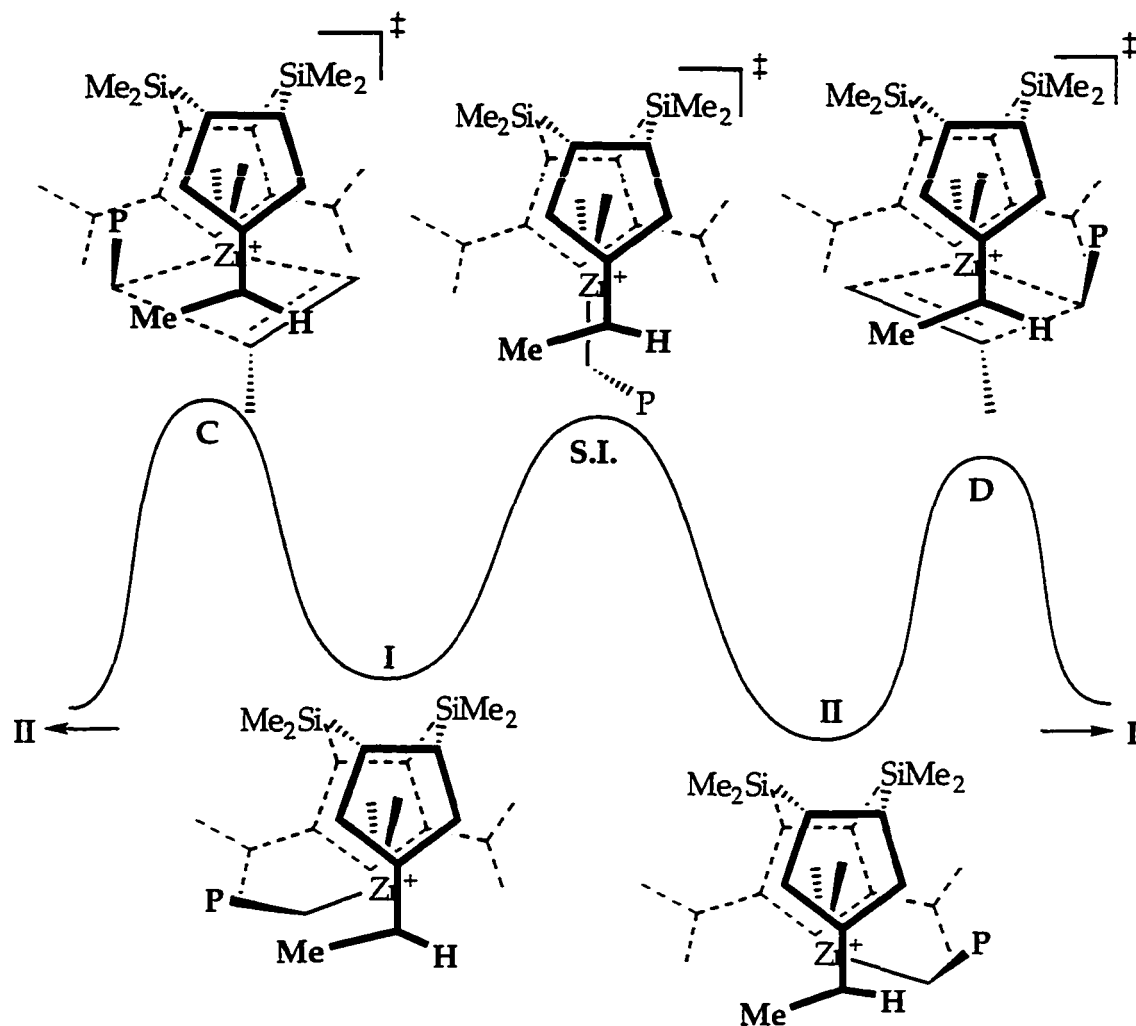
**C<sub>1</sub> symmetric metallocenes:** As opposed to the C<sub>s</sub> symmetric catalysts in which the transition states A and B have the same energy,<sup>48</sup> <sup>s</sup>BuThpZrCl<sub>2</sub> (6B) and MNThpZrCl<sub>2</sub> (7B) are C<sub>1</sub> symmetric and thus transition states C and D, as shown in figure 47, will have different energies.<sup>24</sup>



**Figure 47: Proposed transition states for olefin insertion with C<sub>1</sub> symmetric catalysts 6B and 7B.**

Transition state C is expected to be higher in energy than transition state D since there is presumed to be steric hindrance between the polymer chain and the methyl group of the chiral alkyl.<sup>65</sup> If the mechanism in figure 9 is operating and the olefin inserts from opposite sides after every insertion, then syndiotactic polypropylene is still expected. However, if site isomerization (figure 10) is competitive with olefin insertion, the reaction will proceed mostly through transition state D and isotactic polypropylene is expected.

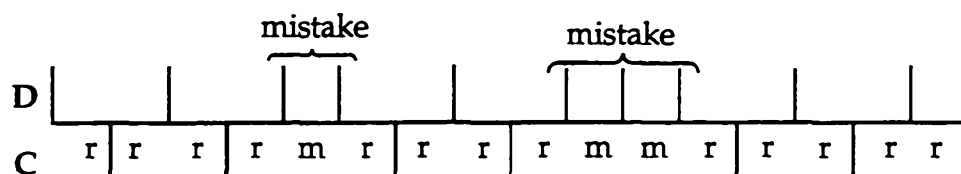
In neat olefin, at 0°C, <sup>s</sup>BuThpZrCl<sub>2</sub> (**4B**) (R' = CH(Me)(Et)) is an active catalyst for propylene polymerization and yields highly syndiotactic polypropylene which has a [r r r] concentration of 83.1%. Despite the fact that transition states **C** and **D** have different energies, it is presumed that the rate of olefin insertion will be very fast relative to site isomerization. If site isomerization is not competitive with olefin insertion, the difference in energy between **C** and **D** will not have a significant effect on the stereospecificity of the reaction. As is the case for the C<sub>s</sub> symmetric catalysts, the [r r r] concentration drops at lower olefin concentration (40 psig) to 20.0%, presumably since site isomerization is now competitive with olefin insertion. The relatively high [mmmm] concentration, compared to the C<sub>s</sub> symmetric catalysts under the same conditions, is likely due to the fact that transition state **C** is higher in energy than transition state **D** as shown below.



**Figure 48: Proposed energy profile for  $C_1$  symmetric catalysts 6B and 7B.**  
 (The R group (Et,  $t$ Bu) was omitted for clarity.)  
 (The relative energy levels are arbitrary.)

On the other hand,  $MNThpZrCl_2$  (**7B**) ( $R' = CH(Me)(tBu)$ ) is far less syndiospecific in neat propylene than the other catalysts, and is remarkably isospecific at lower propylene concentrations. The isospecificity of **7B** at low pressure indicates that site isomerization is competitive with olefin insertion at low olefin concentration. The presence of  $[mmmr]$ ,  $[rrmm]$ , and  $[mrrm]$  in a 2:2:1 ratio respectively, as the only other significant pentads besides  $[mrrm]$ , indicates that only single mistakes occur, consistent with isospecific enantiomeric site control. The syndiospecificity of **7B** at high pressure indicates that olefin insertion is now faster than site isomerization and the catalyst behaves more like a  $C_s$  symmetric system. A key feature of

the microstructure of polymer **7a** is the absence in the  $^{13}\text{C}$  NMR of the [rmm] pentad which indicates that there is still a preference for one site over the other. Presumably most mistakes occur by repeated insertions like D and not like C resulting in a microstructure as shown below:



**Figure 49: Proposed microstructure of polymer 7a.**

Another interesting feature of the microstructure of polymer **7a** is the uncharacteristically high concentration of the [mmmm] pentad. The fact that we have not been able to fit this result to any simple statistical models indicates that more complicated behavior may be involved. One possible explanation is that there are two different forms of the catalyst which are differentiated by a restricted rotation of the chiral group on the Cp.

These results have significant implications to the error mechanisms operating in these systems. If epimerization was the most significant error mechanism, one would predict that stereospecificity would drop for all catalyst systems including  $\text{MNThpZrCl}_2$  (**7B**). It is observed that syndiospecificity drops at lower pressure for the  $C_5$  symmetric catalysts and also for  $^s\text{BuThpZrCl}_2$  (**6B**). However, highly isotactic polypropylene is obtained at low olefin pressure (even 10 psig) with **7B** which is not consistent with an epimerization mechanism.<sup>66</sup> These preliminary results are consistent with a site isomerization mechanism as the primary source of errors in this catalyst system. An interesting experiment to test this idea would be to perform a study like that of Leclerc and Brintzinger,<sup>36</sup> who used isotopic labeling on an isospecific system to determine that epimerization was the main error mechanism in a  $C_2$  symmetric system.

**V. Conclusions of Part 2:** The design, synthesis, and polymerization of a new family of  $C_5$  and  $C_1$  symmetric Ziegler-Natta catalysts has been presented. These catalysts are unique in that they are the first syndiospecific metallocene catalysts not based on fluorenyl like ligands. They are also unique in that they are the first stereospecific doubly bridged metallocenes that are capable of

polymerizing propylene. The fact that these catalysts, even the ones with bulky R' groups, are highly active for the syndiospecific polymerization of olefins gives credence to the idea that a pocket is required in the larger moiety of a syndiospecific catalyst system. The activities of many of these catalysts are higher than those for other syndiospecific catalysts and the syndiospecificity of the  ${}^i\text{PrThpZrCl}_2$  (**4B**)/MAO catalyst system in neat olefin at  $0^\circ\text{C}$  is higher than that for any other catalyst yet reported. The ability to substitute readily in the R' position of these catalyst allows for straightforward variation of stereospecificity and in the case of chiral groups can allow for a complete reversal of stereoselectivity. The variability of these catalysts is evidenced by the polymerization behavior of the  $\text{MNThpZrCl}_2$  (**7B**)/MAO catalyst which produces highly isotactic polypropylene at low olefin concentrations and produces moderately syndiospecific polypropylene in neat olefin.

This catalyst system should also provide an excellent platform for mechanistic studies. These preliminary results are consistent with the idea that site isomerization is the main error mechanism in this new catalyst system, but further studies are certainly necessary to verify this assertion. Studies are currently underway to prepare Group III catalysts using these ligands which should provide excellent model systems for syndiospecific polymerization. Polymerization studies with Group III complexes and these new ligands would also be interesting since there are no reported Group III syndiospecific polymerization catalysts.

## Experimental Section.

**General Considerations.** All air or moisture sensitive chemistry was performed using standard high vacuum line, Schlenk, or drybox techniques<sup>67</sup> under a nitrogen or argon atmosphere. All gases were purified with MnO on vermiculite and activated molecular sieves. Solvents were stored in vacuum transfer flasks over titanocene<sup>68</sup> or sodium benzophenone ketyl. All other reagents were purified using standard methods.<sup>69</sup> Unless otherwise mentioned, all chemicals were purchased from Aldrich and used as received. 6,6-dimethylfulvene is prepared by the method of Little.<sup>70</sup> LAH is purified by ether extraction. Propylene is dried by passage through a Matheson 6110 drying system equipped with an OXISORB™ column. MAO (methylaluminumoxane, Albemarle) was prepared by removing toluene in vacuo. The white MAO solid was dried at 25°C for 48 hours at high vacuum. Dicyclopentadiene was thermally cracked and the distilled cyclopentadiene was stored at -60°C. Alkylchlorosilanes were distilled from CaH<sub>2</sub> immediately prior to use. YCl<sub>3</sub>·3.5THF was prepared using a procedure identical to that reported by Manzer for the corresponding scandium complex.<sup>71</sup> LiCH(SiMe<sub>3</sub>)<sub>2</sub> was prepared by the method of Cowley.<sup>72</sup> Fluorene and potassiumhexamethyldisilazide (KN(TMS)<sub>2</sub>) were sublimed before use. 1,3-di-tert-butylcyclopentadiene was prepared by the method of Casserly.<sup>50</sup>

**Instrumentation.** NMR Spectra were recorded on a Bruker AM500 (<sup>1</sup>H, 500.13 MHz; <sup>13</sup>C, 124.99MHz) spectrometer, a Joel GX-400 (<sup>1</sup>H, 399.7 MHz) spectrometer, and a G.E. QE300 (<sup>1</sup>H, 300.1 MHz) spectrometer.

(CyFlCp)H<sub>2</sub> (**1**) (C<sub>6</sub>H<sub>10</sub>)(C<sub>13</sub>H<sub>9</sub>)(C<sub>5</sub>H<sub>5</sub>). A 2L, 2 neck round bottom flask was charged with fluorene (96.44g, 0.5802 moles) and equipped with a 500 ml addition funnel and a 180° needle valve. 1.3 L of tetrahydrofuran are added to the flask and the addition funnel is charged with 1.5 M MeLi·LiBr (387, 0.580 moles) in ether. The MeLi·LiBr is added to the fluorene solution at 25°C at a rate of 3 drops/sec. The reaction turns a deep red while giving off CH<sub>4</sub> which is vented through a mercury bubbler. After CH<sub>4</sub> evolution stops, the reaction is stirred an additional 30 minutes at 25°C. A solution of tetrahydrofuran (100 ml) and pentamethylenefulvene<sup>52-54</sup> (84.9 g, 0.5804 mmol) are added to the addition funnel and are added to the fluorenyllithium solution over 1.5

hours at 25°C. After 12 hours at 25°C, the red solution is slowly quenched with H<sub>2</sub>O (100 mL). An additional 1L of H<sub>2</sub>O is added and the organic layer is isolated, the solvent is removed in vacuo and the yellow powder is recrystallized in CH<sub>2</sub>Cl<sub>2</sub>/MeOH. 1st crop, yield = 61.8 g. 2nd crop, yield = 81 g. Total = 78%.

**Li<sub>2</sub>(CyFlCp)(THF)<sub>4</sub>** Li<sub>2</sub>(C<sub>6</sub>H<sub>10</sub>)(C<sub>13</sub>H<sub>8</sub>)(C<sub>5</sub>H<sub>4</sub>)(C<sub>4</sub>OH<sub>8</sub>)<sub>4</sub>. A 1L round bottom flask is charged with **1** (61.8 g, 0.198 mol) and is equipped with a 250 mL addition funnel and a 180° needle valve. The flask is cooled to -40°C in an isopropanol bath and tetrahydrofuran (600 mL) is vacuum transferred into the flask. The addition funnel is charged with n-BuLi (1.53 M in hexanes, 271 ml, 0.415 mol) and the n-BuLi is added to the -40°C solution over 1 hour. The reaction is stirred for 6 hours at -40°C. The reaction is then warmed to 25°C and the solvent is removed in vacuo leaving a sticky red solid. The flask is switched to a large swivel frit assembly in the glove box and is washed thoroughly with petroleum ether. Yield 99.38 g (82%).

**[(CyFlCp)ScCl]<sub>2</sub> (1A)** [((C<sub>6</sub>H<sub>10</sub>)(C<sub>13</sub>H<sub>8</sub>)(C<sub>5</sub>H<sub>4</sub>))ScCl]<sub>2</sub>. A 250 ml round bottom flask is charged with Li<sub>2</sub>(CyFlCp)(THF)<sub>4</sub> (7.484g, 12.21 mmol) and ScCl<sub>3</sub>·3THF (4.49 g, 12.21 mmol) and is attached to a swivel frit assembly. At -78°C, toluene (200 ml) is vacuum transferred and the reaction is warmed to 25°C and stirred for 4.5 hours. Toluene is removed in vacuo and 50 ml toluene are vacuum transferred again. The toluene is removed again at 45°C and the solid is dried for 12 hours at 60°C and high vacuum. 100 ml more toluene are vacuum transferred and the resulting suspension is filtered at 50°C. The solution is cooled to -78°C and an orange solid comes out of solution. The solid is filtered and washed with 50 ml of cold toluene. The orange solid is dried overnight at 25°C; 4.20 g (90%).

**[(CyFlCp)YCl]<sub>2</sub> (1C)** [((C<sub>6</sub>H<sub>10</sub>)(C<sub>13</sub>H<sub>8</sub>)(C<sub>5</sub>H<sub>4</sub>))YCl]<sub>2</sub>. A 500 ml round bottom flask is charged with Li<sub>2</sub>(CyFlCp)(THF)<sub>4</sub> (14.26 g, 33.69 mmol) and YCl<sub>3</sub>·3.5THF (13.86 g, 33.69 mmol) and is equipped with a reflux condenser and a 180° needle valve. 300 ml of tetrahydrofuran are vacuum transferred and the red suspension is refluxed under 1 atm. Ar for 12 hours. The solvent is removed in vacuo. 100 ml of dry toluene is vacuum transferred and then removed at 40°C forming an orange powder. The flask is then switched to a swivel frit



assembly and the solid is dissolved in 200 ml Et<sub>2</sub>O. The solution is then stirred for an hour at 35°C at which point the color of the solution has changed from a deep red to pale orange with white solid. The suspension is filtered and the solvent is removed. The solid was then refluxed in 50 ml toluene while some solvent was removed in vacuo. After removing about 10 ml of toluene, the solid became pale yellow. The yellow solid was washed with petroleum ether (3 x 100 ml). The solid was isolated and dried at high vacuum for 8 hours; 12.2 g (83%).

**(CyFlCp)ScCH(SiMe<sub>3</sub>)<sub>2</sub> (1B)** ((C<sub>6</sub>H<sub>10</sub>)(C<sub>13</sub>H<sub>8</sub>)(C<sub>5</sub>H<sub>4</sub>))ScCH(Si(CH<sub>3</sub>)<sub>3</sub>)<sub>2</sub>. A 100 ml round bottom flask is charged with **(1A)** (2.32 g, 3.26 mmol) and LiCH(SiMe<sub>3</sub>)<sub>2</sub> (1.106 g, 6.64 mmol) and is attached to a swivel frit assembly. Toluene (75 ml) is vacuum transferred and the reaction is stirred at 80°C for 3 hours. Volatiles are removed in vacuo leaving an orange solid which is washed with petroleum ether. The solid is transferred to a glass soxhlet thimble in the glove box and is extracted with petroleum ether (50 cycles). The solvent is removed in vacuo leaving an orange microcrystalline solid which is dried at high vacuum for 2 hours; 0.99 g (29%).

**(CyFlCp)YCH(SiMe<sub>3</sub>)<sub>2</sub> (1D)** ((C<sub>6</sub>H<sub>10</sub>)(C<sub>13</sub>H<sub>8</sub>)(C<sub>5</sub>H<sub>4</sub>))YCH(Si(CH<sub>3</sub>)<sub>3</sub>)<sub>2</sub> was obtained analogously by the reaction of **(1C)** (1.011 g, 1.162 mmol) and LiCH(SiMe<sub>3</sub>)<sub>2</sub> (386 g, 2.27 mmol) in toluene at 80°C for 10 hours. 450 mg of an orange microcrystalline solid is obtained (35%).

**Procedure<sup>11</sup> for ethylene polymerization with (CyFlCp)MCH(SiMe<sub>3</sub>)<sub>2</sub> (M = Sc, Y).**

**CAUTION: These manipulations should be performed behind a blast shield!!** A thick walled glass reaction vessel was charged with titanocene (200 mg) and methylcyclohexane (10 mL). Ethylene (2.0 g, 71.3 mmol) was condensed onto the titanocene at 77°K and the mixture was warmed to 25°C and stirred for 1 hour at 25°C. The ethylene/cyclohexane solution was vacuum transferred into a thick walled reaction vessel (cooled to 77°K) containing **3C** or **3D** (~10 mg, 0.018 mmol). The reaction was warmed to -78°C in a dry ice/acetone bath and then, with vigorous stirring, was warmed to 25°C in a water bath and stirred for 1 week. The resulting solid was filtered

and washed with a MeOH/5% HCl solution and acetone. M= Sc; 140 mg (7% based on ethylene). M= Y; 450 mg (23% based on ethylene).

**BTCpH** ( $C_5H_4(SiMe_3)_2$ ) A 3 neck, 3L round bottom flask is charged with NaCp (845 ml, 2.0 M in tetrahydrofuran, 1.69 mol) and equipped with a 500 mL addition funnel.  $Me_3SiCl$  (225 ml, 1.772 mol) is added to the addition funnel and is added to the NaCp solution at a rate of 6 ml/minute. The solution is stirred for 12 hours yielding a brown suspension.  $H_2O$  (600 ml) is added to the reaction and ether (150 ml) is added to the mixture. The organic layer is separated and the aqueous layer is washed with ether (3 X 100 ml). The organic layers are combined and are washed with  $H_2O$  (2 X 200 ml), dried with  $MgSO_4$  and solvent is removed down to about 250 ml. The product is vacuum distilled.

TMSCpH 45°C / 10-12 mm Hg. yield = 80 ml.

$(TMS)_2CpH$  58-60°C / 4 mm Hg. yield = 65 ml.

**Li(BTCp)**  $Li(C_5H_3(SiMe_3)_2)^{73}$  (generated in situ). A 200 ml round bottom flask is charged with BTCpH (10.0 g, 47.5 mmol) and tetrahydrofuran (50 ml), is equipped with a reflux condenser and a 180° needle valve, and is cooled to 0°C in an ice water bath. n-BuLi (32 ml, 1.6M in hexanes, 51 mmol) is added via syringe pump at a rate of 1.5 ml/ min. to the 0°C solution and the solution is allowed to warm to 25°C with stirring as the ice melts overnight. 12 hours after n-BuLi addition, the solution is heated and allowed to reflux for 3 hours. The tetrahydrofuran solution of Li(BTCp) is then cooled to 25°C and was used as a solution.

**$Me_2(BTCp)SiCl$**   $(CH_3)_2(C_5H_3(SiMe_3)_2)SiCl$ . In a frit assembly, a solution of Li(BTCp) (47.5 mmol in 200 ml tetrahydrofuran) is cooled to -78°C and  $Me_2SiCl_2$  (90 mmol) is vacuum transferred. The solution is warmed quickly to 25°C and is stirred for 1 hour. Volatiles are removed and petroleum ether (50 ml) is vacuum transferred. The suspension is filtered, volatiles are removed and the product is isolated as a yellow oil. The oil is kugel-röhr distilled at high vacuum and 100°C, and the yield is approximately 7 g.

**$Et_2(BTCp)SiCl$**   $(C_2H_5)_2(C_5H_3(SiMe_3)_2)SiCl$ . In a frit assembly, the solution of Li(BTCp) (20.43 mmol in 200 ml tetrahydrofuran) is cooled to -78°C and

$\text{Et}_2\text{SiCl}_2$  (3.8 ml, 25 mmol) is vacuum transferred. The solution is warmed quickly to  $25^\circ\text{C}$  and is stirred for 3 hours. Volatiles are removed and petroleum ether (50 ml) is vacuum transferred. The suspension is filtered, volatiles are removed and the product is isolated as a yellow oil which is not distilled; 6.37 g (94%).

$\text{iPr}_2(\text{BTCp})\text{SiCl}$   $(\text{C}_3\text{H}_7)_2(\text{C}_5\text{H}_3(\text{SiMe}_3)_2)\text{SiCl}$ . A solution of  $\text{Li}(\text{BTCp})$  (24.6 mmol in 200 ml tetrahydrofuran) is cooled to  $0^\circ\text{C}$  in an ice water bath and  $\text{iPr}_2\text{SiCl}_2$  (4.55 g, 24.6 mmol) is added slowly to the solution via syringe. The solution is warmed to  $25^\circ\text{C}$  and is stirred for 15 hours. Volatiles are removed and petroleum ether (50 ml) is vacuum transferred. The suspension is filtered, volatiles are removed and the product is isolated as a yellow oil. The oil is kugel-röhr distilled at high vacuum and  $100^\circ\text{C}$ . Yield = 4.35 g of a pale yellow oil. (50%)

$\text{HpH}_2$  (2)  $(\text{C}_3\text{H}_7)_2(\text{C}_5\text{H}_3(\text{SiMe}_3)_2)\text{Si}(\text{C}_5\text{H}_5)$ . A 200 ml round bottom flask is charged with a solution of  $\text{iPr}_2(\text{BTCp})\text{SiCl}$  (0.047 mmol in 100 ml tetrahydrofuran) and equipped with a reflux condenser and  $180^\circ$  needle valve. At  $25^\circ\text{C}$ ,  $\text{NaCp}$  (4.55 g, 52 mmol in 40 ml tetrahydrofuran) is added to the flask. The reaction is refluxed under Ar for 72 hours. Volatiles are removed and petroleum ether (80 ml) is vacuum transferred. The suspension is filtered, volatiles are removed and the product is isolated as a yellow oil. The oil is kugel-röhr distilled at high vacuum and  $120^\circ\text{C}$ . Yield = 6.81 g of a pale yellow oil. (38%)

$\text{K}_2\text{Hp}$   $\text{K}_2[(\text{C}_3\text{H}_7)_2(\text{C}_5\text{H}_2(\text{SiMe}_3)_2)\text{Si}(\text{C}_5\text{H}_4)]$ . A 500 ml round bottom flask is charged with  $\text{HpH}_2$  (6.445 g, 16.57 mmol), tetrahydrofuran (200 ml), and  $\text{KN}(\text{TMS})_2$  (6.62 g, 33.15 mmol) in the glove box. The flask is equipped with a reflux condenser and a  $180^\circ$  needle valve and the solution is refluxed for 48 hours under Ar. Volatiles are removed from the yellow solution yielding a viscous yellow oil. The oil is dried at high vacuum and  $60^\circ\text{C}$  for 12 hours leaving an off white solid. The solid is then recrystallized from hot tetrahydrofuran (100 ml) and a fine white, microcrystalline solid is obtained. The solid is dried overnight at high vacuum; 4.39 g (57%).

**HpZrCl<sub>2</sub> (2A)** [(C<sub>3</sub>H<sub>7</sub>)<sub>2</sub>(C<sub>5</sub>H<sub>2</sub>(SiMe<sub>3</sub>)<sub>2</sub>)Si(C<sub>5</sub>H<sub>4</sub>)]ZrCl<sub>2</sub>. A suspension of ZrCl<sub>4</sub> (460 mg, 1.97 mmol) in tetrahydrofuran (40 ml) is added quickly to a stirred suspension of K<sub>2</sub>Hp (919 mg, 1.97 mmol) in tetrahydrofuran (50 ml) in a 250 ml round bottomed flask attached to a swivel frit assembly at 25°C. The resulting yellow suspension is stirred at 25°C for 7 hours. The solvent is then removed in vacuo leaving an oily yellow solid. The solid is dissolved in hot hexane and the KCl is removed with a medium frit. The product is recrystallized from hot methylcyclohexane and isolated in two crops. Total yield of a pale yellow, air stable, microcrystalline solid is 370 mgs (34%). X-ray quality crystals were obtained by slow cooling a methylcyclohexane solution from 90°C to 25°C. Analysis: Calculated (Found) C: 48.14 (48.10); H: 6.98 (7.00).

**[HpYCl]<sub>2</sub> (2B)** {[(C<sub>3</sub>H<sub>7</sub>)<sub>2</sub>(C<sub>5</sub>H<sub>2</sub>(SiMe<sub>3</sub>)<sub>2</sub>)Si(C<sub>5</sub>H<sub>4</sub>)]YCl}<sub>2</sub>. A 100 ml round bottom flask is charged with K<sub>2</sub>Hp (1.089g, 2.342 mmol) and YCl<sub>3</sub>·3.5THF (964 mg, 2.342 mmol) and is attached to a swivel frit assembly. Tetrahydrofuran (50 ml) is vacuum transferred at -78°C and the white suspension is warmed to 25°C. The reaction is stirred for 2 hours and solvent is removed in vacuo and replaced with 20 ml petroleum ether forming a yellow suspension. Volatiles are removed and the solid is dried at high vacuum for 1 hour. Ether (30 ml) is added and the product is extracted with ether (3 x 30 ml). The ether is removed in vacuo leaving a pale yellow solid. The solid is washed with 3 x 30 ml petroleum ether and the white solid is dried in vacuo for 2 hours. Yield (1st crop) = 180 mg (15%). The reaction mixture is extracted again with ether and the solid is freeze dried<sup>74</sup> with benzene (20 ml). The solid is washed again with 3 x 20 ml petroleum ether and dried in vacuo. Yield (2nd crop) 440 mgs (37%).

**[HpYCH(SiMe<sub>3</sub>)<sub>2</sub>]<sub>2</sub> (2C)** [(C<sub>3</sub>H<sub>7</sub>)<sub>2</sub>(C<sub>5</sub>H<sub>2</sub>(SiMe<sub>3</sub>)<sub>2</sub>)Si(C<sub>5</sub>H<sub>4</sub>)]YCH(SiMe<sub>3</sub>)<sub>2</sub>. A 10 ml round bottom flask is charged with **2B** (153 mg, 0.299 mmol) and LiCH(SiMe<sub>3</sub>)<sub>2</sub> (50 mg, 300 mmol) and attached to a swivel frit assembly. C<sub>6</sub>H<sub>6</sub> (5 ml) is vacuum transferred and the suspension is warmed to 25°C and stirred for 2 hours. Volatiles are removed in vacuo leaving a white solid. The product is extracted with petroleum ether (3 x 10 ml). The petroleum ether solution is concentrated and cooled to -78°C. The resulting white microcrystalline solid is filtered at -78°C and dried at high vacuum for 30 minutes; 89 mg (47%).

**[HpYH]<sub>2</sub> (2D)**  $\{[(C_3H_7)_2(C_5H_2(SiMe_3)_2)Si(C_5H_4)]YH\}_2$ . An NMR tube equipped with a Teflon needle valve is charged with **2C** (5 mg, 0.008 mmol) and C<sub>6</sub>D<sub>12</sub> (.5 ml). The NMR tube is cooled to 77°K in an LN<sub>2</sub> filled dewar and 1 atm H<sub>2</sub> is admitted. The needle valve is then closed and the tube is quickly warmed to 25°C in a water bath. The reaction is quantitative (by <sup>1</sup>H NMR) after 12 hours.

**Li(<sup>t</sup>Bu<sub>2</sub>Cp)[DME]**: A 500 ml flask is charged with di-tert-butylcyclopentadiene (6.4 g, 35.5 mmol) and pentane (200 ml), attached to a swivel frit assembly, and cooled to -78°C. n-BuLi (24 ml, 1.6 M in hexanes, 39 mmol) is added via syringe and the reaction is warmed to 25°C and stirred for 4 hours. DME (5 ml, 48 mmol) is added via syringe resulting in rapid gas evolution and precipitation of a white solid. The suspension is stirred for an additional hour and the solid is isolated on the frit and washed with pentane (3 x 200 ml) and dried at high vacuum for 2 hours; 7.116 g (73%).

**(<sup>t</sup>Bu<sub>2</sub>Cp)Me<sub>2</sub>SiCl**: A 200 ml flask is charged with Li(<sup>t</sup>Bu<sub>2</sub>Cp)[DME] (4.80 g, 17.5 mmol) and tetrahydrofuran (70 ml), attached to a swivel frit assembly, and cooled to -78°C. Dichlorodimethylsilane (4.26 ml, 35 mmol) is vacuum transferred onto the reaction and the reaction is allowed to warm slowly to 25°C without the aid of a water bath. After 9 hours of stirring at 25°C, all volatiles are removed in vacuo and the product is extracted with petroleum ether (3 x 20 mls). The solvent is removed in vacuo leaving a pale yellow oil; 4.47 g (94%).

**Li<sub>2</sub>[(<sup>t</sup>Bu<sub>2</sub>Cp)Me<sub>2</sub>Si(MeCp)][DME]**: A 25 ml schlenk flask is charged with (<sup>t</sup>Bu<sub>2</sub>Cp)Me<sub>2</sub>SiCl (2.0 g, 7.4 mmol) and tetrahydrofuran (15 ml). A suspension of Li(MeCp) (680 mg, 7.9 mmol) in tetrahydrofuran (5 ml) is added via pipette to the stirred solution in the glove box. The clear colorless solution is stirred for 3 hours and solvent is removed in vacuo leaving a white paste. The product is extracted with petroleum ether (2 x 15 ml) using a cannula filter and the solvent is removed in vacuo leaving a yellow oil. The oil is dissolved in pentane (30 ml) and n-BuLi (9.3 ml, 1.6 M in hexanes, 14.8 mmol) is added via syringe. The solution is stirred for 24 hours with no solid formation. DME (1.6 ml, 15.3 mmol) is added to the solution resulting in

precipitate formation. The white suspension is stirred for an additional 2 hours and the solid is isolated on a frit. The white solid is washed with petroleum ether (2 x 10 ml) and dried at high vacuum for 2 hours; 2.25g (60%).

$\text{Li}_2[(^t\text{Bu}_2\text{Cp})\text{Me}_2\text{Si}(^t\text{BuCp})](\text{THF})_n$  is prepared analogously by reaction of  $(^t\text{Bu}_2\text{Cp})\text{Me}_2\text{SiCl}$  (2.47 g, 9.23 mmol) and  $\text{Li}(^t\text{BuCp})$  (1.18 g, 9.2 mmol) in tetrahydrofuran (20 ml) for 6 hours at 25°C. Deprotonation is carried out by reaction of the yellow oil in tetrahydrofuran (20 ml) with *n*-BuLi (11.5 ml, 1.6 M in hexanes, 18.4 mmol). The reaction is stirred for 12 hours and the volatiles are removed in vacuo leaving an oily solid. Petroleum ether (20 ml) is added and the solid is stirred resulting in a white solid in a yellow solution. The solid is isolated on a frit, washed with petroleum ether (2 x 20 ml), and dried at high vacuum for 2 hours; 1.78 g (~40%).

**3-isopropyl-6,6-dimethylfulvene.** Isopropylcyclopentadiene (59.6 g, 0.555 mole), methanol (400 ml), acetone (35 g, 0.603 mole), and pyrrolidine (62 ml, 0.70 mole) were combined in a 1 L flask and stirred in air for 12 hours at 25°C. The solution is neutralized with glacial acetic acid. Water (600 ml) is added and the product is extracted with ether (4 x 400 ml). The organic layer is washed with water (4 x 600 ml) and dried over  $\text{MgSO}_4$ . The solvent is removed in *vacuo*. The yellow oil is kugel-röhr distilled at 90°C and 50 torr yielding a bright yellow oil; 48.3 g (59%).

**6,6-ethyl,methyl-fulvene** was prepared analogously by reaction of cyclopentadiene (29.0g, 438 mmol), 2-butanone (31.6 g, 438 mmole), and pyrrolidine (5 ml, 56 mmole) in methanol (200 ml). The yellow oil is kugel-röhr distilled at 90°C and 50 torr yielding a bright yellow oil; 42.6 g (94%).

**6,-tert-butyl-fulvene** was prepared analogously by reaction of cyclopentadiene (31.7 g, 480 mmole), pivaldehyde (19.825 g, 230 mmol), and pyrrolidine (25 ml, 300 mmole) in methanol (250 ml). The yellow oil is kugel-röhr distilled at 70°C and <1 torr yielding a bright yellow oil; 20.5 g (66.4%).

**isopropylcyclopentadiene**<sup>52-54</sup> "*i*PrCp." A solution of 6,6-dimethylfulvene (70.5 g, 0.663 mole) in anhydrous ether (200 ml) is slowly added via addition

funnel to a well stirred 25°C solution of LAH (0.670 mole) in ether (1 L) in a 3 L flask equipped with air driven overhead stirrer, efficient reflux condenser filled with dry ice/acetone, and N<sub>2</sub> adapter. The addition requires 1 hour. The reaction mixture is stirred for 4 more hours. The reaction mixture is quenched by addition of water (30 ml) via a syringe pump at a rate of 0.4 ml/min. **CAUTION: Reaction is exothermic and produces large amounts of H<sub>2</sub> (g)!** NaOH (30 ml, 15% aqueous solution) is then added at a rate of 0.4 ml/min. and serves to form a pale yellow solution with a granular white solid. After H<sub>2</sub> evolution stops, water (1 L) is added to the reaction mixture. The product is extracted with ether (2 x 500 ml), the organic layer is washed with water (3 x 1 L), and the ether solution is dried with MgSO<sub>4</sub>. The solvent is removed in *vacuo* and the product is distilled at 80°C and ~ 40 torr yielding a pale yellow oil; 65 g (90%).

**sec-butyl-cyclopentadiene "sBuCp"** (C<sub>5</sub>H<sub>5</sub>CH(CH<sub>3</sub>)(CH<sub>2</sub>CH<sub>3</sub>)). A solution of 6,6-ethyl,methyl-fulvene (40 g, 333 mmol) in diethyl ether (300 ml) is slowly added via addition funnel to a well stirred 25°C solution of LAH (553 mmol) in diethyl ether (1 L) in a 3 L flask equipped with air driven overhead stirrer, efficient reflux condenser filled with dry ice/acetone, and N<sub>2</sub> adapter. The addition requires 1 hour. The reaction mixture is stirred for 4 more hours. The reaction mixture is quenched by addition of water (20 ml) via a syringe pump at a rate of 0.4 ml/min. **CAUTION: Reaction is exothermic and produces large amounts of H<sub>2</sub> (g)!** NaOH (20 ml, 15% aqueous solution) is then added at a rate of 0.4 ml/min. and serves to form a pale yellow solution with a granular white solid. After H<sub>2</sub> evolution is complete, H<sub>2</sub>O (300 ml) is added slowly and the ether layer is separated. The reaction mixture is extracted with ether (300 ml) and the organic layers are combined and washed with H<sub>2</sub>O (3 X 200 ml). The yellow ether solution is dried over MgSO<sub>4</sub> and the solvent is removed in *vacuo*. The yellow liquid is kugel-röhr distilled at 100°C and 20 torr; 25.39g (62%).

**1,3-diisopropylcyclopentadiene + isomers "iPr<sub>2</sub>Cp."** A solution of 3-isopropyl-6,6-dimethylfulvene (48 g, 0.323 mole) in anhydrous ether (300 ml) is slowly added via addition funnel to a well stirred 25°C solution of LAH (0.372 mole) in ether (700 ml) in a 3 L flask equipped with air driven overhead stirrer, efficient reflux condenser, and N<sub>2</sub> adapter. The addition requires 1

hour. The reaction mixture is stirred for 4 more hours. The reaction mixture is quenched by addition of water (20 ml) at a rate of 1 ml/min. **CAUTION: Reaction is exothermic and produces large amounts of H<sub>2</sub> (g)!** NaOH (30 ml, 15% aqueous solution) is then added at a rate of 0.4 ml/minute and serves to form a pale yellow solution with a granular white solid. After H<sub>2</sub> evolution stops, water (1 L) is added to the reaction mixture. The product is extracted with ether (2 x 500 ml), the organic layer is washed with water (3 x 1 L), and the ether solution is dried with MgSO<sub>4</sub>. The solvent is removed in *vacuo* and the product is distilled at 80°C and ~ 15 torr yielding a pale yellow oil; 38 g (78%).<sup>55</sup>

**lithium(isopropylcyclopentadienylide)** "Li(<sup>i</sup>PrCp)." A 1 L schlenk flask is charged with <sup>i</sup>PrCp (16.5 g, 153 mmol) and diethyl ether (700 ml). The flask is equipped with a 200 ml addition funnel which is charged with n-BuLi (100 ml, 1.6 M in hexanes, 160 mmol). The n-BuLi is added to the ether solution slowly over 1 hour at 25°C and white solid precipitates upon addition. The white suspension is stirred for 3 hours at 25°C and the solid is filtered in the glove box and washed with diethyl ether (2 x 300 ml). The fine white solid is dried at high vacuum for 8 hours; 13.1 g (75%).

**lithium(sec-butylcyclopentadienylide)** "Li(<sup>s</sup>BuCp)" is prepared analogously by reaction of 6,6-ethyl,methyl-fulvene (25.39 g, 207.7 mmol) and nBuLi (135 ml, 1.6 M in hexanes, 216 mmol) in diethyl ether (1 L) in a 2 L schlenk flask. The white solid is dried at high vacuum and 50°C for 6 hours; 24 g (89.5%).

**lithium(methylneopentyl-cyclopentadienylide)** "Li(MNCp)." A 200 ml Schlenk flask is charged with 6,6-ethyl,methyl-fulvene (5.08 g, 37.8 mmol) and diethyl ether (150 ml). The yellow solution is cooled to 0°C and MeLi (27 ml, 1.4 M in diethylether, 37.8 mmol) is added via syringe over 15 minutes. A white solid precipitates during addition. The white suspension is warmed to 25°C and stirred for 2 hours. The solid is filtered, washed with petroleum ether (4 x 100 ml), and dried at high vacuum for 5 hours; 5.21 g (88%).

**lithium-1,3-diisopropylcyclopentadienylide** "Li(<sup>i</sup>Pr<sub>2</sub>Cp)" Toluene (200 ml) and petroleum ether (150 ml) are cannula transferred onto <sup>i</sup>Pr<sub>2</sub>Cp (24 g, 0.16 mole) in a large swivel frit assembly under argon. <sup>n</sup>BuLi (100 ml, 1.6 M in



hexanes, 0.16 mole) is added via cannula over a period of 30 minutes at 25°C. The solution is stirred overnight and the resulting white solid is filtered and washed with petroleum ether (4x 100 ml). The white solid is dried *in vacuo* resulting in a fine white powder; 22.4 g (90%).

**1-chloro-1-(3,5-diisopropylcyclopentadienyl)-1,1-dimethylsilane**

"(*i*Pr<sub>2</sub>Cp)Me<sub>2</sub>SiCl." Tetrahydrofuran (150 ml) is vacuum transferred onto Li(*i*Pr<sub>2</sub>Cp) (8.03 g, 51.4 mmol) in a medium swivel frit assembly at -78°C with vigorous stirring. Dichlorodimethylsilane (9.57 g, 74.2 mmol) is then vacuum transferred onto the -78°C solution and the reaction mixture is allowed to warm slowly to room temperature in a dry ice/acetone bath over 12 hours. The reaction is stirred at 25°C for an additional 24 hours and then the volatiles are removed *in vacuo* leaving a white paste. The product is extracted away from the lithium chloride with petroleum ether (3 x 100 ml). The solvent is removed *in vacuo* resulting in a yellow oil; 11.85 g (95%).

**1-cyclopentadienyl-1-(3,5-diisopropylcyclopentadienyl)-1,1-dimethylsilane**

"(*i*Pr<sub>2</sub>Cp)Me<sub>2</sub>Si(Cp)."

A suspension of sodiumcyclopentadienylide (4.05 g, 46 mmol) in tetrahydrofuran (50 ml) is added slowly to a solution of (*i*Pr<sub>2</sub>Cp)Me<sub>2</sub>SiCl (9.06 g, 37.3 mmol) in tetrahydrofuran (100 ml). The reaction is stirred at 25°C for 12 hours. The solvent is removed *in vacuo* and the product is extracted from the white sodium chloride with pentane (3 x 100 ml). The solvent is removed *in vacuo* leaving a pale yellow oil which is kugel-röhr distilled at 90°C and <10<sup>-3</sup> torr yielding a colorless oil; 8.22 g (81%).

**1-(isopropyl-cyclopentadienyl)-1-(3,5-diisopropylcyclopentadienyl)-1,1-**

**dimethylsilane** "(*i*Pr<sub>2</sub>Cp)Me<sub>2</sub>Si(*i*PrCp)" is prepared analogously by reaction of (*i*Pr<sub>2</sub>Cp)Me<sub>2</sub>SiCl (5.843 g, 51.202 mmol) and Li(*i*PrCp) (12.286 g, 50.514 mmol). The pale yellow oil is kugel-röhr distilled at 100°C and <10<sup>-3</sup> torr yielding a colorless oil; 13.899 g (87.5%).

**1-(sec-butyl-cyclopentadienyl)-1-(3,5-diisopropylcyclopentadienyl)-1,1-**

**dimethylsilane** "(*i*Pr<sub>2</sub>Cp)Me<sub>2</sub>Si(<sup>s</sup>BuCp)" is prepared analogously by reaction of (*i*Pr<sub>2</sub>Cp)Me<sub>2</sub>SiCl (17.512 g, 71.22 mmol) and Li(<sup>s</sup>BuCp) (9.452 g, 73.18 mmol).

The pale yellow oil is kugel-röhr distilled at 100°C and  $<10^{-3}$  torr yielding a pale yellow oil; 20.77 g (88.7%).

**1-(methylnopentyl-cyclopentadienyl)-1-(3,5-diisopropylcyclopentadienyl)-1,1-dimethylsilane** " $(iPr_2Cp)Me_2Si(MNCp)$ " is prepared analogously by reaction of  $(iPr_2Cp)Me_2SiCl$  (7.033 g, 28.96 mmol) and  $Li(MNCp)$  (4.70 g, 30.1 mmol). The pale yellow oil is kugel-röhr distilled at 110°C and  $<10^{-3}$  torr yielding a pale yellow oil; 8.15g (79%).

**dilithio-1-cyclopentadienylide-1-(3,5-diisopropylcyclopentadienylide)-1,1-dimethylsilane**, " $Li_2[(iPr_2Cp)Me_2Si(Cp)]$ ." Toluene (100 ml) and petroleum ether (150 ml) are cannula transferred onto  $(iPr_2Cp)Me_2Si(Cp)$  (8.22 g, 30.2 mmol) in a medium porosity swivel frit assembly.  $nBuLi$  (39 ml, 1.6 M in hexanes, 62.4 mmol) is added slowly via syringe over 30 minutes at 25°C and a white precipitate forms during addition. The reaction is stirred at 25°C for 18 hours. The white solid is filtered and washed with petroleum ether (3 x100 ml). The solid is dried *in vacuo* for 3 hours resulting in a fine white solid; 8.018g (93%).

**dilithio-1-(3-isopropyl-cyclopentadienylide)-1-(3,5-diisopropylcyclopentadienylide)-1,1-dimethylsilane** " $Li_2[(iPr_2Cp)Me_2Si(iPrCp)]$ ." Diethyl ether (30 ml) is cannula transferred onto  $(iPr_2Cp)Me_2Si(iPrCp)$  (3.066 g, 9.746 mmol) in a 50 ml schlenk flask equipped with a 50 ml addition funnel. The funnel is charged with 13 mls of  $nBuLi$  (13 ml, 1.6 M in hexanes, 21 mmol) and the  $nBuLi$  solution is added over 10 minutes to the 25°C ether solution. A white solid precipitates during addition. The white suspension is stirred at 25°C for 6 hours and filtered in the glove box. The solid is washed with petroleum ether (2 X 25 mL) and dried *in vacuo* for 6 hours; 2.84 g, (89%).

**dilithio-1-(3-sec-butyl-cyclopentadienylide)-1-(3,5-diisopropylcyclopentadienylide)-1,1-dimethylsilane**, " $Li_2[(iPr_2Cp)Me_2Si(sBuCp)]$ " is prepared analogously by the reaction of  $(iPr_2Cp)Me_2Si(sBuCp)$  (19.824 g, 60.326 mmol) and  $nBuLi$  (81 ml, 1.6 M in hexanes, 130 mmol) in diethyl ether (600 ml); 15.5 g, (75%).

**dilithio-1-(3-methylneopentyl-cyclopentadienylyde)-1-(3,5-diisopropylcyclopentadienylyde)-1,1-dimethylsilane,**

"Li<sub>2</sub>[(<sup>i</sup>Pr<sub>2</sub>Cp)Me<sub>2</sub>Si(MNCp)]" is prepared analogously by the reaction of (<sup>i</sup>Pr<sub>2</sub>Cp)Me<sub>2</sub>Si(MNCp) (8.15g, 22.85 mmol) and nBuLi (32 ml, 1.6 M in hexanes, 51.2 mmol) in diethyl ether (600 ml); 15.5 g, (75%).

(<sup>i</sup>Pr<sub>2</sub>Cp)(μ-Me<sub>2</sub>Si)<sub>2</sub>(Cp), (3) "ThpH<sub>2</sub>." A 250 ml round bottom flask is charged with Li<sub>2</sub>[(<sup>i</sup>Pr<sub>2</sub>Cp)Me<sub>2</sub>Si(Cp)] (4.99 g, 17.5 mmol) and tetrahydrofuran (250 ml). The flask is attached to a medium porosity swivel frit assembly and the solution is cooled to -78°C in an acetone/dry ice bath and degassed. Dichlorodimethylsilane (2.265 g, 17.5 mmol) is vacuum transferred onto the well stirred solution and the reaction mixture is stirred for 16 hours at -78°C. The reaction is allowed to warm slowly to 25°C in about 8 hours in a dry ice/acetone bath, and is then stirred for 16 hours at 25°C. Solvent is removed *in vacuo* and the product is extracted away from the lithium chloride with petroleum ether (2 x 50 ml). The solvent is removed *in vacuo* leaving a yellow oil which is kugel-röhr distilled at 90°C and high vacuum yielding a pale yellow oil; 4.946 g (86%).

(<sup>i</sup>Pr<sub>2</sub>Cp)(μ-Me<sub>2</sub>Si)<sub>2</sub>(<sup>i</sup>PrCp), (4) "<sup>i</sup>PrThpH<sub>2</sub>" is prepared analogously by reaction of Li<sub>2</sub>[(<sup>i</sup>Pr<sub>2</sub>Cp)Me<sub>2</sub>Si(<sup>i</sup>PrCp)] (2.84 g, 8.70 mmol) with Me<sub>2</sub>SiCl<sub>2</sub> (1.12 g, 8.70 mmol) in tetrahydrofuran (40 ml). The yellow oil is kugel-röhr distilled at 120°C and high vacuum yielding a pale yellow oil which slowly crystallizes as a white solid; 3.038 g (94.2%).

(<sup>i</sup>Pr<sub>2</sub>Cp)(μ-Me<sub>2</sub>Si)<sub>2</sub>(<sup>s</sup>BuCp), (6) "<sup>s</sup>BuThpH<sub>2</sub>" is prepared analogously by reaction of Li<sub>2</sub>[(<sup>i</sup>Pr<sub>2</sub>Cp)Me<sub>2</sub>Si(<sup>s</sup>BuCp)] (9.036 g, 26.539 mmol) with Me<sub>2</sub>SiCl<sub>2</sub> (3.425 g, 26.538 mmol) in tetrahydrofuran (150 ml). The yellow oil is kugel-röhr distilled at 130°C and high vacuum yielding a pale yellow oil which slowly crystallizes as a white solid; 7.583 g (74.0%).

(<sup>i</sup>Pr<sub>2</sub>Cp)(μ-Me<sub>2</sub>Si)<sub>2</sub>(MNCp), (7) "MNThpH<sub>2</sub>" is prepared analogously by reaction of Li<sub>2</sub>[(<sup>i</sup>Pr<sub>2</sub>Cp)Me<sub>2</sub>Si(MNCp)] (7.60 g, 20.6 mmol) with Me<sub>2</sub>SiCl<sub>2</sub> (2.66 g, 20.6 mmol) in tetrahydrofuran (150 ml). The yellow oil is kugel-röhr distilled at 130°C and high vacuum yielding a pale yellow oil which crystallizes as a white solid; 4.3 g (50.0%).

**$K_2[(iPr)_2Cp](\mu-Me_2Si)_2(Cp)$**  "K<sub>2</sub>Thp." In the glovebox, a suspension of potassium-*tert*-butoxide (2.30 g, 20.49 mmol) in diethyl ether (30 ml) is added to a stirred solution of ThpH<sub>2</sub> (3.345 g, 10.178 mmol) in diethyl ether (100 ml). The resulting white suspension is stirred at 25°C for 30 minutes. The solid is isolated on a medium frit, washed with diethyl ether (3 x 40 ml), and dried *in vacuo* for two hours resulting in a coarse white solid; 4.05g (98%).

**$(iPr)_2Cp(\mu-Me_2Si)_2(TMSCp)$** , (5) "TMSThpH<sub>2</sub>." A 50 ml Schlenk flask is charged with K<sub>2</sub>Thp (0.653 g, 1.613 mmol) and tetrahydrofuran (30 ml). The white suspension is cooled to -78°C with stirring, trimethylsilylchloride (0.175 g, 1.615 mmol) is vacuum transferred into the schlenk flask, and the flask is warmed to 25°C. After six hours, the suspension has turned into a clear yellow solution. The solution is stirred an additional six hours, volatiles are removed *in vacuo* leaving a yellow foam, and diethyl ether (20 ml) is added to form a white suspension. With vigorous stirring, H<sub>2</sub>O (20 ml) is added slowly and the mixture is transferred to a separatory funnel. The ether layer is separated and the aqueous layer is extracted with diethyl ether (2 x 20 ml). The organic layers are combined, washed with H<sub>2</sub>O (2 x 50 ml) and dried over MgSO<sub>4</sub>. Solvent is removed *in vacuo* and the yellow oil is dried at high vacuum for one hour. The oil is kugel-röhr distilled at 130°C and high vacuum yielding a white solid; 0.46 g (71%).

**ThpZrCl<sub>2</sub> (3B)** (Method 1) In the glovebox, ZrCl<sub>4</sub>(THF)<sub>2</sub> (1.89g, 5.01 mmol) is added to a suspension of K<sub>2</sub>Thp (2.024 g, 5.0 mmol) in tetrahydrofuran (20 ml) and the resulting suspension is stirred for three hours. The solvent is removed *in vacuo* and toluene (40 ml) is added to form a brown suspension. The suspension is filtered through a bed of Celite, and the toluene soluble fraction is dried *in vacuo* leaving a yellow orange solid. The solid is washed with pentane (25 ml) and dried *in vacuo* resulting in a fine white solid; 980 mg (40%).

**ThpZr(NMe<sub>2</sub>)<sub>2</sub>. (3A)** A 100 ml schlenk flask is charged with ThpH<sub>2</sub> (3) (3.069 g, 9.338 mmol), xylenes (30 ml), and Zr(NMe<sub>2</sub>)<sub>4</sub> (2.498 g, 9.338 mmol). The flask is equipped with a reflux condenser and a 180° Teflon needle valve. Under a strong argon purge, the reaction is heated to reflux in a 160°C oil

bath. The reaction is monitored by holding a wet piece of pH paper up to the vent needle. The reaction is allowed to cool to 25°C after no more NMe<sub>2</sub>H is released and the pH paper gives a neutral reading. Total reaction time is typically 12 hours, but the reaction time depends on the strength of the Ar flow. The solvent is removed in vacuo and the yellow solid is dried at high vacuum for 12 hours. The solid is recrystallized from petroleum ether yielding yellow microcrystals; 3.5 g (several crops), (74%).

**<sup>i</sup>PrThpZr(NMe<sub>2</sub>)<sub>2</sub> (4A)** is prepared analogously with **<sup>i</sup>PrThp (4)** (3.003 g, 8.100 mmol) and Zr(NMe<sub>2</sub>)<sub>4</sub> (2.175 g, 8.130 mmol) in refluxing xylenes (20 ml) for 18 hours. The solid is dried at high vacuum yielding a yellow/orange solid which is not purified further; 4.40 g (98%).

**TMSThpZr(NMe<sub>2</sub>)<sub>2</sub> (5A)** is prepared analogously with **TMSThp (5)** (379 mg, 0.945 mmol) and Zr(NMe<sub>2</sub>)<sub>4</sub> (254 mg, 0.949 mmol) in refluxing xylenes (15 ml) for 14 hours. The solvent is removed in vacuo leaving an orange oil which is not purified further; 507 mg (93%).

**<sup>s</sup>BuThpZr(NMe<sub>2</sub>)<sub>2</sub> (6A)** is prepared analogously with **<sup>s</sup>BuThp (6)** (2.02 g, 5.25 mmol) and Zr(NMe<sub>2</sub>)<sub>4</sub> (1.41 g, 5.27 mmol) in refluxing xylenes (15 ml) for 15 hours. The solid is dried at high vacuum yielding a fine yellow solid which is not purified further; 2.9 g (98%).

**MNThpZr(NMe<sub>2</sub>)<sub>2</sub> (7A)** is prepared analogously with **MNThp (7)** (4.3 g, 10.32 mmol) and Zr(NMe<sub>2</sub>)<sub>4</sub> (2.76 g, 10.32 mmol) in refluxing xylenes (30 ml) for 28 hours. The solid is dried at high vacuum yielding a yellow/orange solid which is not purified further; 5.59 g (92%).

**ThpZrCl<sub>2</sub> (3B)** (Method 2) A 25 ml Schlenk flask is charged with **3A** (0.714 g, 1.41 mmol) and toluene (10 ml). Excess trimethylsilylchloride (1.0 ml, 7.8 mmol) is syringe added to the solution at 25°C. The solution is stirred for an hour and the solvent is removed in vacuo yielding a pale yellow solid. Petroleum ether (5 ml) is added to the solid and the resulting yellow suspension is filtered and washed with cold petroleum ether (3 x 5 ml). The resulting white solid is dried at high vacuum for 2 hours; 450 mg (65.2%). Analysis: Calculated (Found) C: 49.15 (49.01); H: 6.91 (5.92).

***i*PrThpZrCl<sub>2</sub> (4B).** A 50 ml Schlenk flask is charged with **4A** (4.40 g, 8.02 mmol) and toluene (20 ml). Trimethylsilylchloride (3.5 ml, 27 mmol) is syringe added to the solution at 25°C. After 5 minutes, a white solid begins to precipitate from the yellow solution. The suspension is stirred for an hour and the solvent is removed in vacuo yielding a yellow solid. Petroleum ether (20 ml) is added to the solid and the resulting yellow suspension is filtered and washed with petroleum ether (3 x 20 ml). The resulting white solid is dried at high vacuum for 2 hours; 2.65 g (62.2%). Analysis: Calculated (Found) C: 52.04 (52.10); H: 6.84 (7.14).

**TMSThpZrCl<sub>2</sub> (5B)** is prepared analogously with **5A** (400 mg, 0.69 mmol) and trimethylsilylchloride (0.3 ml, 2.4 mmol) in toluene (10 ml); 296 mg (75%). Analysis: Calculated (Found) C: 49.25 (48.87); H: 6.83 (6.62).

***s*BuThpZrCl<sub>2</sub> (6B)** is prepared analogously with **6A** (2.9 g, 5.16 mmol) and trimethylsilylchloride (3.0 ml, 23 mmol) in toluene (10 ml); 1.64 g (58.3%). Analysis: Calculated (Found) C: 52.91 (52.94); H: 7.03 (7.07).

**MNThpZrCl<sub>2</sub> (7B)** is prepared analogously with **7A** (1.18 g, 2.00 mmol) and trimethylsilylchloride (1.5 ml, 12 mmol) in toluene (20 ml); 437 mg (38%). Analysis: Calculated (Found) C: 54.51 (54.46); H: 7.39 (7.54).

**Polymerization Procedures:** **CAUTION: All of these procedures should be performed behind a blast shield.**

**2a, 3a, 4a, 5a, 7a** (neat olefin, 0°C). A 100 ml high pressure glass reactor equipped with a septa port, large stir bar, and pressure gauge (0-200 psig) is charged with MAO (500 mg, 8.6 mmol). The reactor is connected to a propylene line (120 psig) and the reactor is purged with propylene for approximately 2 minutes at 120 psig. The reactor is placed in a 0°C ice water bath and propylene (~50 ml, ~1.2 mol) is condensed in the reactor. The propylene inlet valve is then shut and a solution containing catalyst (**3B, 4B, 5B, 7B**) (~ 2mg, ~0.004 mmol) in toluene (.5 ml) is added to the vigorously stirred MAO/ propylene suspension via a 1 ml gas tight syringe through the septa. (The addition requires significant force since the pressure in the reactor is ~95 psig.) The reaction is stirred for 10 minutes during which time polymer

is observed to precipitate from the reaction mixture. At this point the reaction is quenched with MeOH (1 ml in a gas tight syringe) by slow addition while venting the propylene from the reactor. An additional 20 ml is added once the pressure in the reactor is below 2 atmospheres and the white suspension is stirred vigorously for 1 hour to ensure complete quenching of the MAO. The suspension is then added to a vigorously stirred HCl (100 ml of a 20% solution in MeOH). The suspension is stirred for 2 hours and is then filtered and washed with MeOH (4 X 50 ml). The resulting white powder is then dried at high vacuum for 4 hours.

**6a** is prepared analogously using catalyst **6B**. After the reaction is complete, a white solid mass has formed in the bottom of the reactor. After quenching with MeOH as above, the polymer is removed from the reactor and is added to a vigorously stirred HCl (100 ml of a 20% solution in MeOH). The polymer is stirred in the solution for 2 hours and is then filtered and washed with MeOH (4 X 50 ml). The resulting polymer is a relatively soft material with some elasticity. The polymer is soxhlet extracted with refluxing toluene for 24 hours. The solvent is removed in vacuo and the solid is dried at high vacuum for 3 hours.

**3b, 4b, 5b, 6b**, (40 psig, toluene, 25°C). A 100 ml high pressure glass reactor equipped with a septa port, large stir bar, and pressure gauge (0-200 psig) is charged with MAO (500 mg, 8.6 mmol), toluene (35 ml), and catalyst (**3B-6B**) (10 mg, ~0.02 mmol). Upon addition of catalyst to the MAO/toluene suspension, the color typically changes from white to pale yellow. The reactor is connected to a propylene line (40 psig) and the reactor is purged with propylene for 5 minutes at 40 psig and 25°C. The reactor vent is closed and the propylene pressure is maintained at 40 psig for an additional 25 minutes with vigorous stirring at 25°C. The propylene inlet is then shut and the reactor is vented to remove the excess propylene. Once the vent is opened, MeOH (10 ml) is added to the reaction mixture to quench the MAO. An additional 20 ml of MeOH are added once the propylene is gone. The suspension is stirred vigorously for two hours, and then all volatiles are removed by rotary evaporation. The resulting polymer is then placed in a soxhlet thimble, and the product is extracted from refluxing toluene over the

course of 24 hours. The product is dried at high vacuum forming a tacky, sticky solid.

**7b** is prepared analogously using catalyst **7B**. However, upon quenching the reaction with MeOH, a fine white powder precipitates and the suspension is stirred vigorously for 1 hour. The suspension is then added to a vigorously stirred HCl solution (200 ml of a 20% solution in MeOH). The suspension is stirred for 2 hours and is then filtered and washed with MeOH (4 X 50 ml). The resulting white powder is then dried at high vacuum for 4 hours.

**7d** is prepared analogously using catalyst **7B**, except that the propylene pressure is now maintained at 10 psig.

**3c**. In the glove box, a stainless steel high pressure bomb, equipped with a mechanical stirrer and pressure gauge, is charged with MAO (800 mg, 14 mmol). An ampoule containing ThpZrCl<sub>2</sub> (11 mg, 0.022 mmol) in toluene (.5 ml) is attached to the stirrer such that it can be broken by rapid stirring. ~ 100 ml of propylene are condensed into the bomb and the propylene/MAO mixture is brought to 60°C in an oil bath and allowed to equilibrate for 1 hour. At this point, the stirrer is started quickly, breaking the ampoule immediately. The reaction temperature increases as evidenced by a pressure increase to ~400 psig, and after 20 minutes the mixture becomes so viscous as to stop the stirrer. The excess propylene is then vented and the reactor is opened. MeOH is added to quench the reaction and the product is scraped out of the reactor; 120g.



**References and Notes:**

- 1) Brintzinger, H. H.; Fischer, D.; Mulhaupt, R.; Rieger, B.; Waymouth, R. M. *Angew. Chem. Intl. Ed. Engl.* **1995**, *34*, 1143-1170; Bochman, M. *J. Chem. Soc. Dalton Trans.* **1996**, 255-270 and references therein.
- 2) Boor, J. *Ziegler-Natta Catalysts and Polymerizations*; Academic Press: New York, 1979.
- 3) Pino, P.; Mulhaupt, R. *Angew. Chem. Intl. Ed. Engl.* **1980**, *19*, 857.
- 4) Tait, P. J. T.; Watkins, N. D. *Comprehensive Polymer Science*; Pergamon Press: Oxford, 1989 Chapter 1, 2.
- 5) Sinn, H.; Kaminsky, W. *Adv. Organomet. Chem.* **1980**, *32*, 325-387.
- 6) Crowther, D. J.; Borkowski, S. L.; Swenson, D.; Meyer, T. Y.; Jordan, R. F. *Organometallics* **1993**, *12*, 2897.
- 7) Shapiro, P. J.; Cotter, W. D.; Schaefer, W. P.; Labinger, J. A.; Bercaw, J. E. *JACS* **1994**, *116*, 4623-4640.
- 8) Mason, M. R.; Smith, J. M.; Bott, S. G.; Barron, A. R. *JACS* **1993**, *115*, 4971-4984.
- 9) Collins, S.; Gauthier, W. J.; Holden, D. A.; Kuntz, B. A.; Taylor, N. J.; Ward, D. G. *Organometallics* **1991**, *10*, 2061-2068.
- 10) Ewen, J. A.; Jones, R. L.; Razavi, A.; Ferrara, J. D. *J. Am. Chem. Soc.* **1988**, *110*, 6255-6256.
- 11) Coughlin, E. B.; Bercaw, J. E. *J. Am. Chem. Soc.* **1992**, *114*, 7606-7607.
- 12) Piers, W. E.; Bercaw, J. E. *JACS* **1990**, *112*, 9406-9407.
- 13) Burger, B. J.; Thompson, M. E.; Cotter, W. D.; Bercaw, J. E. *J. Am. Chem. Soc.* **1990**, *112*, 1566-1577.
- 14) Chacon, S. T.; Coughlin, E. B.; Henling, L. M.; Bercaw, J. E. *J. Organomet. Chem.* **1995**, *497*, 161. and references therein.
- 15) Spaleck, W.; Aulbach, M.; Bachmann, B.; Kuber, F.; Winter, F. *Macromol. Symp.* **1995**, *89*, 237-247. And references therein.
- 16) Kaminsky, W.; Külper, K.; Brintzinger, H. H.; Wild, F. R. W. P. *Angew. Chem. Intl. Ed. Engl.* **1985**, *24*, 507-508.
- 17) Green, M. L. H.; Ishihara, N. *J. Chem. Soc. Dalton Trans.* **1994**, 657-665.
- 18) Chien, J. C. W.; Llinas, G. H.; Rausch, M. D.; Lin, Y. G.; Winter, H. H. *J. Pol. Sci. PC* **1992**, *30*, 2601-2617.
- 19) Ewen, J. A.; Elder, M. J.; Jones, R. L.; Haspeslagh, L.; Atwood, J. L.; Bott, S. J.; Robinson, K. *Makromol. Chem., Macromol. Symp.* **1991**, *48*, 253-295.

- 20) Herrmann, W. A.; Morawietz, M. J. A. *J. Organomet. Chem.* **1994**, *482*, 169-181.
- 21) Rieger, B.; Jany, G.; Fawzi, R.; Steiman, M. *Organometallics* **1994**, *13*, 647-653.
- 22) Syndiotactic polypropylene is characterized by alternating stereochemistry of the methine carbons on the polymer backbone.
- 23) Razavi, A.; Vereecke, D.; Peters, L.; Dauw, K. D.; Nafpliotis, L.; Atwood, J. L. *Manipulation of the Ligand Structure as an Effective and Versatile Tool.*; Springer-Verlag: Berlin, Heidelberg, 1995; Vol. 1, pp 111-147. **Ziegler Catalysts**.
- 24) Razavi, A.; Atwood, J. L. *J. Organomet. Chem.* **1995**, *497*, 105-111.
- 25) Shiomura, T.; Kohno, M.; Inoue, N.; Yokote, Y.; Akiyama, M.; Asanuma, T.; Sugimoto, R.; Kimura, S.; Abe, M. *Studies in Surface Science and Catalysts*. **1994**, *89*, 326-338.
- 26) [r] refers to a racemic (syndiotactic) diad while [m] refers to a meso (isotactic) diad. The triad level [rr] defines the orientation of the next carbon on each side of the one being measured and the pentad level [rrrr] defines the orientation of the next two carbons on each side of the carbon being measured. The higher the ratio of [r] to [m], the higher the syndiotacticity of the polymer.
- 27) Razavi, A.; Atwood, J. L. *J. Organomet. Chem.* **1993**, *459*, 117-123.
- 28) Patsidis, K.; Alt, H. G.; Milius, W.; Palackal, S. J. *J. Organomet. Chem.* **1996**, *509*, 63-71.
- 29) Canich, J. A. M. *Process for producing crystalline poly- $\alpha$ -olefins with a monocyclopentadienyl transition metal catalyst system*, 1992.
- 30) Schmidt, M. A.; Alt, H. G.; Milius, W. *J. Organomet. Chem.* **1995**, *501*, 101-106.
- 31) Miller, S.; Bercaw, J. E. *Candidacy Report 1996*. Personal Communication
- 32) Yamazaki, H.; Takaishi, K.; Kikuchi, H.; Mise, T.; Kageyama, A.; Nakano, M. *42nd Symposium on Organometallic Chemistry, Japan*. **1995**, A207, 116-117.
- 33) Gilchrist, J. C.; Bercaw, J. E. *J. Am. Chem. Soc.* **1996**. Submitted.
- 34) Pino, P.; Galimberti, M. *J. Organomet. Chem.* **1989**, *370*, 1-7.
- 35) Cavallo, L.; Guerra, G.; Vacatello, M.; Corradini, P. *Macromolecules* **1991**, *24*, 1784-1790.
- 36) Leclerc, M. K.; Brintzinger, H. H. *J. Am. Chem. Soc.* **1995**, *117*, 1651-1652.
- 37) Busico, V.; Cipullo, R. *J. Am. Chem. Soc.* **1994**, *116*, 9329-9330.

- 38) Bierwagen, E. P.; Bercaw, J. E.; Goddard, W. A. *J. Am. Chem. Soc.* **1994**, *116*, 1481-1489. The authors predicted that Group III catalysts are unsuitable for syndiospecific polymerizations due to electronic considerations.
- 39) Ewen, J. A.; Jones, R. L.; Razavi, A.; Ferrara, J. D. *J. Am. Chem. Soc.* **1988**, *110*, 6255-6256. Supplementary material.
- 40) Bunel, E. E.; Ph.D. Thesis, Caltech, Pasadena, CA, 1989.
- 41) Jutzi, P. J.; Sauer, R. *J. Organomet. Chem.* **1973**, *50*, C29 - C30.
- 42) Abel, E. W.; Dunster, M. O.; Waters, A. *J. Organomet. Chem.* **1973**, *49*, 287-321.
- 43) The protonated form of the ligand was obtained by reaction of the mixture of I and II with NaCp in THF.
- 44) Razavi, A.; Ferrara, J. *J. Organomet. Chem.* **1992**, *435*, 299-310.
- 45) Cano, A.; Cuenca, T.; Gomez-Sal, P.; Royo, B.; Royo, P. *Organometallics* **1994**, *13*, 1688-1694.
- 46) Lang, H.; Blau, S.; Muth, A.; Weiss, K.; Neugenauer, U. *J. Organomet. Chem.* **1995**, *490*, C32-C36.
- 47) Mengele, W.; Diebold, J.; Troll, C.; Roll, W.; Brintzinger, H. H. *Organometallics* **1993**, *12*, 1931-1935.
- 48) ...assuming that **A** and **B** have opposite chirality at the beta-carbon of the polymer chain.
- 49) Bulls, A. R. *The synthesis of metallation resistant bis(cyclopentadienyl)ligand systems*; Caltech: Pasadena, CA, 1988.
- 50) Venier, C. G.; Casserly, E. W. *J. Am. Chem. Soc.* **1990**, *112*, 2808-2809.
- 51) Sitzmann, H. *J. Organomet. Chem.* **1988**, *354*, 203-214.
- 52) Clark, T. J.; Nile, T. A. *Tett. Lett.* **1990**, 589.
- 53) Clark, T. J.; Nile, T. A. *Polyhedron* **1989**, *8*, 1804-1806.
- 54) Clark, T. J.; Killian, C. M.; Luthra, S.; Nile, T. A. *J. Organomet. Chem.* **1993**, *462*, 247-257.
- 55) Shige Miyake has scaled up this reaction to yield 420 g. The overall yield from <sup>i</sup>PrCp is 74%.
- 56) The only exception is for R' = TMS. TMSThp has been prepared by the addition of one equivalent of trimethylsilylchloride to K<sub>2</sub>Thp. Me<sub>3</sub>Si was only observed on the less substituted Cp. Deprotonation yielded exclusively the C<sub>s</sub> symmetric isomer of the dianion, K<sub>2</sub>TMSThp.
- 57) Chandra, G.; Lappert, M. F. *J. Chem. Soc. (A)* **1968**, 1940-1945.
- 58) Diamond, G. M.; Rodewald, S.; Jordan, R. F. *Organometallics* **1995**, *14*, 5-7.

- 59) Since the amine elimination is an equilibrium process, the thermodynamic product, which is the  $C_s$  symmetric isomer, is formed while deprotonation gives the kinetic product, which is a mixture of isomers.
- 60) Christopher, J. N.; Diamond, G. M.; Jordan, R. F. *Stereoselective Synthesis of  $SiR_2$  Bridged Ansa Metallocenes by Amine Elimination.*: Chicago, 1995, pp 310 INOR.
- 61) Deanna Zubris has recently prepared the *tert*-butyl substituted analog (*t*BuThp) of the Thp ligand and the metallocene, *t*BuThpZrCl<sub>2</sub>. The polymerization data with these catalysts are included for comparison
- 62) Wiesenfeld, H.; Reinmuth, A.; Barsties, E.; Evertz, K.; Brintzinger, H. H. J. *Organomet. Chem.* **1989**, 369, 359-370.
- 63) Wailes, P. C.; Coutts, R. S. P.; Weigold, H. *Organometallic Chemistry of Titanium, Zirconium, and Hafnium*; Academic Press: New York, New York, 1974.
- 64) Hlatky, G. G.; Turner, H. W.; Eckman, R. R. *JACS* **1989**, 111, 2728-2729.
- 65) Molecular mechanics studies using Cache™ in conjunction with the crystal structure reported herein indicate that the chiral group should be directed as shown in figure 47.
- 66) This assumes that epimerization is not stereoselective with this catalyst system.
- 67) Burger, B. J.; Bercaw, J. E. *New Developments in the Synthesis, Manipulation, and Characterization of Organometallic Compounds*, 1987; Vol. 357. ACS Symposium Series.
- 68) Marvich, R. H.; Brintzinger, H. H. J. *Am. Chem. Soc.* **1971**, 93, 203.
- 69) Perrin, D. D.; Armagregó, W. L. F. *Purification of Laboratory Chemicals*, 3rd ed.; Pergamon Press: New York, NY, 1988.
- 70) Stone, K. J.; Little, D. J. *Org. Chem.* **1984**, 49, 1849.
- 71) Manzer, L. E. *Inorg. Synth.* **1982**, 21, 135.
- 72) Cowley, A. H.; Kemp, R. A. *Synth. React. Inorg. Metal-Org. Chem.* **1981**, 11, 591.
- 73) Okuda, J. Personal Communication.
- 74) The compound is dissolved in benzene and the solution is frozen solid by cooling the flask in a dry ice/ acetone bath. The flask is then opened to dynamic vacuum and the cold bath is removed. As long as a strong vacuum is maintained, the benzene does not melt. After a few hours, the benzene has

completely sublimed into the LN<sub>2</sub> trap and the product remains as a fine powder.

Appendix A:  $^1\text{H}$  and  $^{13}\text{C}$  NMR data.Table 1 (in  $\text{C}_6\text{D}_6$ , unless otherwise mentioned).

Compound	Assignments	$\delta$ (ppm)	J <sub>C-H</sub>
cycEwenH <sub>2</sub> ( <b>1</b> )	C <sub>6</sub> H <sub>10</sub>	0.97(s), 1.02(s), 1.12(s), 1.75(s), 1.82(s), 2.79(m), 2.86(m), 3.45(s),	
	Cp, Fl	3.91(s), 4.04(s), 4.15(s), .427(s), 5.73(m), 6.01(m), 6.13(m), 6.31(m), 6.44(m), 6.73(m), 7.09(m), 7.15(s), 7.2(m), 7.38(d), 7.6(m)	
Li <sub>2</sub> [cycEwen](THF) <sub>n</sub> THF-d <sub>8</sub>	cyclohexyl (10H) Fluorenyl(4H) (4H) Cp(4H)	1.4-2.2(b), 3.8(d) 8.34(d), 8.14(d), 7.22(t), 6.83(t) 6.22(t), 5.76(t)	
[cycEwen]ScCl ( <b>1A</b> )	cyclohexyl (10H) Fluorenyl(4H) (4H) Cp(4H)	1.4- 3.0(b) 7.9(d), 7.5(d), 7.0(m) 6.3(t), 5.6(t)	
[cycEwen]Sc- (CH(SiMe <sub>3</sub> ) <sub>2</sub> ) ( <b>1B</b> )	CH(SiMe <sub>3</sub> ) <sub>2</sub> (18H) CH(SiMe <sub>3</sub> ) <sub>2</sub> (1H) C <sub>6</sub> H <sub>5</sub> (10H) Fluorenyl (4H) (4H) Cp(4H)	-0.33(s) -0.79(s) 1.4-3.0(b), 3.2(d) 7.9(d), 7.55(d), 7.0(m) 6.2(t), 5.5(t)	

[cycEwen]YCl (1C)	cyclohexyl (1H) (1H) (2H) (2H) (2H) (2H) Fluorenyl(4H) (4H) Cp(4H)	1.48(m) 1.58(m) 1.73(m) 1.83(q) 2.12(t) 3.22(d) 7.97(b), 7.62(d), 7.08(m) 6.06(b), 5.72(t)	
[cycEwen]Y- (CH(SiMe <sub>3</sub> ) <sub>2</sub> ) (1D)	CH(SiMe <sub>3</sub> ) <sub>2</sub> (18 H) CH(SiMe <sub>3</sub> ) <sub>2</sub> (1 H) cyclohexyl (8H) (2H) Fluorenyl(8H) Cp(4H)	-0.2 ? 1.3-2.2(b) 3.2(d) 8.0(b), 7.6(d), 7.0(m) 6.1(b), 5.7(b)	
(BTCp)Me <sub>2</sub> SiCl (2 isomers)	Me <sub>2</sub> SiCl (5H), (5H) Me <sub>2</sub> SiCl (6H) Me <sub>3</sub> Si (15 H), (15H) Me <sub>3</sub> Si (18H) Cp(5H) Cp(3H)	0.12(s), 0.15(s) 0.51(s) 0.03(s), 0.20(s) -0.08(s) 6.49,6.8,6.85(m) 6.46,6.9,6.95 (m)	
(BTCp)Et <sub>2</sub> SiCl (2 isomers)	Et <sub>2</sub> SiCl (2H), (1.4H) Et <sub>2</sub> SiCl (10H) Me <sub>3</sub> Si (3 H), (3H) Me <sub>3</sub> Si (18H) Cp(0.75H) Cp(3H)	.85(t), .55- .7(m) 0.9(q), 1.05(t) 0.03(s), 0.20(s) -0.06(s) 6.55, 6.87 (m) 6.48,6.9,6.95(m)	
K <sub>2</sub> [(BTCp)Et <sub>2</sub> SiCp] THF-d <sub>8</sub>	(CH <sub>3</sub> CH <sub>2</sub> ) <sub>2</sub> Si (6H) (CH <sub>3</sub> CH <sub>2</sub> ) <sub>2</sub> Si (4H) (CH <sub>3</sub> ) <sub>3</sub> Si (18 H) Cp (2H) (2H) (2H)	1.2(t) 1.1(q) 0.1(s) 5.72(t) 5.84(t) 6.32(s),	

(BTCp) <sup>i</sup> Pr <sub>2</sub> SiCl (1 isomer)	((CH <sub>3</sub> ) <sub>2</sub> CH) <sub>2</sub> SiCl (2H) ((CH <sub>3</sub> ) <sub>2</sub> CH) <sub>2</sub> SiCl (12H) Me <sub>3</sub> Si (18H) Cp(1H) (1H) (1H)	1.2 (b) 1.1 (m) -0.05 (s) 6.48(m) 6.9(m) 7.05(m)	
K <sub>2</sub> (Hp) THF-d <sub>8</sub>	((CH <sub>3</sub> ) <sub>3</sub> Si) <sub>2</sub> (18H) ((CH <sub>3</sub> ) <sub>2</sub> CH) <sub>2</sub> Si (12 H) ((CH <sub>3</sub> ) <sub>2</sub> CH) <sub>2</sub> Si (2H) Cp (2H) (2H) (2H)	0.097(s) 1.347(t) .9(m) 5.76(t) 5.94(t) 6.36(s)	
(Hp)ZrCl <sub>2</sub> (2A) <sup>1</sup> H	((CH <sub>3</sub> ) <sub>3</sub> Si) <sub>2</sub> (18H) ((CH <sub>3</sub> ) <sub>2</sub> CH) <sub>2</sub> Si (12 H) ((CH <sub>3</sub> ) <sub>2</sub> CH) <sub>2</sub> Si (2H) Cp (2H) (2H) (2H)	0.50(s) 1.06(d), 1.09(d) 1.26(h) 5.80(t) 6.48(s) 6.62(t)	
(Hp)ZrCl <sub>2</sub> (2A) <sup>13</sup> C	((CH <sub>3</sub> ) <sub>3</sub> Si) <sub>2</sub> ((CH <sub>3</sub> ) <sub>2</sub> CH) <sub>2</sub> Si ((CH <sub>3</sub> ) <sub>2</sub> CH) <sub>2</sub> Si Cp	1.551 18.506 11.778 106.260 112.587 117.775 127.504 129.368 144.371	
[(Hp)YCl] <sub>2</sub> (2B) (THF free)	((CH <sub>3</sub> ) <sub>3</sub> Si) <sub>2</sub> (18H) ((CH <sub>3</sub> ) <sub>2</sub> CH) <sub>2</sub> Si (12 H) ((CH <sub>3</sub> ) <sub>2</sub> CH) <sub>2</sub> Si (2H) Cp (2H) (2H) (2H)	0.544(s) 1.46(d), 1.51(d) 1.88(m) 6.311(s) 6.644(s) 6.79(s)	



(Hp)Y(CH(SiMe <sub>3</sub> ) <sub>2</sub> ) (2C)	Y-CH(Si(CH <sub>3</sub> ) <sub>3</sub> ) <sub>2</sub> (18H) Y-CH(Si(CH <sub>3</sub> ) <sub>3</sub> ) <sub>2</sub> (1H) ((CH <sub>3</sub> ) <sub>3</sub> Si) <sub>2</sub> (18H) ((CH <sub>3</sub> ) <sub>2</sub> CH) <sub>2</sub> Si (12 H) ((CH <sub>3</sub> ) <sub>2</sub> CH) <sub>2</sub> Si (2H) Cp (4H) (2H)	0.165(s) 0.565(s) .321(s) 1.39(t) 1.72(m) 6.5581(t) 5.9751(s)	
[(Hp)YH] <sub>2</sub> C <sub>6</sub> D <sub>12</sub> (2D)	(Y-H) <sub>2</sub> ((CH <sub>3</sub> ) <sub>3</sub> Si) <sub>2</sub> (18H) ((CH <sub>3</sub> ) <sub>2</sub> CH) <sub>2</sub> Si (12 H) ((CH <sub>3</sub> ) <sub>2</sub> CH) <sub>2</sub> Si (2H) Cp (2H) (2H) (2H)	2.403(t) 0.544(s) 0.996(t) .9(m) 6.27(t) 6.44(t) 6.88(s)	J <sub>Y-H</sub> = 33 Hz
Li( <sup>t</sup> Bu <sub>2</sub> Cp)[DME] THF-d <sub>8</sub>	<sup>t</sup> Bu (18H) Cp-H (2H) (1H) DME (6H) (4H)	1.53(s) 5.88(s) 5.92(s) 2.81(s) 2.52(s)	
( <sup>t</sup> Bu <sub>2</sub> Cp)Me <sub>2</sub> SiCl	(CH <sub>3</sub> ) <sub>2</sub> SiCl (6H) <sup>t</sup> Bu (18H) Cp-H (2H) (1H)	0.218(s) 1.20(s) 7.1(s) 6.48(s)	
Li <sub>2</sub> [( <sup>t</sup> Bu <sub>2</sub> Cp)Me <sub>2</sub> Si- (MeCp)][DME] 2 isomers THF-d <sub>8</sub>	(CH <sub>3</sub> ) <sub>2</sub> SiCl (1H) (CH <sub>3</sub> ) <sub>2</sub> SiCl (6H) <sup>t</sup> Bu (1.3H), (1.3H) <sup>t</sup> Bu (9H), (9H) Cp-Me (<1H) Cp-Me (3H) Cp-H (<1H) Cp-H (5H)	0.42(s) 0.39(s) 1.19(s), 1.25 (s) 1.21(s), 1.26(s) 2.11(s) 2.09(s) 5.5- 6.0 5.5- 6.0	

Li <sub>2</sub> [( <sup>t</sup> Bu <sub>2</sub> Cp)Me <sub>2</sub> Si-( <sup>t</sup> BuCp)](THF) <sub>n</sub> 1 isomer THF-d <sub>8</sub>	(CH <sub>3</sub> ) <sub>2</sub> SiCl (6H) <sup>t</sup> Bu (9H) (9H) (9H) Cp-H (1H) (1H) (1H) (1H) (1H)	0.40(s) 1.21(s) 1.24(s) 1.27(s) 5.71(t) 5.76(d) 5.78(t) 5.88(t) 5.96(d)	
3-isopropyl-6,6-dimethylfulvene CDCl <sub>3</sub>	(CH <sub>3</sub> ) <sub>2</sub> CH (6H) (CH <sub>3</sub> ) <sub>2</sub> CH (1H) (CH <sub>3</sub> ) <sub>2</sub> C (6H) Cp-H (1H) (1H) (1H)	1.18(d) 2.70(h) 2.16(s) 6.16(q) 6.45(q) 6.52(q)	
<sup>i</sup> Pr <sub>2</sub> Cp CDCl <sub>3</sub>	(CH <sub>3</sub> ) <sub>2</sub> CH (12H)  (CH <sub>3</sub> ) <sub>2</sub> CH (2H) Cp-H (4H)	1.07(d), 1.11(d), 1.70(d) 2.3-2.7(b) 2.3-3.0, 5.98- 6.05	
Li( <sup>i</sup> Pr <sub>2</sub> Cp) THF-d <sub>8</sub>	(CH <sub>3</sub> ) <sub>2</sub> CH (12H) (CH <sub>3</sub> ) <sub>2</sub> CH (2H) Cp-H (2H) (1H)	1.15(d) 2.73(h) 5.33(d) 5.37(t)	6.667 6.808 2.447 2.442
( <sup>i</sup> Pr <sub>2</sub> Cp)Me <sub>2</sub> SiCl	(CH <sub>3</sub> ) <sub>2</sub> SiCl (6H) (CH <sub>3</sub> ) <sub>2</sub> CH (12H)  (CH <sub>3</sub> ) <sub>2</sub> CH (2H) Cp-H	0.051(b), 0.23(b) 1.01(d), 1.08(d), 1.11(d) 2.50(h), 3.06(h) 2.58(b), 2.81(b), 3.39(b), 6.26(s), 6.28(m)	
( <sup>i</sup> Pr <sub>2</sub> Cp)Me <sub>2</sub> Si(Cp)	(CH <sub>3</sub> ) <sub>2</sub> Si (6H) (CH <sub>3</sub> ) <sub>2</sub> CH (12H) (CH <sub>3</sub> ) <sub>2</sub> CH (~2H) Cp-H (~8H)	-0.3- 0.2 1.0-1.3 2.5-3 3.0- 3.6, 6.0- 6.8	

Li <sub>2</sub> [( <sup>i</sup> Pr <sub>2</sub> Cp)Me <sub>2</sub> Si(Cp)] THF-d <sub>8</sub>	(CH <sub>3</sub> ) <sub>2</sub> Si (6H) (CH <sub>3</sub> ) <sub>2</sub> CH (6H) (6H) (CH <sub>3</sub> ) <sub>2</sub> CH (1H) (1H) Cp-H (2H) (2H) (1H) (1H)	.334(s) 1.14(d) 1.16(d) 2.76(h) 3.22(h) 5.96(t) 5.80(t) 5.66(d) 5.62(d)	
( <sup>i</sup> Pr <sub>2</sub> Cp)(Me <sub>2</sub> Si) <sub>2</sub> (Cp) = "Thp" <sup>H</sup> <sub>2</sub> (3)	(CH <sub>3</sub> ) <sub>2</sub> Si (12H) (CH <sub>3</sub> ) <sub>2</sub> CH (12H) (CH <sub>3</sub> ) <sub>2</sub> CH (~2H) Cp-H (~6H)	-1.0- 0.6 1.0- 1.3 2.5- 3.3 3.3- 4.0, 6.4- 7.0	
Li <sub>2</sub> (Thp) THF-d <sub>8</sub>	(CH <sub>3</sub> ) <sub>2</sub> Si (3H) (3H) (3H) (3H) (CH <sub>3</sub> ) <sub>2</sub> CH (3H) (3H) (3H) (3H) (CH <sub>3</sub> ) <sub>2</sub> CH (1H) (1H) Cp-H (2H) (1H) (1H)	-0.572(s) 0.206(s) 0.322(s) 0.444(s) 1.11(s) 1.13(s) 1.15(s) 1.25(s) 2.75(h) 3.11(h) 6.008(s) 6.10(s) 6.356(s)	6.809 6.346 6.548 6.863
K <sub>2</sub> (Thp) THF-d <sub>8</sub>	(CH <sub>3</sub> ) <sub>2</sub> Si (12H) (CH <sub>3</sub> ) <sub>2</sub> CH (12H) (CH <sub>3</sub> ) <sub>2</sub> CH (2H) Cp-H (1H) (3H)	0.368(s) 1.23(d) 3.18(h) 5.973(s) 6.241(s)	6.60 6.65

(Thp)Zr(NMe <sub>2</sub> ) <sub>2</sub> (3A)	(CH <sub>3</sub> ) <sub>2</sub> Si (6H) (6H) (CH <sub>3</sub> ) <sub>2</sub> CH (6H) (6H) (CH <sub>3</sub> ) <sub>2</sub> CH (2H) Zr(N(CH <sub>3</sub> ) <sub>2</sub> ) <sub>2</sub> (12H) Cp-H (1H) (1H) (2H)	.575(s) 0.748(s) 1.096(d) 1.314(d) 3.0(m) 2.91(s) 6.202(t) 6.280(s) 6.545(d)	
(Thp)ZrCl <sub>2</sub> (3B) <sup>1</sup> H	(CH <sub>3</sub> ) <sub>2</sub> Si (6H) (6H) (CH <sub>3</sub> ) <sub>2</sub> CH (6H) (6H) (CH <sub>3</sub> ) <sub>2</sub> CH (2H) Cp-H (1H) (1H) (2H)	0.376(s) 0.546(s) 0.926(d) 1.348(d) 2.905(h) 6.348(t) 6.452(s) 6.737(d)	7.16 Hz 6.60 Hz 6.85 Hz
(Thp)ZrCl <sub>2</sub> (3B) <sup>13</sup> C	(CH <sub>3</sub> ) <sub>2</sub> Si  (CH <sub>3</sub> ) <sub>2</sub> CH and (CH <sub>3</sub> ) <sub>2</sub> CH  Cp	-1.542 3.502  20.895 28.645 29.631  110.190 114.043 115.123 116.378 138.196 165.097	
( <sup>i</sup> Pr <sub>2</sub> Cp)(Me <sub>2</sub> Si) <sub>2</sub> - (TMSCp) = "TMSThp" (5)	(CH <sub>3</sub> )Si (21H) (CH <sub>3</sub> ) <sub>2</sub> CH (12H) (CH <sub>3</sub> ) <sub>2</sub> CH (~2H) Cp-H (~5H)	-0.5- 0.7 1.0- 1.3 2.5- 3.5 3.0- 3.5, 6.4- 7.3	

$K_2(TMSThp)$ THF-d8	(CH <sub>3</sub> ) <sub>3</sub> Si (21H) (CH <sub>3</sub> ) <sub>2</sub> CH (12H) (CH <sub>3</sub> ) <sub>2</sub> CH (2H) Cp-H (1H) (2H)	0.15(s) 1.15(d) 3.04(s) 5.79(s) 6.35(s)	6.766 6.793
(TMSThp)Zr(NMe <sub>2</sub> ) <sub>2</sub> (5A)	(CH <sub>3</sub> ) <sub>3</sub> Si (9H) (CH <sub>3</sub> ) <sub>2</sub> Si (6H) (6H) (CH <sub>3</sub> ) <sub>2</sub> CH (6H) (6H) (CH <sub>3</sub> ) <sub>2</sub> CH (2H) Zr(N(CH <sub>3</sub> ) <sub>2</sub> ) <sub>2</sub> (12H) Cp-H (1H) (2H)	0.25(s) 0.60(s) 0.69(s) 1.17(d) 1.32(d) 2.85(m) 2.71(s) 6.40(s) 6.67(s)	6.859 6.697 6.789
(TMSThp)ZrCl <sub>2</sub> (5B) <sup>1</sup> H	(CH <sub>3</sub> ) <sub>3</sub> Si (9H) (CH <sub>3</sub> ) <sub>2</sub> Si (6H) (6H) (CH <sub>3</sub> ) <sub>2</sub> CH (6H) (6H) (CH <sub>3</sub> ) <sub>2</sub> CH (2H) Cp-H (1H) (2H)	0.477(s) 0.4811(s) 0.6176(s) 0.94(d) 1.32(d) 2.91(h) 6.42(s) 6.98(s)	
(TMSThp)ZrCl <sub>2</sub> (5B) <sup>13</sup> C	(CH <sub>3</sub> ) <sub>3</sub> Si and (CH <sub>3</sub> ) <sub>2</sub> Si	-1.664 0.157 -3.381	
	(CH <sub>3</sub> ) <sub>2</sub> CH and (CH <sub>3</sub> ) <sub>2</sub> CH	20.681 28.524 29.618	
	Cp	109.334 114.340 119.557 126.773 143.185 165.064	

6- <i>tert</i> -butylfulvene	(CH <sub>3</sub> )CCH (9H) (CH <sub>3</sub> )CCH (1H) Cp-H (1H) (1H) (1H) (1H)	1.05(s) 6.17(s) 6.19(m) 6.395(m) 6.575(m) 6.69(m)	
Li[CpC(H)(CH <sub>3</sub> )- (CMe <sub>3</sub> )] Li <sup>+</sup> MN <sup>-</sup> THF-d <sub>8</sub>	(CH <sub>3</sub> )CC(CH <sub>3</sub> )H (9H) (CH <sub>3</sub> )CC(CH <sub>3</sub> )H (3H) (CH <sub>3</sub> )CC(CH <sub>3</sub> )H (1H) Cp-H (4H)	.8311(s) 1.179(d) 2.435(q) 5.52(m),5.54(m)	7.15 Hz 7.207 Hz
Li <sub>2</sub> [( <sup>i</sup> Pr <sub>2</sub> Cp)Me <sub>2</sub> Si- ( <sup>i</sup> PrCp)] THF-d <sub>8</sub>	(CH <sub>3</sub> ) <sub>2</sub> Si (6H) (CH <sub>3</sub> ) <sub>2</sub> CH (6H) (6H) (6H) (CH <sub>3</sub> ) <sub>2</sub> CH (1H) (1H) (1H) Cp-H (1H) (2H) (2H)	0.3075(s) 1.144(d) <b>1.158(d)</b> 1.170(d) 2.772(h) <b>2.814(h)</b> 3.233(h) 5.6257(d) 5.69(m) 5.83(m)	6.72 <b>6.86</b> 6.76 6.774 <b>6.835</b> 6.76 2.24
( <sup>i</sup> Pr <sub>2</sub> Cp)(Me <sub>2</sub> Si) <sub>2</sub> ( <sup>i</sup> PrCp) = " <sup>i</sup> PrThp" (4)	(CH <sub>3</sub> ) <sub>2</sub> Si (12H)  (CH <sub>3</sub> ) <sub>2</sub> CH (18H)  (CH <sub>3</sub> ) <sub>2</sub> CH (3H)  Cp-H (5H)	-0.336(s) -0.239(s) 0.555(s) 0.603(s) 1.106(d) 1.280(d) 1.306(d) 2.672(m) 2.862(m) 3.188(m) 3.461(s) 3.558(s) 6.50(s) 7.20(s)	6.692 6.560 6.813 6.547 6.524 6.561

(iPrThp)Zr(NMe <sub>2</sub> ) <sub>2</sub> ( <b>4A</b> )	(CH <sub>3</sub> ) <sub>2</sub> Si (6H)	0.595(s)	
	(6H)	0.720(s)	
	(CH <sub>3</sub> ) <sub>2</sub> CH (6H)	1.187(d)	6.857
	(6H)	1.204(d)	6.816
	(6H)	1.342(d)	6.733
	(CH <sub>3</sub> ) <sub>2</sub> CH (3H)	2.8-2.95(m)	
	Zr(N(CH <sub>3</sub> ) <sub>2</sub> ) <sub>2</sub> (12 H)	2.773(s)	
(iPrThp)ZrCl <sub>2</sub> ( <b>4B</b> ) <sup>1</sup> H	Cp-H (2H)	6.356(s)	
	(1H)	6.387(s)	
	(CH <sub>3</sub> ) <sub>2</sub> Si (6H)	0.461(s)	
	(6H)	0.605(s)	
	(CH <sub>3</sub> ) <sub>2</sub> CH (6H)	0.951(d)	7.142
	(6H)	1.341(d)	~6.167
	(6H)	1.357(d)	~6.145
(CH <sub>3</sub> ) <sub>2</sub> CH (2H)	2.928(h)	6.84	
(1H)	3.200(h)	6.90	
(iPrThp)ZrCl <sub>2</sub> ( <b>4B</b> ) <sup>13</sup> C C <sub>6</sub> D <sub>6</sub> /THF	Cp-H (2H)	6.466(s)	
	(1H)	6.678(s)	
	(CH <sub>3</sub> ) <sub>2</sub> Si	-1.582	
		3.531	
	(CH <sub>3</sub> ) <sub>2</sub> CH and (CH <sub>3</sub> ) <sub>2</sub> CH	20.769	
		23.761	
		28.533	
28.585			
Cp	29.682		
	110.229		
	113.814		
	115.539		
	135.801		
	139.625		
	164.848		

Li <sub>2</sub> [( <sup>i</sup> Pr <sub>2</sub> Cp)Me <sub>2</sub> Si (MNCp)]	(CH <sub>3</sub> ) <sub>2</sub> Si (6H)	0.2965(s)	
	(CH <sub>3</sub> ) <sub>3</sub> CH(CH <sub>3</sub> ) (9H)	0.843(s)	
	(CH <sub>3</sub> ) <sub>3</sub> CH(CH <sub>3</sub> ) (3H)	1.14(d)	
	(CH <sub>3</sub> ) <sub>2</sub> CH (6H)	1.13(d)	
	(6H)	1.17(d)	
	(CH <sub>3</sub> ) <sub>3</sub> CH(CH <sub>3</sub> ) (1H)	2.46(q)	
	(CH <sub>3</sub> ) <sub>2</sub> CH (1H)	2.770(h)	
	(1H)	3.188(h)	
	Cp-H (2H)	5.648(s)	
	(1H)	5.664(s)	
	(1H)	5.804(s)	
(1H)	5.831(s)		
K <sub>2</sub> (MNCp)	(CH <sub>3</sub> ) <sub>2</sub> Si (6H)	0.3714(s)	
	(6H)	0.3805(s)	
	(CH <sub>3</sub> ) <sub>3</sub> CH(CH <sub>3</sub> ) (9H)	0.9266(s)	
	(CH <sub>3</sub> ) <sub>3</sub> CH(CH <sub>3</sub> ) (3H)	1.197(d)	7.117
	(CH <sub>3</sub> ) <sub>2</sub> CH (12H)	1.225(d)	6.643
	(CH <sub>3</sub> ) <sub>3</sub> CH(CH <sub>3</sub> ) (1H)	2.581(q)	7.214
	(CH <sub>3</sub> ) <sub>2</sub> CH (2H)	3.209(h)	6.791
	Cp-H (1H)	5.973(s)	
(2H)	6.023(s)		



(MNThp)Zr(NMe <sub>2</sub> ) <sub>2</sub> (7A)	(CH <sub>3</sub> ) <sub>2</sub> Si (3H)	0.5660(s)	
	(3H)	0.6530(s)	
	(3H)	0.6885(s)	
	(3H)	0.6994(4)	
	(CH <sub>3</sub> ) <sub>3</sub> CH(CH <sub>3</sub> ) (9H)	0.9118(s)	
	(CH <sub>3</sub> ) <sub>3</sub> CH(CH <sub>3</sub> ) (3H)	1.202(d)	6.800
	(CH <sub>3</sub> ) <sub>2</sub> CH (3H)	1.19(d)	7.289
	(3H)	1.215(d)	6.238
	(3H)	1.337(d)	6.691
	(3H)	1.361(d)	6.711
	Zr(N(CH <sub>3</sub> ) <sub>2</sub> ) <sub>2</sub> (6H)	2.7056(s)	
	(6H)	2.8683(s)	
	(CH <sub>3</sub> ) <sub>3</sub> CH(CH <sub>3</sub> ) (1H)	2.64(q)	7.199
	(CH <sub>3</sub> ) <sub>2</sub> CH (2H)	2.87-3.0(m)	
	Cp-H (1H)	6.3609(s)	
	(1H)	6.4093(s)	
(1H)	6.4333(s)		
(MNThp)ZrCl <sub>2</sub> (7B) <sup>1</sup> H C <sub>6</sub> D <sub>6</sub> /THF	(CH <sub>3</sub> ) <sub>2</sub> Si (3H)	0.4754(s)	
	(3H)	0.5020(s)	
	(3H)	0.5646(s)	
	(3H)	0.5986(s)	
	(CH <sub>3</sub> ) <sub>3</sub> CH(CH <sub>3</sub> ) (9H)	0.7947(s)	
	(CH <sub>3</sub> ) <sub>3</sub> CH(CH <sub>3</sub> ) (3H)	1.363(d)	~6.736
	(CH <sub>3</sub> ) <sub>2</sub> CH (3H)	0.952(d)	7.125
	(3H)	0.970(d)	7.934
	(3H)	1.378(d)	~6.7
	(3H)	1.641(d)	7.198
	(CH <sub>3</sub> ) <sub>3</sub> CH(CH <sub>3</sub> ) (1H)	2.892(q)	7.106
	(CH <sub>3</sub> ) <sub>2</sub> CH (1H)	2.9124(h)	6.742
	(1H)	2.9878(h)	6.79
	Cp-H (1H)	6.4864(s)	
	(1H)	6.657(d)	
	(1H)	6.780(d)	

(MNTbp)ZrCl <sub>2</sub> ( <b>7B</b> ) <sup>13</sup> C	(CH <sub>3</sub> ) <sub>2</sub> Si	-1.7099 -1.5796 3.3927 3.7141	
	(CH <sub>3</sub> ) <sub>3</sub> CH(CH <sub>3</sub> ), (CH <sub>3</sub> ) <sub>3</sub> CH(CH <sub>3</sub> ), (CH <sub>3</sub> ) <sub>2</sub> CH, (CH <sub>3</sub> ) <sub>3</sub> CH(CH <sub>3</sub> ), and (CH <sub>3</sub> ) <sub>2</sub> CH	15.5304 20.7513 28.1729 28.5396 28.5639 29.6547 29.7469 34.5829 44.4194	
	Cp	109.7364 110.1156 113.9873 114.2007 115.1752 134.6010 137.2068 140.0237 163.9334 166.1607	
6,6-ethyl,methyl- fulvene	CH <sub>3</sub> CH <sub>2</sub> CCH <sub>3</sub> (3H)	1.156(t)	7.562
	CH <sub>3</sub> CH <sub>2</sub> CCH <sub>3</sub> (3H)	2.1916(s)	
	CH <sub>3</sub> CH <sub>2</sub> CCH <sub>3</sub> (2H)	2.543(q)	7.596
	Cp-H (4H)	6.44-6.52(m)	
Li( <sup>s</sup> BuCp) THF-d <sub>8</sub>	CH <sub>3</sub> CH <sub>2</sub> CHCH <sub>3</sub> (3H)	1.155(d)	6.9
	CH <sub>3</sub> CH <sub>2</sub> CHCH <sub>3</sub> (3H)	0.839(t)	7.5
	CH <sub>3</sub> CH <sub>2</sub> CCH <sub>3</sub> (1H)	1.444(m)	6.6
	(1H)	1.543(m)	6.6
	CH <sub>3</sub> CH <sub>2</sub> CHCH <sub>3</sub> (1H)	2.515(m)	6.9
	Cp-H (4H)	5.526(s)	

Li <sub>2</sub> [( <sup>i</sup> Pr <sub>2</sub> Cp)Me <sub>2</sub> Si-( <sup>s</sup> BuCp)] THF-d <sub>8</sub>	(CH <sub>3</sub> ) <sub>2</sub> Si (6H)	0.299(s)	
	(CH <sub>3</sub> ) <sub>2</sub> CH (6H)	1.14(d)	
	(6H)	1.16(d)	
	CH <sub>3</sub> CH <sub>2</sub> CHCH <sub>3</sub> (3H)	1.17(d)	
	CH <sub>3</sub> CH <sub>2</sub> CHCH <sub>3</sub> (3H)	0.853(t)	7.2
	CH <sub>3</sub> CH <sub>2</sub> CCH <sub>3</sub> (1H)	1.401(m)	7.1
	(1H)	1.565(m)	6.9
	CH <sub>3</sub> CH <sub>2</sub> CHCH <sub>3</sub> (1H)	2.519(m)	6.9
	(CH <sub>3</sub> ) <sub>2</sub> CH (1H)	2.771(h)	6.9
	(1H)	3.217(h)	6.6
	Cp-H (2H)	5.817(m)	
	(2H)	5.668(m)	
(1H)	5.615(m)		
(iPr <sub>2</sub> Cp)(Me <sub>2</sub> Si) <sub>2</sub> -( <sup>s</sup> BuCp) = " <sup>s</sup> BuThp" (6)	(CH <sub>3</sub> ) <sub>2</sub> Si (6H)	-0.40- -0.20	
	(6H)	0.35- 0.8	
	(CH <sub>3</sub> ) <sub>2</sub> CH		
	CH <sub>3</sub> CH <sub>2</sub> CHCH <sub>3</sub>		
	CH <sub>3</sub> CH <sub>2</sub> CHCH <sub>3</sub> (21H)	0.8- 1.8	
	CH <sub>3</sub> CH <sub>2</sub> CCH <sub>3</sub>		
	CH <sub>3</sub> CH <sub>2</sub> CHCH <sub>3</sub>		
	(CH <sub>3</sub> ) <sub>2</sub> CH (2H)	2.4-2.9	
Cp-H (2.3 H)	3.0- 4.0		
Cp-H (2.7H)	6.35- 7.1		

$(^s\text{BuThp})\text{Zr}(\text{NMe}_2)_2$ <b>(6A)</b>	$(\text{CH}_3)_2\text{Si}$ (3H)	0.5452(s)	
	(3H)	0.5575(s)	
	(3H)	0.6641(s)	
	(3H)	0.6819(s)	
	$(\text{CH}_3)_2\text{CH}$ (3H)	0.842(d)	7.39
	(3H)	0.855(d)	7.34
	(3H)	1.092(d)	6.947
	(3H)	1.349(d)	6.698
	$\text{CH}_3\text{CH}_2\text{CHCH}_3$ (3H)	1.463(d)	6.754
	$(\text{CH}_3)_2\text{CH}$ (2H)	3.268(h)	7.115
	$\text{Zr}(\text{N}(\text{CH}_3)_2)_2$ (12 H)	2.828(s)	
	$\text{CH}_3\text{CH}_2\text{CHCH}_3$ (3H)	2.498(q)	6.319
	$\text{CH}_3\text{CH}_2\text{CCH}_3$ (1H)	1.3954(h)	6.919
	(1H)	1.5600(h)	7.091
	$\text{Cp-H}$ (1H)	6.2912(s)	
	(1H)	6.5217(s)	
(1H)	6.5422(s)		
$(^s\text{BuThp})\text{ZrCl}_2$ <b>(6B)</b> $^1\text{H}$	$(\text{CH}_3)_2\text{Si}$ (3H)	0.4661(s)	
	(3H)	0.4770(s)	
	(3H)	0.5913(s)	
	(3H)	0.6079(s)	
	$(\text{CH}_3)_2\text{CH}$ (3H)	0.950(d)	7.100
	(3H)	0.957(d)	7.05
	(3H)	1.356(d)	6.50
	(3H)	1.362(d)	6.50
	$\text{CH}_3\text{CH}_2\text{CHCH}_3$ (3H)	1.460(d)	6.90
	$(\text{CH}_3)_2\text{CH}$ (2H)	2.94(m)	7.0
	$\text{CH}_3\text{CH}_2\text{CHCH}_3$ (3H)	0.8029(t)	7.35
	$\text{CH}_3\text{CH}_2\text{CHCH}_3$ (1H)	1.510(m)	7.35
	(1H)	1.781(m)	
	$\text{CH}_3\text{CH}_2\text{CHCH}_3$ (1H)	3.045(q)	6.85
	$\text{Cp-H}$ (1H)	6.4706(s)	
	(1H)	6.676(s)	
(1H)	6.7125(s)		

$(^s\text{BuThp})\text{ZrCl}_2$ ( <b>6B</b> ) $^{13}\text{C}$ $\text{C}_6\text{D}_6/\text{THF}$	$(\text{CH}_3)_2\text{Si}$	-1.522
		-1.493
		3.527
		3.656
	$(\text{CH}_3)_2\text{CH}$ , $\text{CH}_3\text{CH}_2\text{CHCH}_3$ , $(\text{CH}_3)_2\text{CH}$ , $\text{CH}_3\text{CH}_2\text{CHCH}_3$ , $\text{CH}_3\text{CH}_2\text{CHCH}_3$ , and $\text{CH}_3\text{CH}_2\text{CHCH}_3$	11.583
		19.226
		20.868
		28.647
		29.655
		29.674
	Cp	31.860
		34.906
		110.027
110.139		
113.855		
114.924		
115.961		
135.057		
137.110		
138.971		
164.533		
165.291		

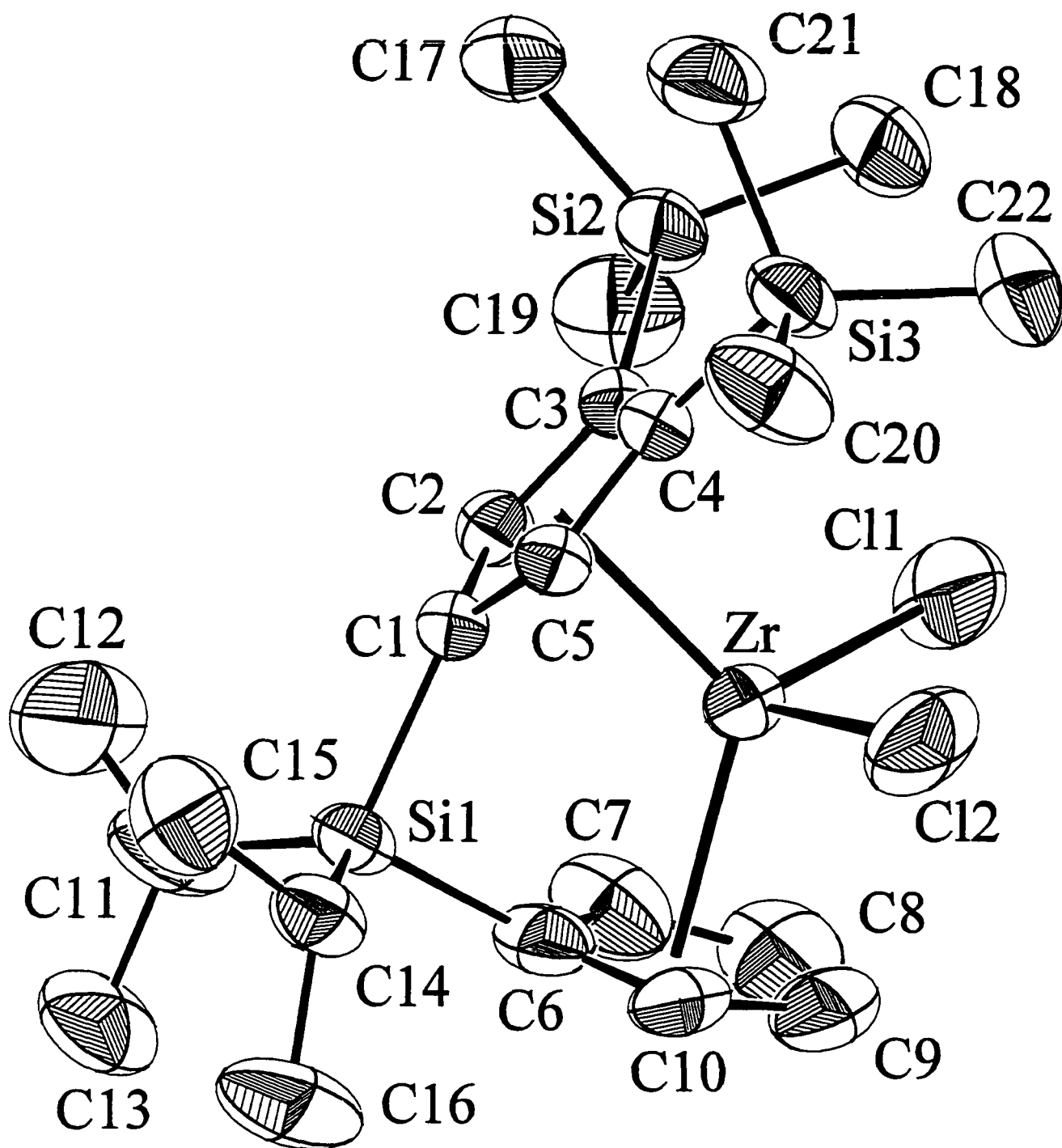
Appendix B: Crystal Structure Data for  $\text{HpZrCl}_2$ .

Figure 1: An ORTEP drawing of  $\text{HpZrCl}_2$  (2A) with 50% probability ellipsoids showing the numbering system.

**Solution and Refinement:**

The structure was solved with SHELXS-86. The hydrogen atom coordinates were placed at calculated positions (C - H = 0.95Å) with a B fixed at 1.2 times that of the attached carbon atom.

Refinement was full-matrix least-squares using CRYM programs.

Weights  $w$  are calculated as  $1/\sigma^2(F_o^2)$ ; variances ( $\sigma^2(F_o^2)$ ) were derived from counting statistics plus an additional term,  $(0.014I)^2$ ; variances of the merged data were obtained by propagation of error plus another additional term,  $(0.014\bar{I})^2$ .

**Definitions:**

$$R = \frac{\sum |F_o - |F_c||}{\sum F_o}; \quad R_w = \left\{ \frac{\sum w(F_o^2 - F_c^2)^2}{\sum w(F_o^2)^2} \right\}^{\frac{1}{2}}$$

$$S = \left\{ \frac{\sum w(F_o^2 - F_c^2)^2}{n - p} \right\}^{\frac{1}{2}} \quad \begin{array}{l} \text{where } n = \text{number of data,} \\ p = \text{number of parameters refined.} \end{array}$$

**Comment:**

One of the isopropyl groups on the linker silicon atom is disordered, apparently with the hydrogen atom on C11 in sites both towards and away from the other isopropyl group. This disorder is evidenced in the large  $U_{eq}$ s for C11 and especially C12 (maximum mean square amplitudes of 0.22 and .39 respectively), the librationaly shortened C11-C12 single bond of 1.330(8)Å, and the near planarity of the angles around C11 (sum of 356.1° vs. 339.1° for the chemically equivalent C14). This disorder was modelled with two separate isotropic partially-populated sites for both C11 and C12; however, as this approach lead to no significant improvement, it was abandoned.

**Table 1. Crystal and Intensity Collection Data for  
HpZrCl<sub>2</sub>**

Formula: C <sub>22</sub> H <sub>38</sub> ZrCl <sub>2</sub> Si <sub>3</sub>	Formula weight: 548.93
Crystal color: Colorless	Habit: Lozenge
Crystal size: 0.18 × 0.44 × 0.49 mm	$\rho_{\text{calc}} = 1.320 \text{ g cm}^{-3}$
Crystal System: Monoclinic	Space group: P2 <sub>1</sub> /c (#14)
$a = 12.351(3)\text{\AA}$	
$b = 12.609(2)\text{\AA}$	$\beta = 100.57(2)^\circ$
$c = 18.042(3)\text{\AA}$	
$V = 2762.1(9)\text{\AA}^3$	$Z = 4$
Lattice parameters: 25 reflections,	$12^\circ \leq \theta \leq 14^\circ$
$\mu = 7.29 \text{ cm}^{-1}$ ( $\mu_{\text{Tmax}} = 0.25$ )	Transmission coeff. = 0.93 – 1.04
CAD-4 diffractometer	$\omega$ scan
MoK $\alpha$ , $\lambda = 0.7107\text{\AA}$	Graphite monochromator
$2\theta$ range: $2^\circ$ – $50^\circ$	$-14 \leq h \leq 14, 0 \leq k \leq 15, -21 \leq l \leq 21$
$T = 295\text{K}$	$F_{000} = 1144$
Number of reflections measured: 10465	Number of independent reflections: 4839
Number with $F_o^2 > 0$ : 4489	Number with $F_o^2 > 3\sigma(F_o^2)$ : 3804
Standard reflections: 3 every 2.5 hrs	Linear Decay: -0.4%
GOF <sub>merge</sub> : 1.17 for 4831 multiples	R <sub>merge</sub> : 0.023 for 4705 duplicates
Number used in refinement: 4839	Criterion: All reflections used
Final R: 0.040 for 3804 reflections with $F_o^2 > 3\sigma(F_o^2)$	
Final R: 0.051 for 4489 reflections with $F_o^2 > 0$	
Final weighted R: 0.089 for 4839 reflections	
Final goodness of fit: 2.19 for 253 parameters and 4839 reflections	
$(\Delta/\sigma)_{\text{max}}$ in final least squares cycle: 0.02	
$\Delta\rho_{\text{max}}$ : $0.65 \text{ e}\text{\AA}^{-3}$ , $\Delta\rho_{\text{min}}$ : $-0.58 \text{ e}\text{\AA}^{-3}$ in final difference map	



**Table 2. Final Heavy Atom Parameters for  
HpZrCl<sub>2</sub>**

$x, y, z$ and $U_{eq}^a \times 10^4$				
Atom	$x$	$y$	$z$	$U_{eq}$
Zr	1300.1(3)	1807.0(3)	6699.4(2)	469(1)
Cl1	2704(1)	453(1)	6868(1)	1027(4)
Cl2	1634(1)	2610(1)	7948(1)	915(4)
Si1	-883.6(7)	2871.7(7)	5585.9(5)	425(2)
Si2	3649.6(8)	1988.7(8)	5365.6(6)	544(2)
Si3	3581.6(7)	4104.3(9)	6997.0(6)	547(3)
C1	640(2)	3109(2)	5694(2)	370(7)
C2	1376(3)	2424(3)	5402(2)	409(7)
C3	2483(2)	2589(3)	5772(2)	395(7)
C4	2444(2)	3381(2)	6340(2)	393(7)
C5	1315(2)	3677(2)	6271(2)	391(7)
C6	-711(3)	1677(3)	6213(2)	559(10)
C7	-233(3)	691(3)	6052(3)	789(13)
C8	119(4)	148(4)	6729(4)	988(18)
C9	-81(4)	774(4)	7311(3)	918(15)
C10	-593(3)	1694(3)	6998(2)	677(11)
C11	-1548(3)	2527(5)	4602(2)	1034(18)
C12	-1145(5)	2831(7)	4001(3)	1744(32)
C13	-2751(3)	2263(4)	4517(3)	922(15)
C14	-1512(3)	3985(3)	6040(2)	541(9)

**Table 2. (Cont.)**

Atom	<i>x</i>	<i>y</i>	<i>z</i>	$U_{eq}$
C15	-1480(4)	5031(3)	5623(3)	861(13)
C16	-2658(3)	3772(4)	6220(3)	957(15)
C17	4028(3)	2965(4)	4689(2)	721(11)
C18	4897(3)	1653(4)	6071(3)	841(13)
C19	3123(4)	783(4)	4835(3)	883(13)
C20	2916(3)	5118(4)	7517(3)	849(13)
C21	4452(3)	4816(4)	6418(3)	789(12)
C22	4458(3)	3244(4)	7693(2)	890(14)

$$^a U_{eq} = \frac{1}{3} \sum_i \sum_j [U_{ij}(a_i^* a_j^*)(\bar{a}_i \cdot \bar{a}_j)]$$

**Table 3. Complete Distances and Angles for  
HpZrCl<sub>2</sub>**

	Distance(Å)	Distance(Å)	
Zr -Cl1	2.412(1)	C14 -C15	1.521(6)
Zr -Cl2	2.435(1)	C14 -C16	1.533(6)
Zr -CpA	2.217	C2 -H2	0.95
Zr -CpB	2.211	C5 -H5	0.95
Zr -C1	2.471(3)	C7 -H7	0.95
Zr -C2	2.486(3)	C8 -H8	0.95
Zr -C3	2.608(3)	C9 -H9	0.95
Zr -C4	2.587(3)	C10 -H10	0.95
Zr -C5	2.483(3)	C11 -H11	0.95
Zr -C6	2.484(4)	C12 -H12a	0.95
Zr -C7	2.473(4)	C12 -H12b	0.95
Zr -C8	2.557(5)	C12 -H12c	0.95
Zr -C9	2.553(5)	C13 -H13a	0.95
Zr -C10	2.498(4)	C13 -H13b	0.95
Si1 -C1	1.880(3)	C13 -H13c	0.95
Si1 -C6	1.872(4)	C14 -H14	0.95
Si1 -C11	1.865(5)	C15 -H15a	0.95
Si1 -C14	1.865(3)	C15 -H15b	0.95
Si2 -C3	1.890(3)	C15 -H15c	0.95
Si2 -C17	1.853(4)	C16 -H16a	0.95
Si2 -C18	1.858(4)	C16 -H16b	0.95
Si2 -C19	1.850(5)	C16 -H16c	0.95
Si3 -C4	1.898(3)	C17 -H17a	0.95
Si3 -C20	1.863(5)	C17 -H17b	0.95
Si3 -C21	1.861(4)	C17 -H17c	0.95
Si3 -C22	1.851(5)	C18 -H18a	0.95
C1 -C2	1.424(4)	C18 -H18b	0.95
C1 -C5	1.405(4)	C18 -H18c	0.95
C2 -C3	1.423(4)	C19 -H19a	0.95
C3 -C4	1.437(4)	C19 -H19b	0.95
C4 -C5	1.427(4)	C19 -H19c	0.95
C6 -C7	1.429(6)	C20 -H20a	0.95
C6 -C10	1.398(5)	C20 -H20b	0.95
C7 -C8	1.399(7)	C20 -H20c	0.95
C8 -C9	1.372(7)	C21 -H21a	0.95
C9 -C10	1.391(6)	C21 -H21b	0.95
C11 -C12	1.330(8)	C21 -H21c	0.95
C11 -C13	1.502(7)	C22 -H22a	0.95

Table 3. (Cont.)

Distance(Å)		Angle(°)
C22 -H22b	0.95	CpA -Zr -CpB 122.5
C22 -H22c	0.95	Cl1 -Zr -Cl2 100.5(0)
		CpA -Zr -Cl1 111.0
		CpA -Zr -Cl2 107.0
		CpB -Zr -Cl1 110.2
		CpB -Zr -Cl2 103.0
		C6 -Si1 -C1 93.7(1)
		C11 -Si1 -C1 113.2(2)
		C14 -Si1 -C1 108.9(1)
		C11 -Si1 -C6 111.6(2)
		C14 -Si1 -C6 110.6(2)
		C14 -Si1 -C11 116.6(2)
		C17 -Si2 -C3 107.0(2)
		C18 -Si2 -C3 114.8(2)
		C19 -Si2 -C3 108.0(2)
		C18 -Si2 -C17 109.0(2)
		C19 -Si2 -C17 108.2(2)
		C19 -Si2 -C18 109.6(2)
		C20 -Si3 -C4 107.4(2)
		C21 -Si3 -C4 108.6(2)
		C22 -Si3 -C4 114.6(2)
		C21 -Si3 -C20 107.8(2)
		C22 -Si3 -C20 108.5(2)
		C22 -Si3 -C21 109.7(2)
		C2 -C1 -Si1 124.1(2)
		C5 -C1 -Si1 127.2(2)
		C5 -C1 -C2 104.6(2)
		C3 -C2 -C1 111.2(3)
		C2 -C3 -Si2 119.6(2)
		C4 -C3 -Si2 133.0(2)
		C4 -C3 -C2 106.3(3)
		C3 -C4 -Si3 131.4(2)
		C5 -C4 -Si3 121.9(2)
		C5 -C4 -C3 106.3(2)
		C4 -C5 -C1 111.6(3)
		C7 -C6 -Si1 125.7(3)
		C10 -C6 -Si1 125.3(3)
		C10 -C6 -C7 104.4(3)

Table 3. (Cont.)

Angle(°)				Angle(°)			
C8	-C7	-C6	108.8(4)	H22c	-C22	-H22a	109.5
C9	-C8	-C7	108.4(5)	H22c	-C22	-H22b	109.5
C10	-C9	-C8	107.5(4)				
C9	-C10	-C6	110.7(4)				
C12	-C11	-Si1	122.9(4)				
C13	-C11	-Si1	113.8(3)				
C13	-C11	-C12	119.4(5)				
C15	-C14	-Si1	112.6(3)				
C16	-C14	-Si1	115.8(3)				
C16	-C14	-C15	111.5(3)				
H12b	-C12	-H12a	109.5				
H12c	-C12	-H12a	109.5				
H12c	-C12	-H12b	109.5				
H13b	-C13	-H13a	109.5				
H13c	-C13	-H13a	109.5				
H13c	-C13	-H13b	109.5				
H15b	-C15	-H15a	109.5				
H15c	-C15	-H15a	109.5				
H15c	-C15	-H15b	109.5				
H16b	-C16	-H16a	109.5				
H16c	-C16	-H16a	109.5				
H16c	-C16	-H16b	109.5				
H17b	-C17	-H17a	109.5				
H17c	-C17	-H17a	109.5				
H17c	-C17	-H17b	109.5				
H18b	-C18	-H18a	109.5				
H18c	-C18	-H18a	109.5				
H18c	-C18	-H18b	109.5				
H19b	-C19	-H19a	109.5				
H19c	-C19	-H19a	109.5				
H19c	-C19	-H19b	109.5				
H20b	-C20	-H20a	109.5				
H20c	-C20	-H20a	109.5				
H20c	-C20	-H20b	109.5				
H21b	-C21	-H21a	109.5				
H21c	-C21	-H21a	109.5				
H21c	-C21	-H21b	109.5				
H22b	-C22	-H22a	109.5				

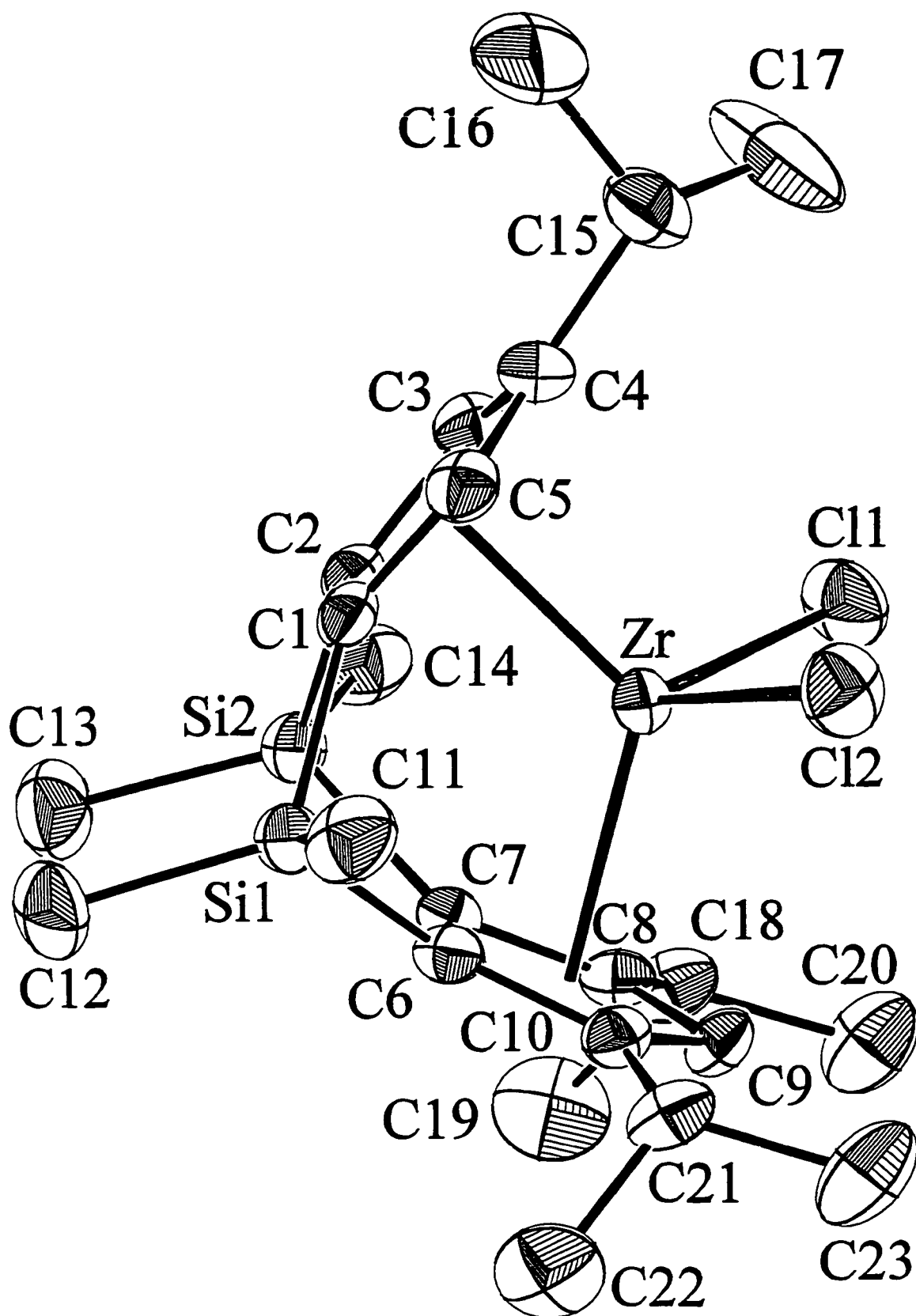
Appendix C: Crystal Structure Data for  $i\text{PrThpZrCl}_2$ .

Figure 1: An ORTEP drawing of  $i\text{PrThpZrCl}_2$  (4B) with 50% probability ellipsoids showing the numbering system.

**Solution and Refinement:**

The structure was solved with SHELXS-86. The hydrogen atom coordinates were placed at calculated positions (C - H = 0.95Å) with a B fixed at 1.2 times that of the attached carbon atom.

Refinement was full-matrix least-squares using CRYM programs.

Weights  $w$  are calculated as  $1/\sigma^2(F_o^2)$ ; variances ( $\sigma^2(F_o^2)$ ) were derived from counting statistics plus an additional term,  $(0.014I)^2$ ; variances of the merged data were obtained by propagation of error plus another additional term,  $(0.014\bar{I})^2$ .

**Definitions:**

$$R = \frac{\sum |F_o - |F_c||}{\sum F_o}; \quad R_w = \left\{ \frac{\sum w(F_o^2 - F_c^2)^2}{\sum w(F_o^2)^2} \right\}^{\frac{1}{2}}$$

$$S = \left\{ \frac{\sum w(F_o^2 - F_c^2)^2}{n - p} \right\}^{\frac{1}{2}} \quad \begin{array}{l} \text{where } n = \text{number of data,} \\ p = \text{number of parameters refined.} \end{array}$$

**Comment:**

The crystals were macroscopically twinned about the  $a$  axis, and appeared to be monoclinic rather than triclinic. One crystal was successfully broken to produce a triclinic fragment, which was used for data collection.

**Table 1. Crystal and Intensity Collection Data for  
iPrThpZrCl<sub>2</sub>**

Formula: C <sub>23</sub> H <sub>36</sub> ZrSi <sub>2</sub> Cl <sub>2</sub>	Formula weight: 530.84
Crystal color: Colorless	Habit: Twinned tabular
Crystal size: 0.2 × 0.2 × 0.3 mm	$\rho_{\text{calc}} = 1.383 \text{ g cm}^{-3}$
Crystal System: Triclinic	Space group: $P\bar{1}$ (#2)
$a = 8.612(2)\text{\AA}$	$\alpha = 85.19(3)^\circ$
$b = 9.708(3)\text{\AA}$	$\beta = 77.85(2)^\circ$
$c = 16.662(5)\text{\AA}$	$\gamma = 69.41(2)^\circ$
$V = 1274.8(6)\text{\AA}^3$	$Z = 2$
Lattice parameters: 25 reflections,	$9^\circ \leq \theta \leq 11^\circ$
$\mu = 7.42 \text{ cm}^{-1}$	
CAD-4 diffractometer	$\omega$ scan
MoK $\alpha$ , $\lambda = 0.7107\text{\AA}$	Graphite monochromator
	$-10 \leq h \leq 10, -11 \leq k \leq 11, -14 \leq l \leq -14$
T = 293K	$F_{000} = 520$
Number of reflections measured: 8571	Number of independent reflections: 4084
Number with $F_o^2 > 0$ : 3866	Number with $F_o^2 > 3\sigma(F_o^2)$ : 3356
Standard reflections: 3 every 1 hr	Linear Decay: 0.32%
GOF <sub>merge</sub> : 0.99 for 4084 multiples	R <sub>merge</sub> : 0.026 for 3746 duplicates
Number used in refinement: 4084	Criterion: All reflections used
Final R: 0.046 for 3356 reflections with $F_o^2 > 3\sigma(F_o^2)$	
Final R: 0.053 for 3866 reflections with $F_o^2 > 0$	
Final weighted R: 0.106 for 4084 reflections	
Final goodness of fit: 2.12 for 253 parameters and 4084 reflections	
$(\Delta/\sigma)_{\text{max}}$ in final least squares cycle: 0.01	
$\Delta\rho_{\text{max}}$ : 1.14 e $\text{\AA}^{-3}$ , $\Delta\rho_{\text{min}}$ : -0.67 e $\text{\AA}^{-3}$ in final difference map	



**Table 2. Final Heavy Atom Parameters for  
iPrThpZrCl<sub>2</sub>**

$x, y, z$ and $U_{eq}^a \times 10^4$				
Atom	$x$	$y$	$z$	$U_{eq}$
Zr	2054.2(6)	5289.1(5)	2569.8(3)	237(1)
Cl1	2245(2)	3656(2)	1495(1)	438(4)
Cl2	1320(2)	3904(2)	3779(1)	449(4)
Si1	2099(2)	8060(2)	3496(1)	301(3)
Si2	3032(2)	7752(2)	1371(1)	285(3)
C1	3864(6)	6491(5)	2935(3)	278(11)
C2	4254(6)	6337(5)	2050(3)	261(11)
C3	5135(6)	4815(5)	1886(3)	306(12)
C4	5303(6)	4022(5)	2633(3)	333(13)
C5	4530(6)	5040(5)	3266(3)	299(12)
C6	553(6)	7850(5)	2903(3)	252(11)
C7	947(6)	7736(5)	2006(3)	258(12)
C8	-198(6)	7117(5)	1784(3)	258(12)
C9	-1184(6)	6803(5)	2517(3)	288(12)
C10	-810(6)	7298(5)	3196(3)	282(12)
C11	1772(7)	7566(7)	4605(4)	471(15)
C12	2377(8)	9887(6)	3409(4)	504(16)
C13	3396(8)	9541(6)	1269(4)	509(16)
C14	3571(7)	6980(6)	326(4)	449(15)
C15	6298(8)	2408(6)	2752(4)	476(16)

**Table 2. (Cont.)**

Atom	<i>x</i>	<i>y</i>	<i>z</i>	$U_{eq}$
C16	8028(11)	2239(9)	2860(8)	1229(39)
C17	6326(12)	1417(7)	2117(6)	972(32)
C18	-399(6)	6935(6)	922(3)	353(14)
C19	-989(9)	8423(8)	493(4)	612(20)
C20	-1612(8)	6109(7)	905(4)	506(17)
C21	-1759(6)	7328(6)	4075(3)	342(14)
C22	-2688(8)	8919(7)	4345(4)	573(19)
C23	-2996(8)	6500(8)	4191(4)	538(18)

$$^a U_{eq} = \frac{1}{3} \sum_i \sum_j [U_{ij}(a_i^* a_j^*)(\vec{a}_i \cdot \vec{a}_j)]$$

**Table 3. Complete Distances and Angles for  
iPrThpZrCl<sub>2</sub>**

	Distance(Å)	Distance(Å)	
Zr -Cl1	2.432(2)	C18 -C20	1.530(9)
Zr -Cl2	2.424(2)	C21 -C22	1.524(9)
Zr -CpA	2.217	C21 -C23	1.520(9)
Zr -CpB	2.240	C3 -H3	0.95
Zr -C1	2.441(5)	C5 -H5	0.95
Zr -C2	2.428(5)	C9 -H9	0.95
Zr -C3	2.550(5)	C11 -H11a	0.95
Zr -C4	2.652(5)	C11 -H11b	0.95
Zr -C5	2.565(5)	C11 -H11c	0.95
Zr -C6	2.415(5)	C12 -H12a	0.95
Zr -C7	2.418(5)	C12 -H12b	0.95
Zr -C8	2.624(5)	C12 -H12c	0.95
Zr -C9	2.673(5)	C13 -H13a	0.95
Zr -C10	2.617(5)	C13 -H13b	0.95
Si1 -C1	1.875(5)	C13 -H13c	0.95
Si1 -C6	1.888(5)	C14 -H14a	0.95
Si1 -C11	1.859(6)	C14 -H14b	0.95
Si1 -C12	1.861(7)	C14 -H14c	0.95
Si2 -C2	1.870(5)	C15 -H15	0.95
Si2 -C7	1.887(5)	C16 -H16a	0.95
Si2 -C13	1.858(7)	C16 -H16b	0.95
Si2 -C14	1.856(6)	C16 -H16c	0.95
C1 -C2	1.450(7)	C17 -H17a	0.95
C1 -C5	1.432(7)	C17 -H17b	0.95
C2 -C3	1.423(7)	C17 -H17c	0.95
C3 -C4	1.414(7)	C18 -H18	0.95
C4 -C5	1.395(7)	C19 -H19a	0.95
C4 -C15	1.518(8)	C19 -H19b	0.95
C6 -C7	1.467(7)	C19 -H19c	0.95
C6 -C10	1.435(7)	C20 -H20a	0.95
C7 -C8	1.441(7)	C20 -H20b	0.95
C8 -C9	1.410(7)	C20 -H20c	0.95
C8 -C18	1.514(7)	C21 -H21	0.95
C9 -C10	1.404(7)	C22 -H21a	0.95
C10 -C21	1.517(7)	C22 -H21b	0.95
C15 -C16	1.488(12)	C22 -H21c	0.95
C15 -C17	1.480(11)	C23 -H22a	0.95
C18 -C19	1.523(9)	C23 -H22b	0.95

Table 3. (Cont.)

Distance(Å)		Angle(°)	
C23	-H22c	0.95	
CpA	-Zr	-CpB	120.3
Cl1	-Zr	-Cl2	100.4(1)
CpA	-Zr	-Cl1	109.1
CpA	-Zr	-Cl2	108.1
CpB	-Zr	-Cl1	107.7
CpB	-Zr	-Cl2	109.5
C6	-Si1	-C1	91.6(2)
C11	-Si1	-C1	108.1(3)
C12	-Si1	-C1	117.2(3)
C11	-Si1	-C6	116.4(3)
C12	-Si1	-C6	115.9(3)
C12	-Si1	-C11	107.1(3)
C7	-Si2	-C2	92.1(2)
C13	-Si2	-C2	116.2(3)
C14	-Si2	-C2	108.4(2)
C13	-Si2	-C7	116.8(3)
C14	-Si2	-C7	115.3(2)
C14	-Si2	-C13	107.5(3)
C2	-C1	-Si1	123.9(4)
C5	-C1	-Si1	125.2(4)
C5	-C1	-C2	106.2(4)
C1	-C2	-Si2	121.5(4)
C3	-C2	-Si2	127.4(4)
C3	-C2	-C1	106.7(4)
C4	-C3	-C2	109.8(5)
C5	-C4	-C3	107.0(5)
C15	-C4	-C3	127.9(5)
C15	-C4	-C5	124.7(5)
C4	-C5	-C1	110.3(5)
C7	-C6	-Si1	121.8(4)
C10	-C6	-Si1	128.0(4)
C10	-C6	-C7	107.1(4)
C6	-C7	-Si2	122.5(4)
C8	-C7	-Si2	127.2(4)
C8	-C7	-C6	106.9(4)
C9	-C8	-C7	107.7(4)
C18	-C8	-C7	126.4(4)
C18	-C8	-C9	125.8(5)

Table 3. (Cont.)

Angle(°)			Angle(°)			
C10	-C9	-C8	110.2(4)	H21c	-C22 -H21a	109.5
C9	-C10	-C6	107.9(4)	H21c	-C22 -H21b	109.5
C21	-C10	-C6	126.3(4)	H22b	-C23 -H22a	109.5
C21	-C10	-C9	125.6(5)	H22c	-C23 -H22a	109.5
C16	-C15	-C4	109.8(6)	H22c	-C23 -H22b	109.5
C17	-C15	-C4	114.9(6)			
C17	-C15	-C16	112.2(7)			
C19	-C18	-C8	110.8(5)			
C20	-C18	-C8	112.6(5)			
C20	-C18	-C19	109.8(5)			
C22	-C21	-C10	109.5(5)			
C23	-C21	-C10	112.7(5)			
C23	-C21	-C22	110.0(5)			
H11b	-C11	-H11a	109.5			
H11c	-C11	-H11a	109.5			
H11c	-C11	-H11b	109.5			
H12b	-C12	-H12a	109.5			
H12c	-C12	-H12a	109.5			
H12c	-C12	-H12b	109.5			
H13b	-C13	-H13a	109.5			
H13c	-C13	-H13a	109.5			
H13c	-C13	-H13b	109.5			
H14b	-C14	-H14a	109.5			
H14c	-C14	-H14a	109.5			
H14c	-C14	-H14b	109.5			
H16b	-C16	-H16a	109.5			
H16c	-C16	-H16a	109.5			
H16c	-C16	-H16b	109.5			
H17b	-C17	-H17a	109.5			
H17c	-C17	-H17a	109.5			
H17c	-C17	-H17b	109.5			
H19b	-C19	-H19a	109.5			
H19c	-C19	-H19a	109.5			
H19c	-C19	-H19b	109.5			
H20b	-C20	-H20a	109.5			
H20c	-C20	-H20a	109.5			
H20c	-C20	-H20b	109.5			
H21b	-C22	-H21a	109.5			